



# CENTER FOR INFRASTRUCTURE ENGINEERING STUDIES

## THE ENGINEERING OF CONSTRUCTION SPECIFICATIONS FOR EXTERNALLY BONDED FRP COMPOSITES

by

**Xinbao Yang**

**Antonio Nanni**

**Genda Chen**

**Lokesh R. Dharani**



**CIES  
99-09**

University of Missouri-Rolla

**Disclaimer**

The contents of this report reflect the views of the author(s), who are responsible for the facts and the accuracy of information presented herein. This document is disseminated under the sponsorship of the Center for Infrastructure Engineering Studies (CIES), University of Missouri -Rolla, in the interest of information exchange. CIES assumes no liability for the contents or use thereof.

The mission of CIES is to provide leadership in research and education for solving society's problems affecting the nation's infrastructure systems. CIES is the primary conduit for communication among those on the UMR campus interested in infrastructure studies and provides coordination for collaborative efforts. CIES activities include interdisciplinary research and development with projects tailored to address needs of federal agencies, state agencies, and private industry as well as technology transfer and continuing/distance education to the engineering community and industry.

Center for Infrastructure Engineering Studies (CIES)  
University of Missouri-Rolla  
223 Engineering Research Lab  
1870 Miner Circle  
Rolla, MO 65409-0710  
Tel: (573) 341-6223; fax -6215  
E-mail: [cies@umr.edu](mailto:cies@umr.edu)  
[www.umr.edu/~cies](http://www.umr.edu/~cies)

## ABSTRACT

This dissertation, consisting of six technical papers, presents the results of research on the theme of developing engineering and the construction specifications for externally bonded FRP composites. For particular, the work focuses on three critical aspects of the performance of FRP systems: fiber misalignment, corner radius, and lap splice length. Based on both experimental and theoretical investigations, the main contribution of this work is the development of recommendations on fiber misalignment limit, minimum corner radius, lap splice length to be used as guidance in the construction practice of FRP strengthening of concrete structures.

The first three papers focus on the strength and stiffness degradation of CFRP laminates from fiber misalignment. It was concluded that misalignment affects strength more than stiffness. In practice, when all fibers in a laminate can be regarded as through fibers, it is recommended to use a reduction factor for strength and no reduction factor for stiffness to account for fiber misalignment. Findings from concrete beams strengthened with misaligned CFRP laminates verified these recommendations.

The fourth and fifth papers investigate the effect of corner radius on the mechanical properties of CFRP laminates wrapped around a rectangular cross section. A unique reusable test device was fabricated to determine fiber stress and radial stress of CFRP laminates with different corner radii. Comparison performed with finite element analyses shows that the test method and the reusable device were viable and the stress concentration needs to be considered in FRP laminate wrapped corners. A minimum of 1.0 in. corner radius was recommended for practice.

The sixth paper summarizes the research on the lap splice length of FRP laminates under static and repeated loads. Although a lap splice length of 1.5 in. is sufficient for CFRP laminates to develop the ultimate static tensile strength, a minimum of 4.0 in. is recommended in order to account for repeated loads.

## ACKNOWLEDGMENTS

The author would like to express his sincere appreciation to his two co-advisors, Drs. Antonio Nanni and Genda Chen for their continuous guidance, advice and support in his research.

The author's appreciation is also extended to the other members of his advisory committee: Drs. Abdeldjelil Belarbi, Franklin Y. Cheng, and Lokeswarappa R. Dharani for their time, advice and help.

Special thanks are given to his colleagues and friends: Jeff Bradshaw, Jason Cox, Yumin Yang, Chung Leung Sun, Ji Shen, and Danielle Stone, for their cooperation and generous help.

The financial support from the Federal Highway Administration (FHWA) and the University Transportation Center based at UMR are gratefully acknowledged.

Finally, the author wishes to express his deepest appreciation to his parents, and especially to his wife, Yaping Zhao, for their consistent encouragement, patience and understanding.

## TABLE OF CONTENTS

	Page
ABSTRACT.....	iv
ACKNOWLEDGMENTS.....	v
LIST OF ILLUSTRATIONS.....	x
LIST OF TABLES.....	xvii
INTRODUCTION.....	1
<b>PAPER</b>	
<b>Paper 1: Strength and Modulus Degradation of CFRP Laminates from Fiber Misalignment</b>	
ABSTRACT .....	21
INTRODUCTION .....	21
TEST SPECIMENS.....	22
Material Properties.....	22
Specimen Characteristics.....	22
Specimen Aspect Ratio.....	23
Specimen Dimensions and End Anchors.....	23
Instrumentation and Test Protocol.....	23
TEST RESULTS.....	24
Series I.....	24
Series II.....	25
RESULTS DISCUSSION.....	25
CONCLUSIONS.....	26
ACKNOWLEDGEMENT.....	26
APPENDIX I: REFERENCES.....	26
<b>Paper 2: Concrete Beams Strengthened with Misaligned CFRP Laminates</b>	
ABSTRACT.....	40
INTRODUCTION.....	40
EXPERIMENTAL PROGRAM.....	41

Material Properties.....	41
Specimens and Test Setup.....	42
TEST RESULTS.....	43
Strength and Deformation.....	43
Strain Distribution and Failure Modes of CFRP Laminates.....	45
CONCLUSIONS.....	47
ACKNOWLEDGEMENT.....	47
REFERENCES.....	47
<b>Paper 3: EFFECT OF FIBER MISALIGNMENT ON FRP LAMINATES AND STRENGTHENED CONCRETE BEAMS</b>	
ABSTRACT.....	48
INTRODUCTION.....	48
TEST SPECIMENS.....	49
Material Properties.....	49
Coupon Specimens.....	49
Scaled Concrete Beams.....	51
TEST RESULTS.....	52
Coupon Tensile Specimens.....	52
Scaled Concrete Beams.....	56
CONCLUSIONS.....	58
ACKNOWLEDGEMENT.....	59
REFERENCES.....	59
<b>Paper 4: Effect of Corner Radius on the Performance of Externally Bonded FRP Reinforcement</b>	
ABSTRACT.....	60
INTRODUCTION.....	60
EXPERIMENTAL PROGRAM.....	61
Material Properties.....	61
Design of Test Specimen.....	61
Installation of Laminate.....	62
Instrumentation.....	63

TEST RESULTS.....	64
Strength of CFRP laminates.....	64
Strain Distribution.....	65
Failure Modes.....	66
CONCLUSIONS.....	67
ACKNOWLEDGEMENT.....	67
REFERENCES.....	67
<b>Paper 5: STRESSES IN FRP LAMINATES WRAPPED AROUND CORNERS</b>	
ABSTRACT.....	68
INTRODUCTION.....	68
TEST PROGRAM.....	69
Materials.....	69
Test Specimen Design.....	69
Installation of Laminate.....	70
Instrumentation.....	70
ANALYSIS OF EXPERIMENTAL RESULTS.....	71
Strength of CFRP Laminates.....	71
Radial Stress Distribution.....	72
FINITE ELEMENT ANALYSIS.....	73
Analytical Model.....	73
Results and Discussions.....	74
CONCLUSIONS.....	75
ACKNOWLEDGEMENT.....	76
REFERENCES.....	76
<b>Paper 6: LAP SPLICE LENGTH AND FATIGUE PERFORMANCE OF LAP SPLICED CFRP LAMINATES</b>	
ABSTRACT.....	77
RESEARCH SIGNIFICANCE.....	77
INTRODUCTION.....	78
TEST PROGRAM.....	79
Materials.....	79

Test Specimens and Setup.....	79
EXPERIMENTAL RESULTS AND ANALYSIS.....	80
Lap Splice Length.....	80
Fatigue Performance of Lap Spliced CFRP Laminates.....	81
Residual Strength and Stiffness.....	83
VALIDATION OF ACI 440 GUIDE SPECIFICATION.....	84
CONCLUSIONS.....	84
ACKNOWLEDGEMENT.....	84
REFERENCES.....	85
CONCLUSIONS .....	102
APPENDIX 1 Proposed Standard Test Method for Determining the Effect of Corner Radius on Tensile Strength of Fiber Reinforced Polymers.....	104
APPENDIX 2 Stress Strain Curve of Misaligned CFRP Laminates.....	114
APPENDIX 3 Stress Strain Curve of FRP Laminates with Different Corner Radius and Confining Stress between Curvature Changing Points.....	127
APPENDIX 4 Load Strain Curve of Lap Spliced CFRP Laminates.....	153
APPENDIX 5 Recommendations to the AASHTO LRFD Design Specifications, US Units, Second Edition, 1998.....	163
VITA.....	168

## LIST OF ILLUSTRATIONS

Figure	Page
 Paper 1	
1 Width of through fibers of misaligned CFRP laminates.....	31
2 One-ply CFRP specimens.....	32
3 Specimen in the testing machine.....	33
4 Stress-strain curve of one-ply specimen.....	34
5 Stress-strain curve of two-ply specimen.....	34
6 Normalized strength of one-ply specimens.....	35
7 Normalized modulus of one-ply specimens.....	35
8 Normalized strength of two-ply specimens.....	36
9 Normalized modulus of two-ply specimens.....	36
10 Failure modes of selected specimens for Series I.....	37
11 Size effect on strength of CFRP laminate.....	37
12 Size effect on tensile modulus of CFRP laminate.....	38
13 Normalized gross strength vs. percent of effective width of all specimens.....	38
14 Normalized gross modulus vs. percent of effective width of all specimens.....	39
 Paper 2	
1 Specimen and strengthening.....	42
2 Strain gage arrangement.....	43
3 Load-midspan deflection of all beams.....	44
4 Degradation of ultimate load.....	44
5 Degradation of midspan deflection.....	44
6 Modulus degradation of tensile coupons and beams.....	45
7 Strain distribution of all beams.....	46
8 Delamination of CFRP laminates.....	46
 Paper 3	
1 CFRP coupon specimens.....	50
2 Specimen in the testing machine.....	50

3	Width of through fibers of misaligned CFRP laminates.....	50
4	Design of beams and CFRP system.....	52
5	Strain gage arrangement.....	52
6	Stress-strain curves of one-ply specimens.....	53
7	Normalized strength of one-ply specimens.....	54
8	Normalized modulus of one-ply specimens.....	54
9	Size effect on strength of CFRP laminate.....	55
10	Size effect on tensile modulus of CFRP laminate.....	56
11	Load-midspan deflection of all beams.....	56
12	Change in of ultimate load.....	57
13	Change in midspan deflection.....	57
14	Modulus degradation of CFRP laminate.....	57
15	Strain distribution of all beams.....	58
16	Delamination of CFRP laminates.....	58
<b>Paper 4</b>		
1	Test apparatus .....	62
2	Strain gage arrangement.....	63
3	Test setup.....	63
4	Ultimate load and stress vs. corner radius.....	64
5	Stress-strain curves of CFRP laminates.....	65
6	Strain distribution around a corner.....	66
7	Failure modes of CFRP laminates.....	67
<b>Paper 5</b>		
1	Test apparatus.....	69
2	Test setup.....	71
3	Ultimate stress vs. corner radius.....	71
4	Normalized ultimate stress of CFRP laminate.....	72
5	Pressure film.....	73
6	Radial stress distribution.....	73
7	(a) A quarter of the test apparatus, (b) Finite element analytical model.....	73
8	Ultimate radial stress by FEA and test.....	74

9	Radial stress distribution in corner area for R=25.4 mm.....	74
10	Stress concentration factor.....	75
11	Stress concentration factor distribution.....	75
Paper 6		
1	Couple in Single Layer Specimen.....	90
2	Symmetrical Configuration of a Specimen.....	91
3	Coupon Specimen and Test Setup.....	92
4	Failure Load versus Lap Splice Length.....	93
5	Strain Gage Distribution of 101.6-mm Lap-spliced Specimens.....	94
6	Load-Strain Curves on CFRP Laminates.....	95
7	Strain Distribution in Lapped and Non-lapped Areas (101.6-mm lap splice length).....	96
8	FRP Laminate Fatigue Life.....	97
9	Load-Strain Curves after Fatigue Loading.....	98
10	Strain Change with Fatigue Cycles.....	99
11	Residual Strength of CFRP Laminates.....	100
APPENDIX 1		
1	Assembled Test Fixture.....	106
2	Upper Part of Test Fixture(mm).....	109
3	Lower Part of Test Fixture(mm).....	107
4	Interchangeable Corner Inserts(mm).....	107
5	Tensile Fixture(Two sets needed) (mm).....	108
6	Installation of Specimen and Suggested Strain Gage Arrangement(mm).....	108
APPENDIX 2		
1	Stress strain curve of one-ply CFRP laminate ( $\theta = 0^\circ$ ).....	115
2	Stress strain curve of one-ply CFRP laminate ( $\theta = 5^\circ$ ).....	115
3	Stress strain curve of one-ply CFRP laminate ( $\theta = 10^\circ$ ).....	116
4	Stress strain curve of one-ply CFRP laminate ( $\theta = 15^\circ$ ).....	116
5	Stress strain curve of one-ply CFRP laminate ( $\theta = 20^\circ$ ).....	117
6	Stress strain curve of one-ply CFRP laminate ( $\theta = 30^\circ$ ).....	117
7	Stress strain curve of one-ply CFRP laminate ( $\theta = 40^\circ$ ).....	118

8	Stress strain curve of two-ply CFRP laminate ( $\theta = 0^\circ \sim 0^\circ$ ) (based on gross sectional area).....	118
9	Stress strain curve of two-ply CFRP laminate ( $\theta = 0^\circ \sim 5^\circ$ ) (based on gross sectional area).....	119
10	Stress strain curve of two-ply CFRP laminate ( $\theta = 0^\circ \sim 10^\circ$ ) (based on gross sectional area).....	119
11	Stress strain curve of two-ply CFRP laminate ( $\theta = 0^\circ \sim 15^\circ$ ) (based on gross sectional area).....	120
12	Stress strain curve of two-ply CFRP laminate ( $\theta = 0^\circ \sim 30^\circ$ ) (based on gross sectional area).....	120
13	Stress strain curve of two-ply CFRP laminate ( $\theta = 0^\circ \sim 45^\circ$ ) (based on gross sectional area).....	121
14	Stress strain curve of two-ply CFRP laminate ( $\theta = 0^\circ \sim 60^\circ$ ) (based on gross sectional area).....	121
15	Stress strain curve of two-ply CFRP laminate ( $\theta = 0^\circ \sim 90^\circ$ ) (based on gross sectional area).....	122
16	Stress strain curve of two-ply CFRP laminate ( $\theta = 0^\circ \sim 0^\circ$ ) (based on sectional area of through fibers).....	122
17	Stress strain curve of two-ply CFRP laminate ( $\theta = 0^\circ \sim 5^\circ$ ) (based on sectional area of through fibers).....	123
18	Stress strain curve of two-ply CFRP laminate ( $\theta = 0^\circ \sim 10^\circ$ ) (based on sectional area of through fibers).....	123
19	Stress strain curve of two-ply CFRP laminate ( $\theta = 0^\circ \sim 15^\circ$ ) (based on sectional area of through fibers).....	124
20	Stress strain curve of two-ply CFRP laminate ( $\theta = 0^\circ \sim 30^\circ$ ) (based on sectional area of through fibers).....	124
21	Stress strain curve of two-ply CFRP laminate ( $\theta = 0^\circ \sim 45^\circ$ ) (based on sectional area of through fibers).....	125
22	Stress strain curve of two-ply CFRP laminate ( $\theta = 0^\circ \sim 60^\circ$ ) (based on sectional area of through fibers).....	125
23	Stress strain curve of two-ply CFRP laminate ( $\theta = 0^\circ \sim 90^\circ$ ) (based on sectional area of through fibers).....	126

### APPENDIX 3

1	Stress strain curve of one ply CFRP laminates (R=0.0 mm, Specimen 1).....	128
2	Stress strain curve of one ply CFRP laminates (R=0.0 mm, Specimen 2).....	128
3	Stress strain curve of one ply CFRP laminates (R=0.0 mm, Specimen 3).....	129

4	Stress strain curve of one ply CFRP laminates (R=6.35 mm, Specimen 1).....	129
5	Stress strain curve of one ply CFRP laminates (R=6.35 mm, Specimen 2).....	130
6	Stress strain curve of one ply CFRP laminates (R=6.35 mm, Specimen 3).....	130
7	Stress strain curve of one ply CFRP laminates (R=12.7 mm, Specimen 1).....	131
8	Stress strain curve of one ply CFRP laminates (R=12.7 mm, Specimen 2).....	131
9	Stress strain curve of one ply CFRP laminates (R=12.7 mm, Specimen 3).....	132
10	Stress strain curve of one ply CFRP laminates (R=19.0 mm, Specimen 1).....	132
11	Stress strain curve of one ply CFRP laminates (R=19.0 mm, Specimen 2).....	133
12	Stress strain curve of one ply CFRP laminates (R=19.0 mm, Specimen 3).....	133
13	Stress strain curve of one ply CFRP laminates (R=25.4 mm, Specimen 1).....	134
14	Stress strain curve of one ply CFRP laminates (R=25.4 mm, Specimen 2).....	134
15	Stress strain curve of one ply CFRP laminates (R=25.4 mm, Specimen 3).....	135
16	Stress strain curve of one ply CFRP laminates (R=38.1 mm, Specimen 1).....	135
17	Stress strain curve of one ply CFRP laminates (R=38.1 mm, Specimen 2).....	136
18	Stress strain curve of one ply CFRP laminates (R=38.1 mm, Specimen 3).....	136
19	Stress strain curve of one ply CFRP laminates (R=50.8 mm, Specimen 1).....	137
20	Stress strain curve of one ply CFRP laminates (R=50.8 mm, Specimen 2).....	137
21	Stress strain curve of one ply CFRP laminates (R=50.8 mm, Specimen 3).....	138
22	Stress strain curve of two ply CFRP laminates (R=0.0 mm, Specimen 1).....	138
23	Stress strain curve of two ply CFRP laminates (R=0.0 mm, Specimen 2).....	139
24	Stress strain curve of two ply CFRP laminates (R=6.35 mm, Specimen 1).....	139
25	Stress strain curve of two ply CFRP laminates (R=6.35 mm, Specimen 2).....	140
26	Stress strain curve of two ply CFRP laminates (R=12.7 mm, Specimen 1).....	140
27	Stress strain curve of two ply CFRP laminates (R=12.7 mm, Specimen 2).....	141
28	Stress strain curve of two ply CFRP laminates (R=19.0 mm, Specimen 1).....	141
29	Stress strain curve of two ply CFRP laminates (R=19.0 mm, Specimen 2).....	142
30	Stress strain curve of two ply CFRP laminates (R=25.4 mm, Specimen 1).....	142
31	Stress strain curve of two ply CFRP laminates (R=25.4 mm, Specimen 2).....	143
32	Stress strain curve of two ply CFRP laminates (R=38.1 mm, Specimen 1).....	143
33	Stress strain curve of two ply CFRP laminates (R=38.1 mm, Specimen 2).....	144
34	Stress strain curve of two ply CFRP laminates (R=50.8 mm, Specimen 1).....	144

35	Stress strain curve of two ply CFRP laminates (R=50.8 mm, Specimen 2).....	145
36	Stress strain curve of one ply AFRP laminates (R=6.35 mm, Specimen 1).....	145
37	Stress strain curve of one ply AFRP laminates (R=6.35 mm, Specimen 2).....	146
38	Stress strain curve of one ply AFRP laminates (R=12.7 mm, Specimen 1).....	146
39	Stress strain curve of one ply AFRP laminates (R=12.7 mm, Specimen 2).....	147
40	Stress strain curve of one ply AFRP laminates (R=25.4 mm, Specimen 1).....	147
41	Stress strain curve of one ply AFRP laminates (R=25.4 mm, Specimen 2).....	148
42	Stress strain curve of one ply AFRP laminates (R=38.1 mm, Specimen 1).....	148
43	Stress strain curve of one ply AFRP laminates (R=38.1 mm, Specimen 2).....	149
44	Stress strain curve of one ply AFRP laminates (R=50.8 mm, Specimen 1).....	149
45	Confining stress between curvature changing points (R=6.35 mm (0.25 in))...	150
46	Confining stress between curvature changing points (R=12.7 mm (0.5 in))....	150
47	Confining stress between curvature changing points (R=19.0 mm (0.75 in))...	151
48	Confining stress between curvature changing points (R=25.4 mm (1.0 in))....	151
49	Confining stress between curvature changing points (R=38.1 mm (1.5 in))....	152
50	Confining stress between curvature changing points (R=50.8 mm (2.0 in))....	152

#### APPENDIX 4

1	Load strain curve of lap spliced CFRP laminates (Lap splice length $d=12.7$ mm, specimen 1).....	154
2	Load strain curve of lap spliced CFRP laminates (Lap splice length $d=12.7$ mm, specimen 2).....	154
3	Load strain curve of lap spliced CFRP laminates (Lap splice length $d=12.7$ mm, specimen 3).....	155
4	Load strain curve of lap spliced CFRP laminates (Lap splice length $d=25.4$ mm, specimen 1).....	155
5	Load strain curve of lap spliced CFRP laminates (Lap splice length $d=25.4$ mm, specimen 2).....	156
6	Load strain curve of lap spliced CFRP laminates (Lap splice length $d=25.4$ mm, specimen 3).....	156
7	Load strain curve of lap spliced CFRP laminates (Lap splice length $d=38.1$ mm, specimen 1).....	157
8	Load strain curve of lap spliced CFRP laminates (Lap splice length $d=38.1$ mm, specimen 2).....	157
9	Load strain curve of lap spliced CFRP laminates	

(Lap splice length $d=38.1$ mm, specimen 3).....	158
10 Load strain curve of lap spliced CFRP laminates (Lap splice length $d=50.8$ mm, specimen 1).....	158
11 Load strain curve of lap spliced CFRP laminates (Lap splice length $d=50.8$ mm, specimen 2).....	159
12 Load strain curve of lap spliced CFRP laminates (Lap splice length $d=50.8$ mm, specimen 3).....	159
13 Load strain curve of lap spliced CFRP laminates (Lap splice length $d=76.2$ mm, specimen 1).....	160
14 Load strain curve of lap spliced CFRP laminates (Lap splice length $d=76.2$ mm, specimen 2).....	160
15 Load strain curve of lap spliced CFRP laminates (Lap splice length $d=76.2$ mm, specimen 3).....	161
16 Load strain curve of lap spliced CFRP laminates (Lap splice length $d=101.6$ mm, specimen 1).....	161
17 Load strain curve of lap spliced CFRP laminates (Lap splice length $d=101.6$ mm, specimen 2).....	162

## LIST OF TABLES

Table	Page
Paper 1	
1 Manufacturer provided CFRP properties.....	28
2 Strengths and moduli of one-ply specimens.....	28
3 Strengths and moduli of two-ply specimens.....	29
4 Variation of strengths and moduli with aspect ratio (misalignment angle $\theta = 5^\circ$ , width $W = 38.1$ mm).....	30
5 Variation of strengths and modulus with aspect ratio (misalignment angle $\theta = 10^\circ$ , width $W = 38.1$ mm).....	30
Paper 2	
1 Mechanical properties of CF130 tow sheet.....	41
2 Mechanical properties of MBrace saturant.....	41
3 Ultimate load and deflection of all beams.....	44
Paper 3	
1 Manufacturer provided CFRP properties.....	49
2 Strengths and moduli of specimens Series I.....	53
3 Variation of strengths and moduli with aspect ratio.....	55
4 Variation of strengths and modulus with aspect ratio.....	55
5 Ultimate load and deflection of all beams.....	57
Paper 4	
1 Manufacturer provided CFRP properties.....	61
2 Average ultimate results.....	64
Paper 6	
1 Failure Load.....	89
2 Fatigue Test Matrix and Results.....	89

## INTRODUCTION

### **1: Background of Fiber Reinforced Polymer (FRP) Materials**

Composite materials are made of two or more distinct constituents, which can be categorized as reinforcement phase(s) and binder phase(s). The most popularly used advanced composite materials are fibers impregnated in a polymeric resin, also known as fiber reinforced polymer (FRP) materials. In a composite material, the fibers take the role of the principal load-bearing constituent and the resin (matrix) has the role of transferring the load, providing a barrier against adverse environment, and protecting the surface of fibers from mechanical abrasion.

Composites using fiber-reinforced materials of various types have created a revolution in high-performance structures in recent years. They offer significant advantages in strength and stiffness coupled with light-weight relative to conventionally used metallic materials. Along with this structural performance comes the freedom to select the orientation of the fibers for optimum performance. In this sense, advanced composite materials have been described as being revolutionary because the materials can be designed as well as the structure (Swanson 1997).

FRP materials are anisotropic and are characterized by excellent tensile strength in the fiber direction. No yielding is exhibited in FRP materials, but instead they are elastic up to failure. The current commercially available FRP reinforcements are usually made of continuous fibers of aramid (AFRP), carbon (CFRP), or glass (GFRP). They can be produced by different manufacturing methods in many shapes and forms; the most popular ones for concrete reinforcement are rebars, prestressing tendons, precured laminates/shells and fiber sheets. Commonly used FRP rods have various types of deformation systems, including externally wound fibers, sand coatings, and separately formed deformations. These rods are commonly used for internal or near surface mounted concrete reinforcement. FRP prefabricated laminates and sheets are commonly used for external reinforcement for strengthening/repairing concrete structures. FRP plane laminates have been used to replace bonded steel plates (Sharif and Baluch 1996) and FRP shells have been used as jackets for columns (Xiao and Ma 1997).

Figures 1 and 2 show some types of FRP composites used in the structural engineering lab of the University of Missouri-Rolla. Figure 1 shows unidirectional glass, aramid, and carbon fiber sheets. Different kinds of FRP rods are shown in Figure 2.

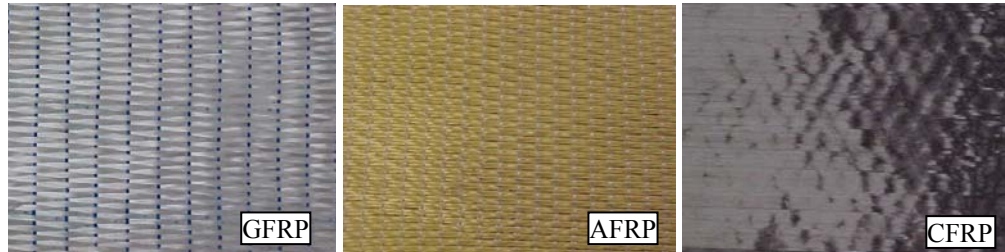


**Fig. 1 Glass, Aramid and Carbon FRP Sheet**



**Fig. 2 Carbon and Glass FRP Rods**

To give an idea of the basic mechanical properties of fiber sheets, the strength, modulus, and strain of glass, carbon, and aramid fibers are listed in Tables 1 and 2. Compared with conventional materials (e.g. steel), the advantages of fiber composites are often related to the ratios of stiffness and strength to weight, durability, creep and fatigue performance. Along with these advantages are the easy handling and installation, lower transportation cost, lower dead load, and excellent environmental resistance, which make FRP materials suitable for use with concrete structures and perform better than other construction materials in terms of weathering behaviors. Usually the tensile strength of FRP sheets is 10~20% less than that of fibers with equivalent volume. This is because fibers in a sheet are not uniformly arranged and there is strength redistribution due to the reorientation of fibers under load (Maruyama 1997).

Table 1 Mechanical Properties of Different Types of Fibers (MBrace 1998)

Fiber	Ultimate Strength ksi (MPa)	Design Strength ksi (MPa)	Modulus of Elasticity ksi (MPa)	Design Strain in/in	Thickness per Ply in (mm)
CF 130 High Strength Carbon	620(4275)	550(3790)	33,000(228,000)	0.017	0.0065(0.165)
CF 530 High Modulus Carbon	584(4027)	510(3517)	54,000(372,000)	0.009	0.0065(0.165)
EG900 E-Glass	251(1730)	220(1517)	10,500(72,400)	0.021	0.0139(0.353)
Aramid* AK-60	348(2401)	298(2058)	17,400(120,000)	0.017	0.0286(0.726)

\* Properties of aramid AK-60 were provided by Chang, K of DuPont.

Table 2 Typical Density of FRP Materials, lb/ft<sup>3</sup>(g/cm<sup>3</sup>) (MBrace 1998)

GFRP	CFRP	AFRP	Steel
75~130 (1.2~2.1)	90~100 (1.2~1.6)	75~90 (1.2~1.5)	492.5 (7.9)

Conventionally used polymeric resins with FRP systems include primers, putty fillers, saturants, and adhesives. The primer is used to penetrate the concrete surface to provide an improved adhesive bond for the saturating resin of adhesive. The putty is used to fill small surface voids in the concrete substrate and to provide a smooth surface to which the FRP can be bonded. Filled surface voids can also prevent bubbles from forming during curing of saturant and from creating stress concentration and load failure of FRP laminates due to realignment in case of bridging voids. The saturant is used to impregnate the fibers, fix them in place, and provide a shear path to effectively transfer load between fibers. The saturant also serves as the adhesive for wet lay-up systems providing a shear path between the previously primed concrete substrate and the FRP system. For prefabricated FRP laminate systems, adhesives are used to bond them to concrete substrate, which provides a shear path between the concrete substrate and the laminates. Adhesives are also used to bond together multiple layers of prefabricated FRP laminates. Figure 3 indicates a complete CFRP strengthening system bonded to concrete substrate.

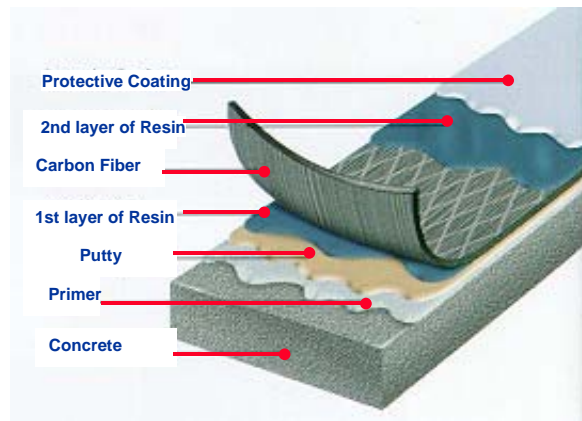


**Fig. 3 CFRP strengthening system**

It is of importance that the integrity of the FRP systems be achieved and maintained which depends on the construction quality to apply the FRP, the strength and the quality of the concrete. A generally accepted application process is described step by step as follows (MBrace 1998):

Step 1: preparation of the concrete substrate

Prior to installing the FRP strengthening system, the concrete substrate need to be prepared to accept the system, the surface of the concrete should be free of loose and unsound materials. All laitance, dirt, dust, oil, etc. should be removed. Sandblasting, water jetting, mechanical grinding or other approved methods should be used to open the pore structure of the concrete and make the surface rough as expected.

Step 2: application of primer

Primer is applied to the properly prepared concrete surface using a short or medium nap roller with a volume coverage of 200~250 ft<sup>2</sup>/gal.

Step 3: application of putty

Putty is applied to the primed surface using a trowel. The putty should be used to fill any surface defects; complete coverage is not necessary. The putty may be applied to a freshly primed surface without waiting for the primer to cure. The volume coverage for putty is 6~12 ft<sup>2</sup>/gal.

Step 4: application of first coat of saturant

Saturant is applied to primed and puttied surface with a medium nap roller. The saturant is blue in color and should be applied to a thickness of 0.015 to 0.02 in. The volume of saturant used depends on the FRP sheet used.

#### Step 5: application of fiber sheet

The FRP sheets should be measured and pre-cut prior to installing on the surface. The sheet is placed on the concrete surface and gently pressed into the saturant. Prior to removing the backing paper, a squeegee or trowel may be used to remove any air bubbles. After the backing paper is removed, a ribbed roller is rolled in the direction of the fibers to facilitate impregnation by separating the fibers. The ribbed roller should never be used in a direction transverse to the fibers since fibers could be damaged. Streaks of blue colored saturant should be visible on the fiber sheet after rolling.

#### Step 6: application of second coat of saturant

A second coat of saturant is applied 30 minutes after placing and rolling the fiber sheet. This period of time allows the first coat of saturant to be completely absorbed by the sheet. The second coat of saturant is applied to the FRP sheet with a medium nap roller to a thickness of 0.015 to 0.02 inch. More saturant is required for glass sheets because they are thickness than carbon sheets.

#### Step 7: application of additional fiber plies

If required, additional fiber plies may be installed by resaturating the surface 30 minutes after the second saturant coat is applied and repeating Steps 4, 5, and 6. This process should be repeated for as many plies as necessary. After completion of this step, the fiber sheet layers are encapsulated in laminate form.

#### Step 8: application of finish coats (optional)

After the saturant has cured tack free, one or more finish coats may be applied for protection or aesthetic purposes.

However, compared with the application process of FRP sheets, the application of near surface mounted (NSM) FRP rods is much simpler. Installation of the NSM rods is achieved by grooving the surface of the concrete. Traditionally, surface mounted reinforcement is placed parallel to the existing reinforcement. The grooves may have a square cross section with dimensions exceeding the diameter of the FRP rod to allow for embedment. Concrete can be grooved by making two parallel saw cuts on the concrete surface using conventional tools and technology. The two cuts have a predetermined depth and are spaced at a distance equal to the required width of the groove. The concrete in between the two cuts is then chipped off, thus creating the groove. After the groove is

cleaned, it is initially filled half way with a high viscosity binder (e.g. epoxy paste) compatible with the FRP rod. The high viscosity binder ensures easier field execution, especially for the case of over-head application. An FRP rod is then placed into the groove and lightly pressed in place. This action forces the paste to flow around the rod and cover the sides of the groove. The rod can be held in place using wedges at an appropriate spacing. The groove is then filled with the same binder and the surface is leveled (Nanni 2000a). In regard of the dimensions of the grooves, there is a trade off between the performance and the constructability. Larger groove dimensions may result in less stress concentration and thus higher ultimate capacity. However, constructability calls for the grooves as smaller as possible. So far no literature addressing the effect of groove dimensions on the bond performance for near surface mounted rods is available. However, the optimum value should be a function of groove size and the diameter of FRP rods (CIES 1999).

## **2. Strengthening of Infrastructures with FRP Composite Materials**

Concrete structures are conventionally reinforced with steel bars and/or prestressed with steel tendons. For concrete structures subjected to aggressive environments (e.g. bridges treated with deicing salt and marine structures), combinations of moisture, temperature and chlorides may result in the corrosion of the reinforcing and prestressing steel eventually leading to premature structural deterioration and loss of serviceability. In addition, the increasing service loads (e.g. growing traffic volume) and seismic upgrade requirements result in a need to strengthen many of these structures. To resolve corrosion problems, professionals have turned to alternative reinforcements such as epoxy-coated steel bars. It has been determined, however, that such remedies merely slow down the corrosion process rather than eliminating it. For flexural and shear strengthening of structural members, the use of externally bonded steel plates was well established for interior applications and for non-corrosive environments (Swamy et al. 1987). The corrosion problem has limited the use of this technique for outdoor application and technical problems have limited the use for long span applications.

Recently, fiber-reinforced polymer (FRP) advanced composite materials have emerged as an alternative and practical solution to steel reinforcement and its inherent

corrosion problems. FRP materials exhibit several properties suitable for their use as structural reinforcement (Nanni 1993, Nanni and Dolan 1993). FRP composites are corrosion resistant, and therefore should perform better than other construction materials such as steel in harsh environments.

The most important characteristic of FRP in repair and strengthening application is the speed and ease of installation combined with the higher ratios of strength and stiffness to weight. Lower labor and shut-down costs, and almost free of site constraints which typically offset the material cost of FRP composites making them very competitive with traditional strengthening techniques such as steel plate bonding and section enlargement. Concrete structures may need strengthening due to deterioration, design/construction errors, a change in use or loading, or for a seismic upgrade. Bonded FRP essentially works as additional reinforcement to provide tensile strength. FRP may be used on beams, girders, and slabs to provide additional flexural strength, on the sides of beams and girders to provide additional shear strength, or wrapped around columns to provide confinement and additional ductility (a primary concern in seismic upgrades).

Europe. Research on the use of FRP in concrete structures started in Europe in the sixties (Robinsky and Robinsky 1954, Wines et al. 1966). In the field of strengthening with FRP composites, pioneering work took place in the 1980's, in Switzerland and resulted in successful practical applications (Meier and Kaiser 1991). It was in Switzerland where the first on-site repair by externally bonded FRP took place in 1991 (Meier 1996). Since the first FRP reinforced highway bridge in 1986, programs have been implemented to increase the research and use of FRP reinforcement in Europe. The European BRITE/EURAM Project, "Fiber Composite Elements and Techniques as Non-Metallic Reinforcement," conducted extensive testing and analysis of the FRP materials from 1991 to 1996 (Taerwe, 1997). A pan-European collaborative research program (EUROCRETE) was established. The program started in December 1993 and ended in 1997. It aimed at developing FRP reinforcement for concrete and included industrial partners from the United Kingdom, the Netherlands, Switzerland, France, and Norway. Currently, more efforts and interests than ever have been given to FRP both in research and application in Europe (Taerwe et al. 2001).

Asia. Most activities of using FRP composite materials in infrastructures in Asia are concentrated in Japan (Maruyama 1997) and in Singapore (Tan 1997). Japan had its first FRP application in the early 1980's (Sonobe 1993). At the first stage, FRP rods, tendons, and sheets were used for counter measures to corrosion problem of concrete structures. However, a sudden increase in the use of FRP materials was attained after the 1995 Great Hanshin Earthquake, when extensive damages were identified in concrete structures. To strengthen/retrofit the damaged structures, continuous fiber sheets have played an important role and have gained tremendous applications due to their lightweight, speed and ease of installation and high tensile strength. The main applications are using FRP sheets to wrap bridge and building columns for enhanced ductility as well as shear capacity (Park 1995) and to strengthen bridge decks for improved flexural performance to accommodate the growing service loading. As of 1997, the Japanese led the FRP reinforcement usage with more than 1000 demonstration/commercial projects (JSCE 1997). To date, this technique is gradually attracting the attention of numerous research institutes, construction companies, and public agencies in Singapore and many projects involving the strengthening of beams, columns, and slabs have been carried out (Tan 1997).

North America. The use of advance composite materials in construction in North America is an exciting and rapidly expanding market even though the application of these materials to concrete structures was only the subject of research until only a few years ago. In this field, America and Canada hold the leadership (Nanni 1993, Neale and Labossiere 1997, Dolan, Rizkalla, and Nanni 1999). Today, many companies are involved in the manufacturing, design, and installation of these systems in construction projects (Gangarao et al. 1997). Tens of projects in the U.S. alone have been completed accounting for millions of square feet of this material both in strengthening existing structures and new construction. In addition, accepted building codes for using composite materials are beginning to surface from organizations such as ACI (ACI Committee 440, 2001). This material has quickly risen from state-of-the-art to mainstream technology (Nanni 1999). The dramatic increase of using FRP materials in infrastructures in America is due to the fact that many US bridges are made of reinforced concrete and were designed in accordance with older codes to accommodate traffic loads smaller than

currently permitted. Moreover, most of these structures were designed for gravity loads only with no consideration to seismic vulnerability. It may be economically unfeasible to replace every outdated bridge across the country due to many reasons including cost, time of construction, and traffic disturbance. A potential solution is the use of new technologies that allow for the upgrading of deficient structures at low cost and with minimal users' inconvenience. To this extent, strengthening systems that utilize FRP systems in the form of "external" reinforcement have attracted great interest of the civil engineering community (Nanni 1997, Dolan, Rizkalla, and Nanni 1999). One reinforced concrete bridge strengthened/retrofitted with FRP composite materials is introduced here as an example of successful application of this new technology and new material in America. All the work for this bridge was conducted under the cooperation of University of Missouri-Rolla (UMR) and Missouri Department of Transportation (MoDOT).

Bridge J857, built in 1932, located on Route 72 in Phelps County, MO, was strengthened in August of 1998 while in service (Alkhrdaji et al. 1999, Nanni 2000b). The three-span structure had a roadway width of 25 ft. with each deck spanning 26 ft. and a thickness of 18 inches reinforced concrete slab. The bridge deck was supported by two abutments and two bents. Each bent consisted of two piers connected at the top by a RC cap beam. The piers had a 2 by 2 feet square cross-section and were supported by 4 by 4 by 2.5 feet square spread footings. The bridge needed to be demolished due to the road realignment. Prior to its demolition, two of the three bridge decks were strengthened with externally bonded FRP reinforcement. The first was strengthened using near surface mounted carbon FRP rods and the second using externally bonded carbon FRP sheets leaving the third deck unstrengthened as the control span. The decks were tested to failure under static load. The piers, originally designed for gravity loads, were seismically upgraded using NSM carbon FRP rods, as well as jackets made of unidirectional carbon or glass FRP sheets. All strengthening work was carried out on the bridge while in service. Bridge upgrading was rapid with no interruption of traffic flow. The test results of the NSM CFRP rods strengthened span showed that an increase in moment capacity of 27% over the unstrengthened deck had been obtained which made the bridge deck enough to accommodate American Association of State Highway and Transportation Officials (AASHTO) HS20—modified truck loading. However, the design only called for

20 NSM CFRP sandblasted rods with a diameter of 7/16 in. spacing at 15 inch center-to-center. The rods were embedded in 20-ft. long, 3/4-in. deep, and 9/16-in. wide grooves cut into the soffit of the bridge deck parallel to its longitudinal axis.

Due to the inherent mechanical properties and interaction mechanisms between FRP systems and concrete structures, applications where existing FRP systems may not be useful include correcting punching shear problems in slabs or footings, correcting vibration problems, and providing greater compression strength to walls. In cases where FRP is useful, it should be recognized that there are reasonable limits to the additional strength afforded with FRP. Typically, increases in strength up to 50% are reasonable. It is also important to recognize that in cases where FRP is being used to address a deterioration problem, the FRP system will not stop the deterioration from occurring and may conceal visual signs of deterioration. The source of the deterioration should always be addressed and corrected prior to installing FRP. A common example is corrosion of steel reinforcement in a concrete beam or column. FRP should never be used to contain corrosion. FRP will not stop corrosion from progressing (the FRP may actually accelerate the corrosion process), and, in case of externally bonded FRP systems, the corrosion will eventually result in failure due to debonding. Fire protection is a concern when implementing an FRP system. FRP will not be capable of sustaining its structural properties under excessive heat due to a loss of composite action upon softening of the resin matrix (Nanni 1999). In addition, the lower modulus of elasticity of GFRP and AFRP composites may limit its use in long span structures such as bridges and slabs without implementing other materials with higher modulus of elasticity.

### **3. Research Background and Project Description**

At present, there are no nationally accepted specifications for construction process control of bonded FRP composite materials for structural repairs and strengthening. The long-term performance of these materials is very sensitive to the process in which the material is stored, handled, installed, and cured. Long-term performance is also sensitive to concrete condition as well as the surface of the underlying concrete. Bonded FRP composites require a higher level of process control than is required for bonded steel. Hence, there is a need to verify the quality control of the construction process and the

constituent materials of the composites to ensure acceptable performance of structures repaired with FRP. With the rapid and wide spread use of these materials, the process of quality control and quality assurance is becoming particularly important since there are potentials for inexperienced contractors and suppliers of materials with varying degree of quality to enter the market.

Currently, there are no methods for quantifying the relationship between the long-term performance of composite repairs and the processes by which they are manufactured and applied. As a result, DOTs and bridge owners do not have a rational basis to write construction specifications, for either procedures or tolerances. In order to develop construction and application specifications, focused research is required that takes into account the body of recent and past work, nationally and internationally, and tailors an analytical and experimental program to accomplish the objectives of individual tasks.

This project involved the elaboration of a research program to develop model construction specifications for public agencies engaged in the construction of FRP strengthening/repairing of highway bridges, and in the inspection of FRP repair work. The principal recipients for these model specifications are the Federal Highway Administration (FHWA), AASHTO and its member organizations. The study developed recommended specifications, supporting tests, and field procedures to FHWA and state highway agencies who supervise the activities in product acceptance, construction contracting, inspection, and repair. These particular specifications were also intended to place specifications, supporting testing, and field practice in these areas on a scientifically-valid, widely-accepted, and public foundation.

Research tasks were tailored to address construction issues that affect the performance of FRP systems. The program developed acceptance test specifications for FRP repair for bridge decks and superstructures. The program also developed criteria for field inspection of FRP repair/strengthening systems and bonded FRP repairs of concrete structures. These criteria were based on the identification of critical sections of FRP structures or repairs and the determination of critical accumulated damage thresholds. The results of the experimental tasks were used to develop recommendations for rapid and economical techniques to detect accumulated damage approaching or exceeding these thresholds.

The work that the UMR team has been coordinating with AASHTO Technical Committee T-21 includes holding periodic meetings with the committee and providing technical assistance as requested by the committee. UMR team has also communicated on a regular basis with composites industry and industry-sponsored organizations that are developing industry standards which would be compatible with AASHTO specifications, and with professional and trade organizations that are compiling syntheses of existing specifications.

During the investigation of this project, both laboratory and field test and verification have been conducted to provide the required background materials for the specifications. The first task of this research program was to collect and review all literature, research findings, performance data, and current practices relative to construction and inspection specifications for FRP repair and strengthening of RC structures. Research results are being implemented with the production of an AASHTO Guide Specification for Construction Process Control for Bonded FRP Repairs of Concrete Structures. The research did not involve the development of design specifications for different repair applications.

The research program has identified the construction procedures that ensure the long-term performance for FRP repair and retrofit systems bonded to concrete structural elements. The aim to this objective was the ability to predict the long-term performance of FRP systems using short-duration (accelerated) test methods. The research was tailored to concentrate on those factors, which are most critical to performance, and allow greater leeway on those which are not. The research program did not involve the manufacturing process for constituent materials or plant-fabricated composite components. It was strictly concerned with those aspects of field fabrication and quality control tests, which would affect the long-term performance of composite structural repairs and strengthening.

The main topics are divided into three major types, namely externally bonded FRP sheets and prefabricated laminates; near surface mounted FRP rods; and external FRP post-tensioning, which are listed in Tables 3, 4 and 5, respectively (CIES 1999).

Table 3 Topics Related to Repair/Strengthening with  
FRP Sheets and Prefabricated Laminates

Main Topic	Sub-topic
1. Externally Bonded Sheets and Prefabricated Laminates	
1.1 Substrate Condition	Surface Profile
	Surface Strength
	Intimate Contact
	Presence of Moisture or Frost
	Moisture Vapor Transmission
	Crack Injection
	Moving Cracks
1.2 Materials and Material Handling	Dust Control
	Fiber Irregularities
	Storage
1.3 Installation	Epoxied Surface Smoothness
	Unattended Epoxy Surfaces
	<b>Fiber Alignment</b>
	Voids/Delaminations
	Cure Time Limits
	<b>Corner Radius</b>
	FRP Strip Spacing
	Bonded Length
<b>Lap Splice Length</b>	
Inspection Devices and Methods	Surface Roughness Test
	Pull-off Test (Bond)
	Torque Test (Bond)
	Voids/Delaminations Test
2. Durability of FRP Repair	
2.1 Aggressive Environment	Freeze-Thaw Cycles
	Extreme Thermal Gradients (non- freeze)
	UV Exposure
	Relative Humidity
	Long-term Exposure to Salts
3. End Anchorage	
3.1 Installation Purpose	Shear Strengthening
	Flexural Strengthening
3.2 Anchor Details	Groove Dimensions
	Type of FRP Bar

Table 4 Topics Related to Repair/Strengthening with  
Near Surface Mounted FRP Rods

Main Topic	Sub-topic
1. Substrate Condition	Surface Preparation
2. Materials and Material Handling	Type of Rod
3. Installation	Dimensions of Groove
4. Inspection Devices and Methods	N/A

Table 5 Topics Related to Repair/Strengthening  
with External Post-Tensioned FRP

MAIN TOPIC	SUB-TOPIC
1. Substrate Condition	N/A
2. Materials and Material Handling	Characterization of Mechanical Properties
3. Installation	Tendon Anchorage
4. Inspection Devices and Methods	N/A

#### 4. Report Organization

The research work covered in this report include three subtasks regarding the installation of externally bonded CFRP laminates namely fiber misalignment; corner radius; and lap splice length (Table 3).

##### 4.1 Fiber Misalignment

The performance of unidirectional FRP laminates is highly dependent on fiber orientation with respect to applied load direction. In the case of fabrication by manual lay-up, it is possible to have fiber plies installed with improper orientation. If not considered, fiber misalignment will generally reduce FRP strength as well as stiffness. The reduction is usually magnified by the stress concentration resulted from opening of cracks. In this project, the degradation of strength and modulus of carbon FRP laminates from fiber misalignment was first investigated experimentally using tensile coupons. Then verification tests were performed using concrete beams strengthened with misaligned CFRP laminates. For the coupon tests, the specimens consisted of one and two plies of unidirectional carbon FRP impregnated with a two-component epoxy. The misalignment angles varied from 0 to 40° for the one-ply samples, and from 0 to 90° for one ply of the two-ply samples. The size effect on the strength and modulus was also investigated for one-ply specimens with misalignments of 5 and 10°. For these

specimens, the ply width was maintained constant and the length was varied so that the aspect ratio ranged between 2 and 8. For the verification tests, five unreinforced concrete inverted Tee beams were cast and strengthened with misaligned CFRP laminates on the tension surfaces. The laminates had off-axis angles of 0 to 10°, respectively. The beams were tested under four-point loading to total failure to investigate (1) strength and stiffness degradation of beams, (2) flexural performance, and (3) strain distribution and failure modes of CFRP laminates

#### 4.2 Corner Radius

Externally bonded FRP reinforcement is wrapped around concrete members in order to provide confinement and/or shear strengthening. The need for bending the fibers over the member corners affects the performance of the FRP laminate and the efficiency of its confining/strengthening action. In this project, both experimental and analytical study focusing on the effects of corner radius on FRP mechanical properties have been performed. A unique re-usable test device was designed and used for this purpose such that plies of FRP could be applied over interchangeable corner inserts. The radius of the inserts ranged from a minimum of 0 to a maximum of 2.0 inches, and one or two plies of CFRP and AFRP were tested. The monitored parameters included strain distribution in the FRP laminate and load. For the one-ply CFRP laminates, the radial stress was measured using pressure films to get a picture of the confining effect exerted by CFRP laminates on the structural cross sections. The relationship between radial stress distribution and corner radius, and the stress concentration in the laminates were analyzed numerically using the finite element method and compared with experimental results.

#### 4.3 Lap Splice Length

Most FRP laminates are applied externally with manual lay up. With this technique, the convenient handling length is usually less than 20 feet. When FRP laminates strengthen long members or in cases when there are some geometrical restrictions, lap splicing is usually adopted to maintain the continuity of laminates and force transition. To obtain assurance of the performance of lap-spliced FRP laminates and avoid failure before developing the strength of FRP laminates, the effective lap splice

length needs to be investigated before installation of FRP laminates. In this project, the lap splice length of CFRP and the long-term (fatigue) performance of lap-spliced CFRP laminates were investigated. Lap-spliced CFRP coupon specimens were fabricated with a splice length of 0.5 to 4.0 inches. To eliminate the bending on the lap splice joints, a symmetric specimen configuration was adopted. The width of the specimens was 1.5 inches. These specimens were tested to failure under tension load. The ultimate load, failure mode, and strain distribution on the surface of both the non-lapped and lapped areas were monitored. Tension-tension fatigue tests were performed only on 4-inch lap-spliced specimens to investigate the long-term performance of CFRP laminates. A stress ratio versus number of cycles curve was constructed using the test data and compared with theoretical results. In addition, the residual strength and stiffness of the specimens subjected to 2.5 million cycles of fatigue loading were also investigated.

#### 4.4 Concluding Remarks

Based on the research of these three projects, the general conclusions were stated at the end of this report and an appendix shows the recommendations to the AASHTO LRFD Bridge Design Specifications (Second Edition, 1998) for implementing FRP composite materials in the design and construction of bridge structures. Four additional appendices were attached to this report to provide the original experimental results which are not covered in the papers. A flowchart of Figure 4 gives a general picture of the organization of this report.

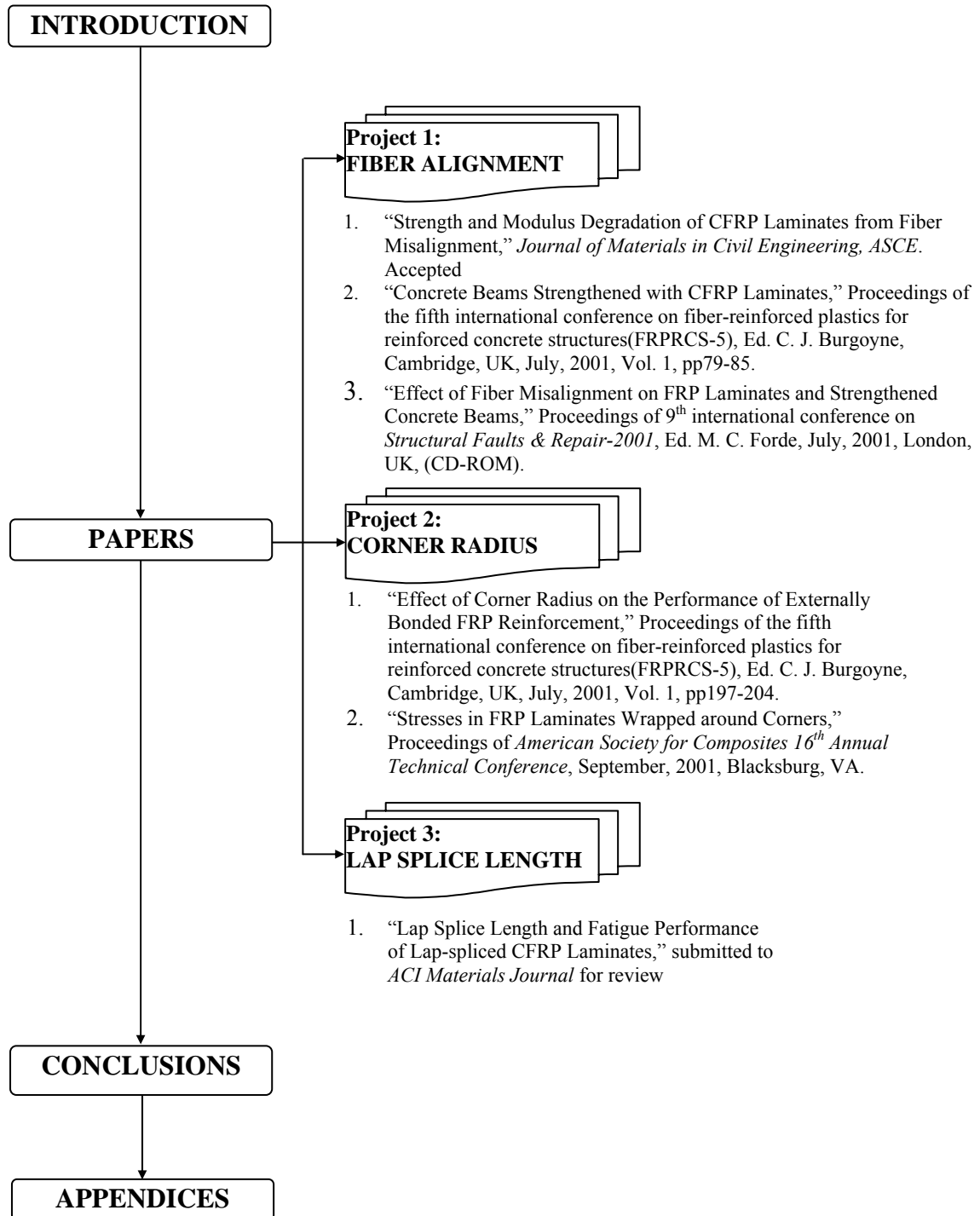


**Fig. 4 General Organization of Report**

## REFERENCES

- ACI Committee 440 (2001), "Guide for the Design and Construction of Externally Bonded FRP Systems for Strengthening Concrete Structures," American Concrete Institute, Detroit, MI. (In print)
- Alkhrdaji, T., Nanni, A., Chen, G., and Barker, M. (1999), "Upgrading the Transportation Infrastructure: Solid RC Decks Strengthened with FRP," *Concrete International*, American Concrete Institute, Vol. 21, No. 10, October, pp. 37-41.
- Center for Infrastructure Engineering Studies (CIES), UMR (1999), "Construction Specifications and Inspection Process for FRP Repair/Strengthening of Concrete Structures," Project proposal to Federal Highway Administration (FHWA).
- Dolan, C. W., Rozkalla, S. H., and Nanni, A. Editors (1999), "Fourth International Symposium on Fiber Reinforced Polymer Reinforcement for Reinforced Concrete Structures (FRPRCS-4)," SP-188, American Concrete Institute, Farmington Hills, Michigan. 1182pp.
- GangaRao, H.V.S., Thippeswamy, H.K., Kumar, S.V., and Franco, J.M., (1997) "Design, Construction, and Monitoring of the First FRP Reinforced Concrete Bridge Deck in the United States," *Non-Metallic (FRP) Reinforcement for Concrete Structures*, Proceedings of the 3<sup>rd</sup> Int. Symposium, Sapporo, Japan, Vol. 1, 647-656.
- JSCE Sub-Committee on Continuous Fiber Reinforcement (1992), "Utilization of FRP-Rods for Concrete Reinforcement," *Proc.*, Japan Society of Civil Engineers, Tokyo, Japan, 314 pp.
- Maruyama, K. (1997), "JCI Activities on Continuous Fiber Reinforced Concrete," Proceedings of the 3<sup>rd</sup> international symposium on non-metallic(FRP) reinforcement for concrete structures(FRPRCS-3), Vol. 1, Oct. 1997, Japan Concrete Institute, Sapporo, Japan, pp3-12.
- MBrace <sup>TM</sup> (1998), "Composite Strengthening System, Engineering Design Guideline", 2<sup>nd</sup> Ed., Structural Preservation Systems, Inc., Cleveland, OH, pp109.
- Meier, U., and Kaiser, H. P., (1991), "Strengthening of Structures with CFRP Laminates," *Advanced Composite Materials in Civil Engineering Structures*, ASCE Speciality Conference, pp. 224-232.

- Meier, U., (1996), "Composites for Structural Repair and retrofitting," Proceedings of the 1<sup>st</sup> international conference on composites in infrastructure (ICCI), Jan. 1996, Tucson, Arizona, pp1202-1216.
- Nanni, A., Editor, (1993), "Fiber-Reinforced-Plastic (FRP) Reinforcement for Concrete Structures: Properties and Applications," Developments in Civil Engineering, Elsevier, Amsterdam, The Netherlands, Vol. 42, 450 pp.
- Nanni, A. and Dolan, C.W., Eds. (1993), "FRP Reinforcement for Concrete Structures," Proc., ACI SP-138, American Concrete Institute, Detroit, MI, pp. 977.
- Nanni, A. (1997), "Carbon FRP Strengthening: New Technology Becomes Mainstream," Concrete International: Design and Construction, Vol. 19, No. 6, pp. 19-23.
- Nanni, A. (1999), "Composites: Coming on Strong," Concrete Construction, Vol. 44, pp120-127.
- Nanni, A. (2000a), "FRP reinforcement for Bridge Structures," Proceedings of Structural Engineering Conference, The University of Kansas, Lawrence, Kansas.
- Nanni, A. (2000b), "Carbon Fibers in Civil Structures: Rehabilitation and New Construction," proceedings of the Global Outlook for Carbon Fiber 2000," San Antonio, Texas.
- Neale, K. W. and Labossiere, P. (1997), "State-of-the-Art Report on Retrofitting and Strengthening by Continuous Fibre in Canada," Proceedings of the 3<sup>rd</sup> international symposium on non-metallic(FRP) reinforcement for concrete structures(FRPRCS-3), Vol. 1, Oct. 1997, Japan Concrete Institute, Sapporo, Japan, pp25-40.
- Park, R. (1996), "Analysis of the Failure of the Columns of a 600-meter-length of the Hanshin Elevated Expressway during the Great Hanshin Earthquake of Jan. 17, 1995," Bulletin of New Zealand National Society of Earthquake Engineering, Vol. 29, No. 2.
- Rubinsky, I. A., and Rubinsky, A., (1954), "An Investigation into the Use of Fiber-Glass for Prestressed Concrete," Magazine of Concrete Research, V. 6.
- Sharif, A. and Baluch, M. H. (1996), "External FRP Plates to Strengthen Reinforced Concrete Beams," Proceedings of the 1<sup>st</sup> international conference on composites in infrastructures(ICCI-96), Tucson, AR, pp814-828.

- Sonobe, Y. (1993), "An Overview of R&D in Japan," Fiber-Reinforced-Plastic (FRP) Reinforcement for Concrete Structures: Properties and Applications, Ed. Nanni, A., Elsevier, Amsterdam, The Netherlands, pp115-128.
- Swamy, R.N., Jones, R. and Bloxham, J.W., (1987), "Structural Behavior of Reinforced Concrete beams Strengthened by Epoxy-Bonded steel Plates", The Structural Engineer, Vol. 65A, No. 2, pp. 59-68.
- Swanson, S. R. (1997), Introduction to Design and Analysis with Advanced Composite Materials, Simon & Schuster/A Viacom Company, Prentice-Hall, Inc., Upper Saddle, NJ, 249pp.
- Taerwe, L., Khalil, H., and Matthys, S., (1997), "Behavior of RC Beams Strengthened in Shear by External CFRP Sheets," Proceeding of the Third International Symposium on Non-Metallic (FRP) Reinforcement for Concrete Structures (FRPRCS-3), Japan Concrete Institute, Sapporo, Japan, Vol. 1, pp. 483-490.
- Taerwe, L. et al. (2001), "European Activities on the Use of FRP Reinforcement, fib Task Group 9.3 and the ConFiberCrete Network," Proceeding of the fifth international conference on fiber0reinforced plastics for reinforced concrete structures, Cambridge, United Kingdom, pp3-15.
- Tan, K. H. (1997), "State-of-the-Art Report on Retrofitting and Strengthening by Continuous Fibers: Southeast Asian Perspective-Status, Prospects and Research Needs," Proceedings of the 3<sup>rd</sup> international symposium on non-metallic(FRP) reinforcement for concrete structures(FRPRCS-3), Vol. 1, Oct. 1997, Japan Concrete Institute, Sapporo, Japan, pp13-24.
- Wines, J. C., et al., (1966), "Laboratory Investigation of Plastic-Glass Fiber Reinforcement for Reinforced and Prestressed Concrete," U.S. Army Corps of Engineers, WES, V. 1 & 2, Vicksburg, MS, 228 pp.
- Xiao, Y. and Ma, R. (1997), "Seismic Retrofit of RC Circular Columns Using Prefabricated Composite Jacketing," Journal of Structural Engineering - ASCE, Vol. 123, No. 10, pp. 1357-1364.

## Strength and Modulus Degradation of CFRP Laminates from Fiber Misalignment

Xinbao Yang, Antonio Nanni, Stephen Haug, and Chung Leung Sun  
Center for Infrastructure Engineering Studies  
University of Missouri-Rolla  
Rolla, MO 65409

**ABSTRACT:** Fiber reinforced polymer (FRP) laminates are being used as external reinforcement for strengthening concrete members. The performance of unidirectional FRP laminates is highly dependent on fiber orientation with respect to applied load direction. In the case of fabrication by manual lay-up, it is possible to have fiber plies installed with improper orientation. In this project, the degradation of strength and modulus of carbon FRP laminates from fiber misalignment was investigated experimentally using tensile coupons. The specimens consisted of one and two plies of unidirectional carbon FRP impregnated with a two-component epoxy. The misalignment angles varied from 0 to 40° for the one-ply samples, and from 0 to 90° for one ply of the two-ply samples. The size effect on the strength and modulus was investigated for one-ply specimens with misalignments of 5 and 10°. For these specimens, the ply width was maintained constant and the length was varied so that the aspect ratio ranged between 2 and 8. It was concluded that misalignment affects strength more than elastic modulus. However, provided that mechanical parameters are related to the cross sectional area of laminate with fibers continuous from end to end of the coupon, the degradation of strength can be accounted with a knock down factor that is independent of misalignment angle.

**KEYWORDS:** carbon fiber; fiber reinforced polymer; laminate; misalignment; strength; stiffness; tensile modulus; size effect.

### INTRODUCTION

Fiber reinforced polymer (FRP) laminates have been used extensively in the past decade as externally bonded reinforcement for the upgrade of reinforced concrete (RC) and prestressed concrete (PC) structures (Nanni and Dolan 1993, Taerwe 1995, Ueda et al. 1997, Dolan et al. 1999). The majority of this work has been conducted with composites installed by manual lay-up. Experimental investigations of RC and PC members strengthened with FRP have shown satisfactory performance in both strength and ductility or other special requirements. When FRP laminates are intended for strengthening, the analysis and design of the member can be performed under the conventional principles of RC and PC theory based on assumed material properties (Saadatmanesh and Malek 1998, Nanni et al. 1998). Typically, the material properties used for FRP are those provided by the material manufacturers and are based on tensile tests of “perfect” coupons (Hamada et al. 1997). Obviously, there are concerns about the performance of a structural member when errors in installation may result in fiber misalignment. Depending on the severity of the misalignment, the difference between

actual strength and stiffness of the FRP from the assumed nominal values may become unacceptable or, at least, warrant a reduction of performance expectations.

An experimental investigation on the effect of fiber misalignment on strength and stiffness degradation is crucial for the successful use of FRP in the upgrade of the concrete infrastructure. The results of such an investigation should be implemented into corresponding construction and design specifications for guidance in field practice. In this paper, experimental results of coupon tests for misaligned carbon FRP laminates are reported. Two issues were addressed by the tests, namely: the degradation of strength and stiffness as a function of the misalignment angle for one and two-ply laminates, and the degradation of strength and stiffness as a function of the specimen aspect ratio for one-ply laminates.

## TEST SPECIMENS

### Material Properties

Coupons used in the research project were cut from CFRP laminate panels made of high tensile strength, unidirectional carbon tow sheets (MBrace 1998). The carbon tow sheets were impregnated using the two-part epoxy polymer saturant provided by the manufacturer. The guaranteed mechanical properties of the CFRP laminate as per manufacturer's literature are listed in Table 1. It is to be noted that in this table, as for the rest of the paper, the FRP mechanical properties are based on fiber cross sectional area rather than composite area. This is due to the following reasons: a) in manual lay-up fabrication, it is rather difficult to control the amount of resin being used; b) small variations in the amount of resin, provided that the fibers are fully impregnated, do not affect the composite mechanical performance; and c) resin mechanical properties are significantly lower than those of fibers.

### Specimen Characteristics

Laminate panels were fabricated by the hand lay-up technique and coupons were cut from the panels after complete cure. A 610×460×16 mm plywood sheet was set as the base of the mold which was a rectangular plastic plate covered with a thin polyethylene film as the release agent. After the mold was prepared, the two-part saturant was thoroughly mixed and a thin layer was placed on the mold with a roller. Then the carbon fiber ply was spread on the saturant layer and its backing paper was removed after application of gentle pressure. A plastic roller was used to remove air entrapped between fiber ply and saturant. After approximately 30 minutes, a second layer of saturant was applied and the plastic roller was used again to work the resin into the fibers. The wet laminate was left to cure for seven days and then released from the mold. The laminate panel was then ready to be cut into coupons along predetermined lines in order to obtain different misalignment angles. The final laminate surface in contact with the mold was smooth enough for attaching the strain gages prior to testing.

For the two-ply samples, the fabrication process included an additional step. Furthermore, the two plies were placed with fiber directions forming a predetermined angle  $\theta$ . The first fiber ply was placed at the angle  $\theta$  with respect to the mold edge using a triangular wedge. The second ply was then applied with fibers parallel to the mold

edge. Coupons from the cured laminate were cut along the fiber direction of the upper ply so that only the first ply had a misalignment angle equal to  $\theta$ .

### Specimen Aspect Ratio

Due to the finite width,  $W$ , length,  $L$ , and misalignment angle,  $\theta$ , for each coupon type, not all fibers can be continuous from end to end of the specimen. The width of continuous or through fibers,  $W'$ , is clearly shown in Fig. 1. This figure shows the relevance of the specimen aspect ratio for the case of  $\theta = 10^\circ$ . When  $L/W = 2$  only 65% of the fiber area is continuous from end to end; if  $L/W = 4$ , then that area becomes 29%. Obviously, the larger the aspect ratio (and the misalignment angle), the smaller is the percentage of the through fibers. In the case of  $L/W = 4$ , no continuous fiber (i.e.,  $W' = 0$ ) is present when  $\theta > 14^\circ$ .

### Specimen Dimensions and End Anchors

*Series I.* All one-ply and two-ply specimens for Series I had the same width of 38.1 mm and gage length of 152.4 mm for an aspect ratio  $L/W = 4$ . The carbon fiber thickness,  $t$ , was 0.165 and 0.330 mm for one-ply and two-ply specimens, respectively. To provide appropriate anchorage during testing, rectangular aluminum tabs were used at both ends of each specimen in order to diffuse clamping stresses. According to previous research (Hojo et al. 1994), the shape of the tabs does not significantly influence the tensile properties. Squared-off tabs with dimensions of 51.0×38.1×1.6 mm were used in this project. Two tabs were glued at each end of a specimen using an epoxy-based adhesive (Fig. 2). During testing, only the initial 38.1 mm in the longitudinal direction of the tabs was held by the grips of the testing machine. This was intended to further reduce the stress concentration at the onset of the specimen gage length as compared to the case of tabs totally clamped by the grips (Fig. 3).

For one-ply specimens, six misalignment angles were investigated in addition to perfectly aligned fibers; the angles were 5, 10, 15, 20, 30, and 40°. Five identical specimens were tested for each case. As shown in Table 2, no fiber is continuous from end to end (i.e.,  $W' = 0$ ) for the last four groups of specimens.

For the two-ply specimens, one ply had fiber aligned with the direction of the load (0°), while the other ply had fibers at an angle to the loading direction, which included values of 0, 5, 10, 15, 30, 45, 60, and 90°. For each case, three identical specimens were tested. As shown in Table 3, only one of two plies had continuous fibers from end to end (i.e.,  $W' = 38.1 + 0$ ) for the last five groups of specimens.

*Series II.* One-ply specimens for investigation of the size effect were limited at misalignment angles of 5 and 10°. Aspect ratios were varied from 2 to 8 for both groups of specimens (see Tables 4 and 5). The width of these specimens was always constant and equal to 38.1 mm, the gage length varied between 76.2 and 304.8 mm. No through fibers existed between tabs ( $W' = 0$ ) for the specimen with aspect ratio of 6 and 8 when  $\theta$  is 10° as shown in Table 5.

### Instrumentation and Test Protocol

Strain gages were attached to the mold-side surface of the specimens of Series I and II to record strain in the longitudinal and transverse directions. In this paper, only the strain measurements recorded by gages applied along the centerline of the coupon in the

direction of the load application are reported. For Series I readings, the gage of reference was that applied at mid height (center point, CP). For Series II readings, one additional gage located at quarter length (quarter point, QP) is reported.

The load was acquired by the built-in hydraulic line pressure transducer of the MTS 880 testing machine. In this testing frame, the loading head is rotationally self-aligning, which eliminates the potential of bending and twisting the specimen. The wedge grips are self-tightening, to keep a constant pressure, so the clamping conditions do not change due to laminate contraction. All specimens were tested under displacement control with a constant loading speed of 2 mm/min (ASTM 1995; Tarnopol'skii and Kincis 1985).

## TEST RESULTS

### Series I

Figures 4 and 5 show representative stress-strain diagrams obtained from specimens of Series I. The stress of the laminate as plotted is based on the assumption that the load was solely carried by fibers and is computed as a nominal gross value based on load divided by gross fiber area ( $t \times W$ ).

Figure 4 shows four diagrams related to one-ply specimens. The stress-strain curve is almost a perfect line for specimens with  $\theta = 0^\circ$  or  $\theta = 15^\circ$  and higher. These are the perfectly aligned fiber specimen and the ones with no through fibers. For specimens with  $\theta = 5$  and  $10^\circ$ , the diagram shows a sudden drop at a strain value of approximately 0.007 mm/mm, signaling the formation of cracking.

Figure 5 shows three diagrams related to two-ply specimens. For all two-ply specimens, irrespective of the misalignment angle of the first ply, the stress strain diagram was a straight line, indicating that the  $0^\circ$  ply would prevent the formation of cracks.

A summary of strength and stiffness results for Series I is shown in Tables 2 and 3. Two values of strength are reported:  $f_g$  is the gross strength based on load divided by gross fiber area ( $t \times W$ ), and  $f_t$  is the strength of through fibers based on load divided by through fiber area ( $t \times W$ ). The elastic modulus  $E_g$  is calculated from the gross stress and strain values, with the latter measured at the center point along the gage length of specimens.  $E_g$  is obtained by fitting the best straight line for given experimental data and calculating the slope of such line. It is to be noted that, for one-ply specimens with misalignment angles of 5 and  $10^\circ$ ,  $E_g$  refers to the slope of the first leg of the stress-strain curve prior to the stress drop.

Average gross and through strengths, and elastic modulus of all specimens are normalized with respect to the values of the specimens perfectly aligned fibers (i.e.  $0^\circ$  and  $0^\circ-0^\circ$ ) and reported in Tables 2 and 3. Normalized individual (not average) specimen strengths and modulus are plotted in Figures 6 to 9 for all specimens of Series I as a function of the misalignment angle. In this paper, no specific consideration is made with respect to the statistical significance of the experimental work; however, the data plotted in these figures show a remarkable repeatability as also indicated by the standard deviation values on strength and stiffness shown in Tables 2 and 3. Typical failure modes of specimens for Series I are illustrated in Figure 10. Through fibers broke

suddenly and disintegrated, while non-through fibers slid along the cracks as the applied load was increasing.

## Series II

The gross strength,  $f_g$ , and elastic modulus,  $E_g$ , for specimens of Series II are calculated as described previously and reported in Tables 4 and 5. Two specimens were tested for each aspect ratio. The aspect ratios ranged from 2 to 8 for both groups of specimens. All individual strength and modulus data are listed in Tables 4 and 5 including the modulus calculated using the strain of the quarter point of the centerline of specimen number 2. The tables also report the values of thorough fiber width,  $W'$ , corresponding to each aspect ratio.

The average strength and modulus are normalized using the strength and modulus of the one-ply, perfectly aligned fiber specimens with an aspect ratio of 4, in order to allow for consistent comparisons. The normalized average strength and modulus are shown as a function of the aspect ratio in Figures 11 and 12, respectively.

## RESULTS DISCUSSION

The experimental investigation presented challenges to be resolved, or at least logically addressed, if tensile coupons were to be used to predict the performance of misaligned FRP laminates externally bonded to concrete.

- In practical cases, the misalignment is typically small. It is rather difficult to consistently produce specimens with a small misalignment angle and, unless the number of repetitions is high, there is the risk of losing statistical significance. The minimum misalignment angle as well as the minimum angle increment was set equal to  $5^\circ$ .
- Even in the presence of misalignment, all fibers are through fibers in practical cases. For example, consider an FRP laminate applied to the soffit of a beam for flexural strengthening. Independent of quality of installation, all fibers are continuous and well anchored across any potential crack, whether perpendicular or not to the beam longitudinal axis. In the case of a tensile coupon, some fibers are always discontinuous as long as the misalignment angle is different from  $0^\circ$ . It was decided to use the present results as a function of nominal as well as through width for analysis.
- Single or multi-ply laminates are used in practical cases with similar frequency. One- and two-ply laminates were used in the project.

The overall summary of the experimental work conducted in this project can be illustrated with the diagrams of Figures 13 and 14. In Figure 13, the average normalized gross strength,  $f_g$ , is plotted as a function of the effective fiber width percentage, defined as  $W'/W \times 100$ , for all specimens. In Figure 14, the same is done for the case of the average normalized gross modulus,  $E_g$ . In both figures, the points corresponding to an effective width equal to 0 have been omitted since they represent the saturant contribution rather than fiber's.

From Figure 13, it is apparent that  $f_g$  is directly proportional to the effective width. One could conclude that, provided that all fibers are properly anchored, there is an insignificant effect of fiber misalignment on strength. For design purposes in

strengthening use, it is suggested that the nominal strength of a CFRP laminate be reduced by a knock down factor,  $k$ , equal to 13.6% to account for potential fiber misalignment. The  $k$  value is based on the 80 percentile (see lower line in Figure 13) for the sample population of this project. If some fibers are not anchored, strength should be related to effective width.

From Figure 14, one could draw similar conclusions with reference to stiffness rather than strength. The only difference is that a knock down factor is not needed in this case.

## CONCLUSIONS

Based on the experimental results of this investigation on the strength and modulus degradation of misaligned CFRP laminates, the following conclusions can be reached:

- Strength more than elastic modulus is affected by fiber misalignment.
- In practice, when all fibers in a laminate can be regarded as through fibers, it is recommended to use a reduction factor for strength and no reduction factor for stiffness to account for fiber misalignment. The reduction (knock down) factor is constant and equal to 13.6%.
- size effects need to be further investigated in future research

## ACKNOWLEDGEMENT

The financial support of the Federal Highway Administration (FHWA) and the University Transportation Center based at UMR are gratefully acknowledged. The authors wish to thank Mr. J. Bradshaw for his generous help during lab testing.

## APPENDIX I: REFERENCES

- ASTM D3039/D3039M (1995), "Standard Test Method for Tensile Properties of Polymer Matrix Composite Material", American Society for Testing and Materials, West Conshohocken, PA, 10 pp.
- Dolan, C.W., Rizkalla, S.H., and Nanni, A., (1999), "Fiber Reinforced Polymer Reinforcement for Reinforced Concrete Structures," FRPRCS-4, *Proc. 4<sup>th</sup> Int. Symposium*, Baltimore, MD, SP-188, American Concrete Institute, Farmington Hills, MI, 1181 pp.
- Hamada, H., Oya, N., Yamashita, K., and Maekawa, Z.-I. (1997), "Tensile Strength and Its Scatter of Unidirectional Carbon Fiber Reinforced Composites", *Journal of Reinforced Plastics and Composites*, 16(2), pp119-130.
- Hojo, M., Sawada, Y. and Miyairi, H. (1994), "Influencing of Clamping Method on Tensile Properties of Unidirectional CFRP in 0° and 90° Directions-Round Robin Activity for International Standardization in Japan", *Composites*, 25(8), pp786-796.
- MBrace<sup>TM</sup> (1998), "Composite Strengthening System, Engineering Design Guideline", 2<sup>nd</sup> Ed., Structural Preservation Systems, Inc., Cleveland, OH, pp109.
- Nanni, A. and Dolan, C.W., Editors, Fiber Reinforced-Plastic Reinforcement of Concrete Structures - International Symposium, ACI Special Publication No. 138, American Concrete Institute, Detroit, MI, 1993, 988 pp.

- Nanni, A., Focacci, F., and Cobb, C.A., (1998) "Proposed Procedure for the Design of RC Flexural Members Strengthened with FRP Sheets," *Proc., ICCI-98*, Tucson, AZ, Jan. 5-7, 1998, Vol. I, pp.187-201
- Saadamanesh, H. and Malek, A. M. (1998), "Design Guideline for Flexural Strengthening of RC Beams with FRP Plates", *Journal of Composites for Construction*, ASCE, 2(4), pp158-164.
- Taerwe, L., ed., 1995, "Non-Metallic (FRP) Reinforcement for Concrete Structures," Proceedings of the Second International RILEM Symposium (FRPRCS-2), Ghent, Belgium, 714 pp.
- Tarnopol'skii, Yu. M. and Kincis, T. (1985), "Static Test Methods for Composites", Van Nostrand Reinhold Company, New York, pp301.
- Ueda, T., Nakai, H., and Tottori, S. (1997), "JCI State-of-the-Art Report on Retrofitting by CFRM-Guidelines for Design, Construction and Testing", FRPRCS-3, *Proc. 3<sup>rd</sup> Int. Symposium*, Sapporo, Japan, Oct. 14-16, 1997, Vol. I, pp. 621-628.

**Table 1: Manufacturer provided CFRP properties**

Ultimate strength (MPa)	4275
Design strength (MPa)	3790
Tensile modulus (MPa)	228
Ultimate strain (mm/mm)	0.017

**Table 2: Strengths and moduli of one-ply specimens**

Angle (deg.)	W (mm)	W' (mm)	Properties based on w				Properties based on w'	
			E <sub>g</sub> (GPa) [std]*	Normalized E <sub>g</sub>	f <sub>g</sub> (MPa) [std]*	Normalized f <sub>g</sub>	f <sub>t</sub> (MPa) [std]*	Normalized f <sub>t</sub>
0	38.1	38.1	264 [18]	1.00	4323 [172]	1.00	4323 [172]	1.00
5		24.8	221 [18]	0.84	2603 [254]	0.60	4004 [391]	0.93
10		11.2	142 [11]	0.54	1210 [80]	0.28	4106 [272]	0.95
15		0	88 [7]	0.33	586 [117]	0.14	-	-
20		0	58 [7]	0.22	396 [57]	0.09	-	-
30		0	33 [6]	0.12	261 [21]	0.06	-	-
40		0	27 [2]	0.10	116 [8]	0.03	-	-

Note \* = Standard deviation based on 5 repetitions

**Table 3: Strengths and moduli of two-ply specimens**

Angle (deg.)	W (mm)	W' (mm)	Properties based on w				Properties based on w'	
			E <sub>g</sub> (GPa) [std]*	Normalized E <sub>g</sub>	f <sub>g</sub> (MPa) [std]	Normalized f <sub>g</sub>	f <sub>t</sub> (MPa) [std]	Normalized f <sub>t</sub>
0-0	38.1+38.1	38.1+38.1	259 [7]	1.00	4315 [320]	1.00	4315 [320]	1.00
0-5		38.1+24.8	228 [22]	0.88	3273 [112]	0.76	3967 [136]	0.92
0-10		38.1+11.2	186 [15]	0.72	2643 [112]	0.61	4083 [173]	0.95
0-15		38.1+0	170 [11]	0.66	2311 [227]	0.54	4623 [455]	1.07
0-30		38.1+0	124 [9]	0.48	2167 [159]	0.50	4335 [318]	1.00
0-45		38.1+0	124 [15]	0.48	2106 [212]	0.49	4212 [425]	0.98
0-60		38.1+0	124 [1]	0.48	2157 [176]	0.50	4315 [351]	1.00
0-90		38.1+0	115 [11]	0.44	1971 [158]	0.46	3943 [315]	0.91

Note \* = Standard deviation based on 3 repetitions

**Table 4: Variation of strengths and moduli with aspect ratio (misalignment angle  $\theta = 5^\circ$ , width  $W = 38.1$  mm)**

Aspect ratio L/W	2	4	6	8
W' (mm)	31.4	24.8	18.1	11.4
Strength $f_g$ (MPa)				
Specimen-1	3141	2610	1798	2039
Specimen-2	2655	2570	1961	1890
Modulus $E_g$ (GPa)				
CP of specimen-1	225	194	225	250
CP of specimen-2	252	247	187	239
QP of specimen-2	197	216	198	232

Note: CP = center point, and QP = quarter point of the longitudinal centerline refer to the position of the strain gage

**Table 5: Variation of strengths and modulus with aspect ratio (misalignment angle  $\theta = 10^\circ$ , width  $W = 38.1$  mm)**

Aspect ratio L/W	2	4	6	8
W' (mm)	24.7	11.2	0	0
Strength $f_g$ (MPa)				
Specimen-1	1752	1132	950	727
Specimen-2	1651	-	746	758
Modulus $E_g$ (GPa)				
CP of specimen-1	144	146	137	132
CP of specimen-2	167	156	136	137
QP of specimen-2	149	177	146	129

Note: CP = center point, and QP = quarter point of the longitudinal centerline refer to the position of the strain gage

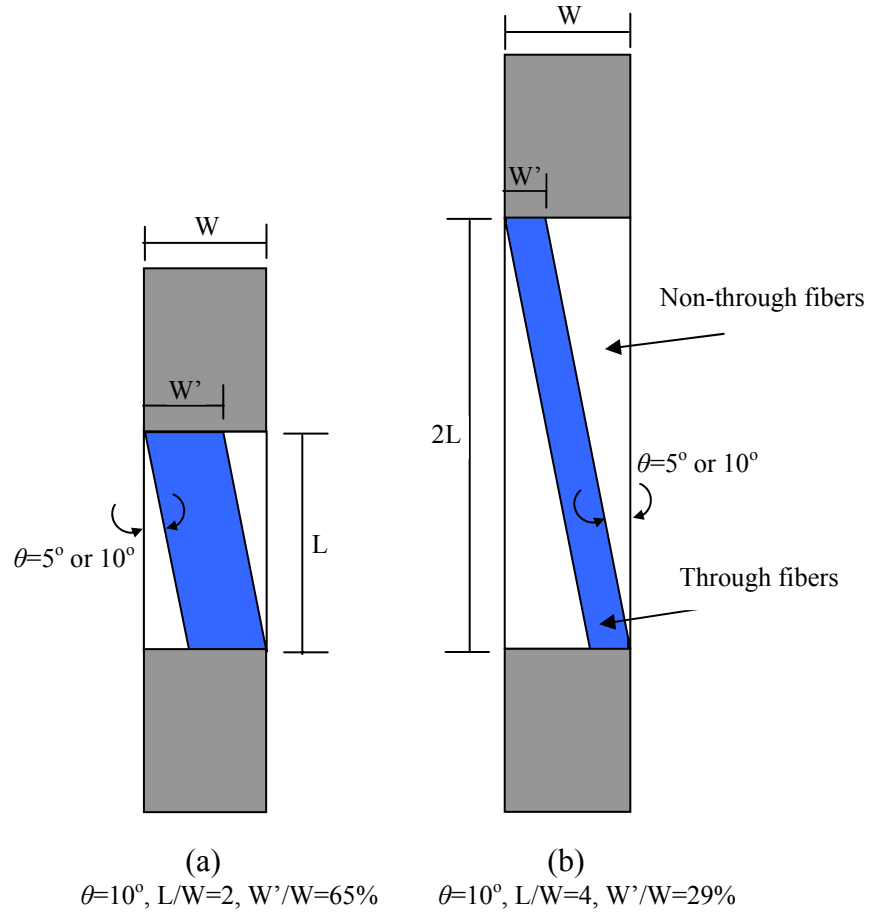


**Fig. 1: Width of through fibers of misaligned CFRP laminates**

**( $\theta=10^\circ$ ,  $L/W=2$  or  $L/W=4$ )**

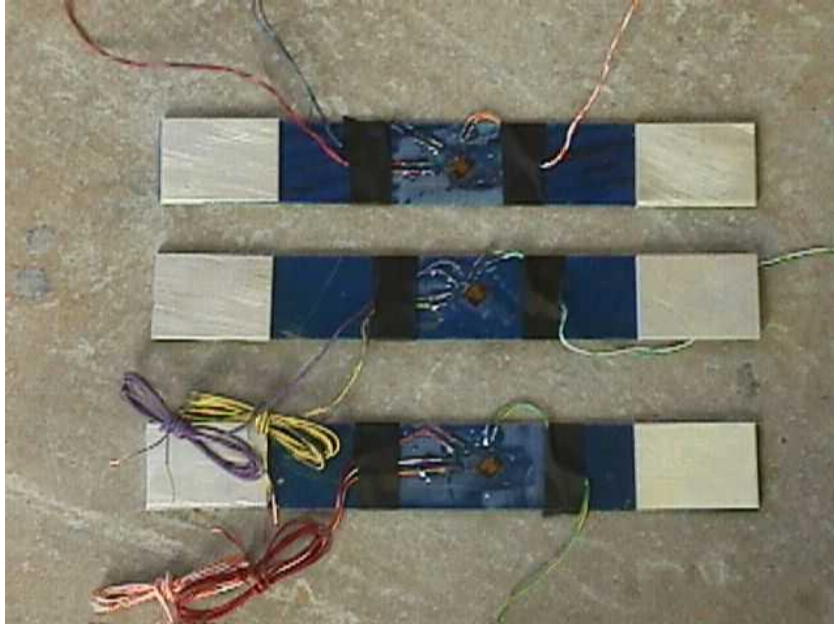


**Fig. 2: One-ply CFRP specimens**



**Fig. 3: Specimen in the testing machine**

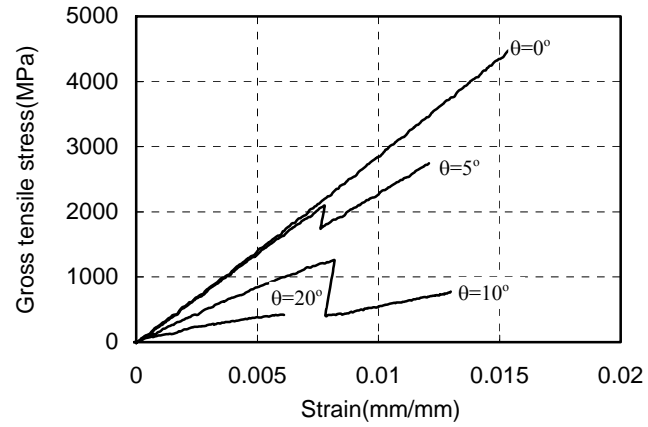


**Fig 4: Stress-strain curves of one-ply specimens**

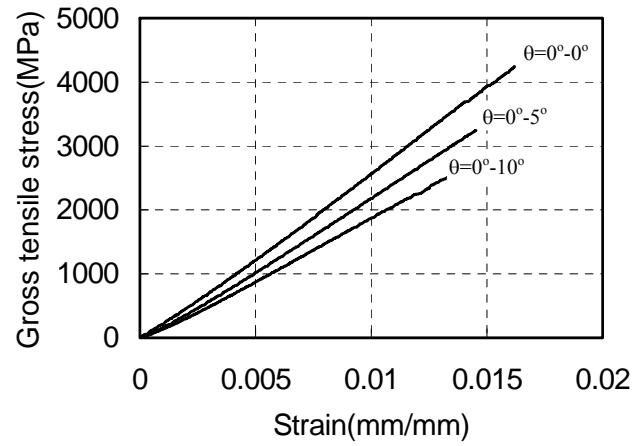


**Fig. 5: Stress-strain curves of two-ply specimens**

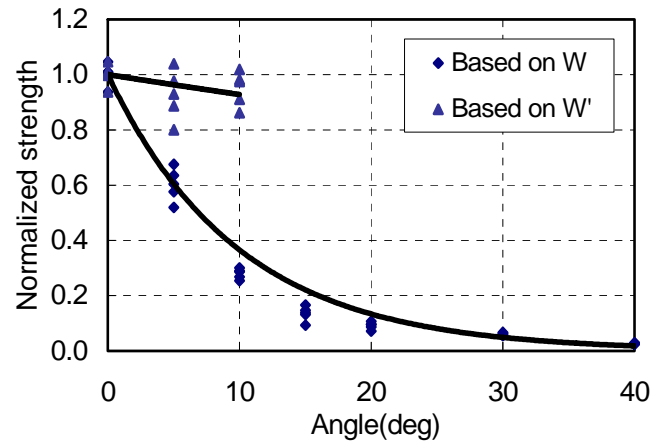


**Fig. 6: Normalized strength of one-ply specimens**

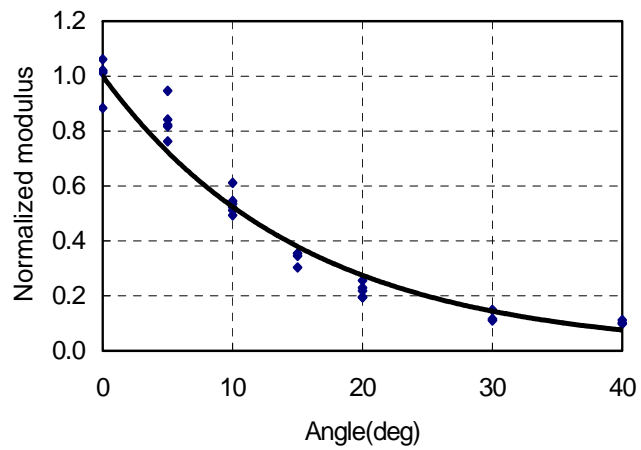


**Fig. 7: Normalized modulus of one-ply specimens**

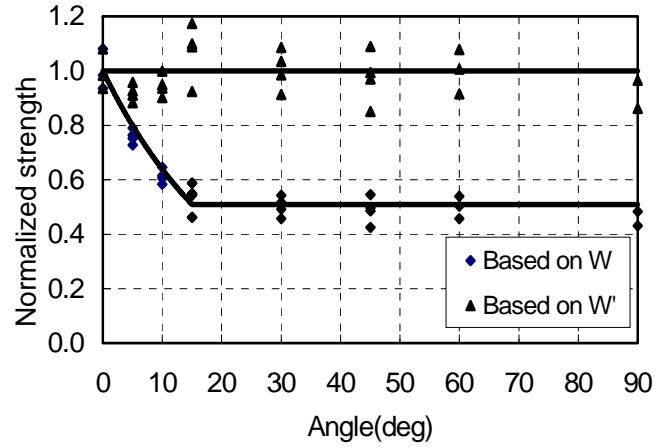


**Fig. 8: Normalized strength of two-ply specimens**

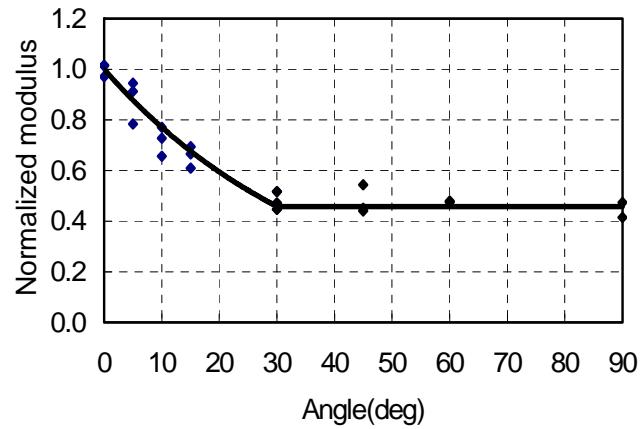
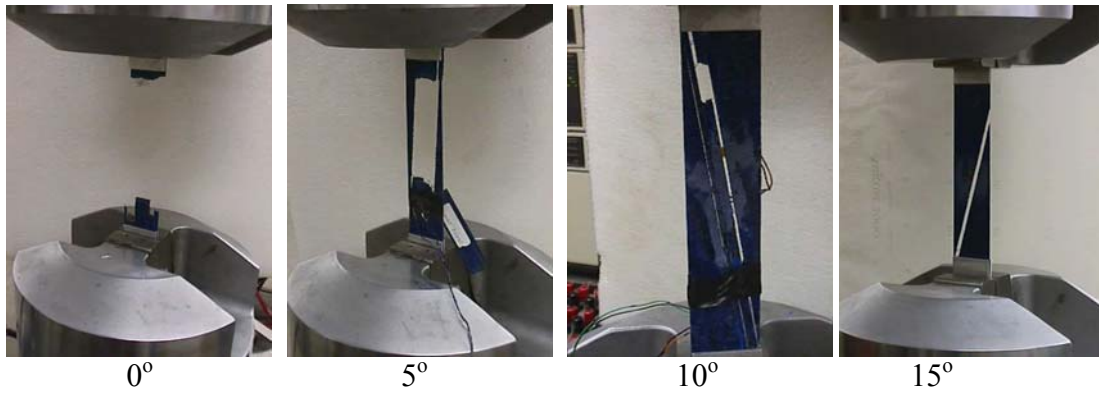
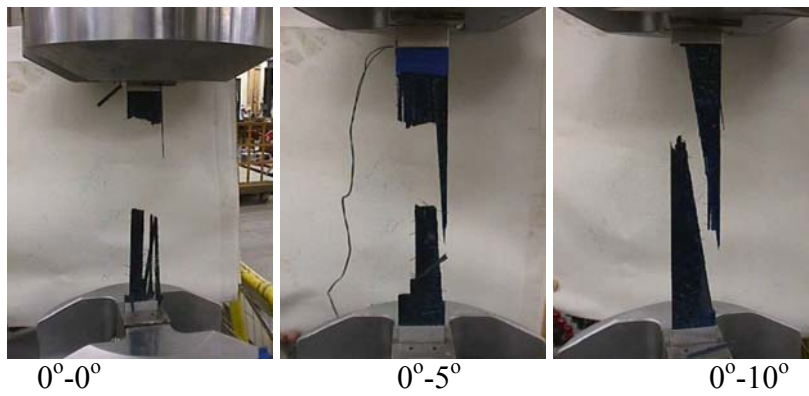


**Fig. 9: Normalized modulus of two-ply specimens**



(a) One-ply



(b) Two-ply

**Fig. 10: Failure modes of selected specimens for Series I**

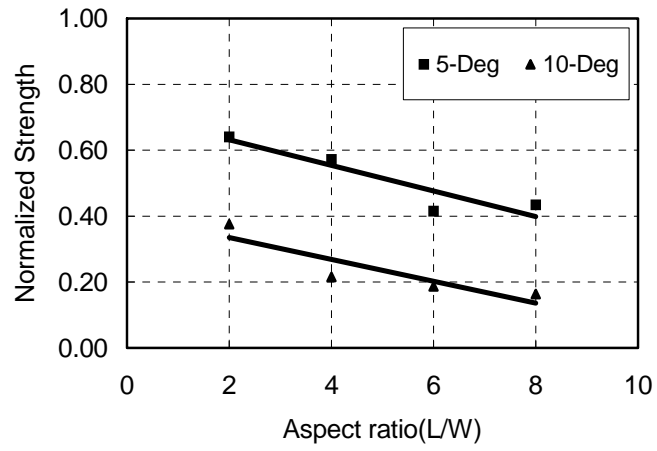


**Fig. 11: Size effect on strength of CFRP laminate**

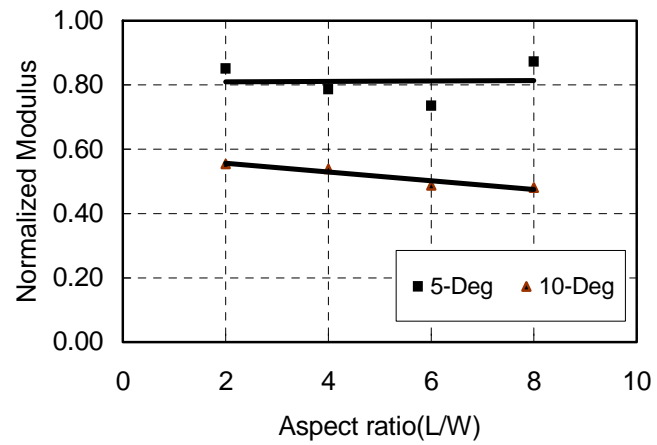


**Fig. 12: Size effect on tensile modulus of CFRP laminate**

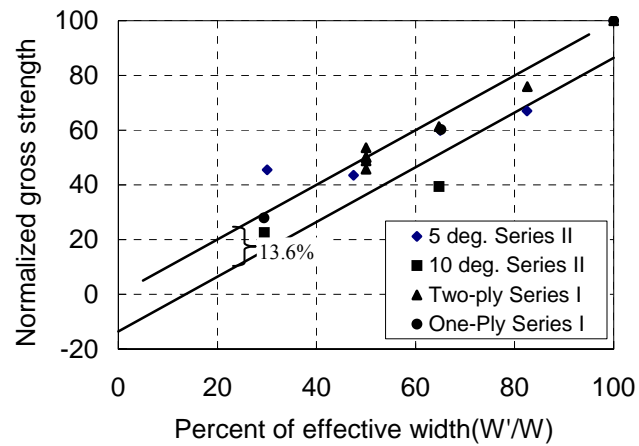


**Fig. 13: Normalized gross strength vs. percent of effective width of all specimens**

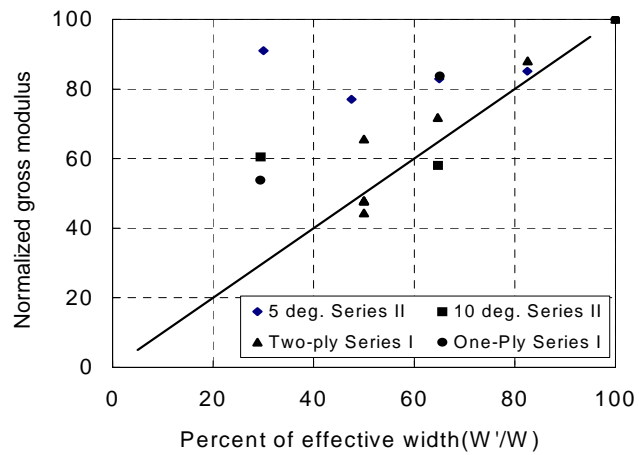


**Fig. 14: Normalized gross modulus vs. percent of effective width of all specimens**

# Concrete Beams Strengthened with Misaligned CFRP Laminates

XINBAO YANG

Research Assistant, Department of Civil Engineering, University of Missouri-Rolla,  
Rolla, MO 65409, USA

ANTONIO NANNI

V. & M. Jones Professor, Department of Civil Engineering, University of Missouri-Rolla,  
Rolla, MO 65409, USA.

## ABSTRACT

A unidirectional carbon fiber reinforced polymer (CFRP) laminate has its maximum strength and stiffness in the fiber direction. However, misalignment of fibers can be introduced intentionally or unintentionally during design or construction of structures. In this paper, the effect of fiber misalignment on the performance of concrete beams strengthened with CFRP laminates is experimentally investigated. Five unreinforced concrete Tee beams were cast and strengthened with CFRP laminates. The laminates had an off-axis angle of 0, 2, 5, 8, and 10°, respectively. The beams were tested under four-point loading to total failure. The objectives of this research were to investigate (1) strength and stiffness of beams, (2) strain distribution of CFRP laminates and, (3) failure modes. It was found that the variation of beam capacity with the severity of misalignment showed a different trend from that of midspan deflection and that failure by rupture of the CFRP laminate was experienced by all beams. A bond length of 127 mm was sufficient to develop the strength of the CFRP laminate.

## INTRODUCTION

Composite materials are generally applied in the optimal direction so their performance (stiffness and strength) can be well developed. However, it is unavoidable that FRP may not be applied in the exact direction as expected and some misalignment may exist. The misalignment can be introduced unintentionally by errors in design and construction or intentionally by the restriction in the structure's geometry. Because FRP laminates are orthotropic materials, the maximum stiffness and strength are exhibited along the fiber direction. Any deviation from this direction will cause strength and stiffness degradation. The influence of this degradation needs to be investigated to obtain an accurate evaluation of the performance of strengthened structures. The ultimate goal of this investigation is that the effect of misalignment on stiffness and strength degradation be implemented into design and analysis. M'Bazaa(1996) tested three RC beams strengthened with two symmetric misaligned CFRP plies and one CFRP ply in the direction of the longitudinal axis of the beam. The results indicated that the strength and deflection did not change significantly compared with the beams strengthened with three CFRP plies having fibers applied with the longitudinal beam axis. There is no other literature available on the subject.

In this paper, five 1.22 m plain concrete beams were constructed and strengthened with one ply of misaligned CFRP laminate. The beams had a saw-cut crack at the midspan of the tension face and a fixed hinge was installed at the midspan of the compression face. After cracking of concrete at the center, only the CFRP laminate sustained the tension force, which allowed to investigating the performance of the laminate, to determine the strain distribution, and to identify the effective bond length.

Before testing the concrete beams, CFRP laminate coupons consisting of one and two-ply were tested to investigate the strength and stiffness degradation with misalignment. All coupon specimens had an aspect ratio of 4 and a width of 38 mm. The specimens were tabbed at both ends and tested in an MTS 880 testing machine. For the two-ply laminates, one ply was oriented in the loading direction and the other ply was oriented at angles ranging from a minimum of 0-deg to a maximum of 90-deg. Coupon size effect on the strength and stiffness of misaligned CFRP laminates was addressed by making samples with the same width but different aspect ratios ranging from 2 to 8 until no through fibers existed between end tabs (Yang *et al.* 2000). This paper only reports part of the results of the entire project.

## EXPERIMENTAL PROGRAM

### Material Properties

The design properties of carbon fiber and saturant are listed in Tables 1 and 2 as provided by the manufacturer (MBrace, 1998).

The CFRP system was applied to the beam tension surface with a hand lay-up technique according to the procedure specified by the manufacturer. After the concrete surface was sandblasted and cleaned by pressure air, a thin layer of primer was applied to the surface using a roller. Following the application of the primer, putty was applied to the areas with small holes in order to smooth the concrete surface. Then the first layer of saturant and fiber ply were applied when the primer was still sticky. After smoothing the ply into the saturant with a nap roller, a second layer of saturant coat was applied to obtain thorough epoxy impregnation.

Table 1 Mechanical properties of CF130 tow sheet

Ultimate strength	4275 MPa (4525 MPa *)
Design strength	3790 MPa
Yielding modulus	228 GPa (264 GPa *)
Ultimate strain	0.017 mm/mm

\* results from coupon tests (Yang *et al.* 2000)

Table 2 Mechanical properties of MBrace saturant

Maximum stress	55 MPa
Maximum strain	0.03 mm/mm
Yielding strain	0.025 mm/mm
Modulus of elasticity	30 GPa

Concrete cylinders were tested showing concrete strength of 24.96MPa to 38.24MPa. Miller (1999) indicated that concrete strength does not play a critical role on bond strength of CFRP laminates on concrete and only affects the cracking load. The ultimate load was controlled by the CFRP strength and bond strength. This conclusion was justified by the results of current research, where all beams experienced the same failure by rupture of the CFRP laminate regardless of concrete strength.

### Specimens and Test Setup

Five plain concrete inverted Tee beams were constructed with dimensions as shown in Figure 1. A 51mm-deep artificial crack was cut at the center of the tension face. A steel hinge was installed into a 51mm-deep saw-cut groove at the center point of the top compression surface. After cracking of the beam, the force was sustained by the CFRP laminate only to facilitate the evaluation of the bond characteristics between CFRP laminate and concrete substrate. After cracking, a constant moment arm of 222 mm was produced from the center of steel hinge to the CFRP laminate.

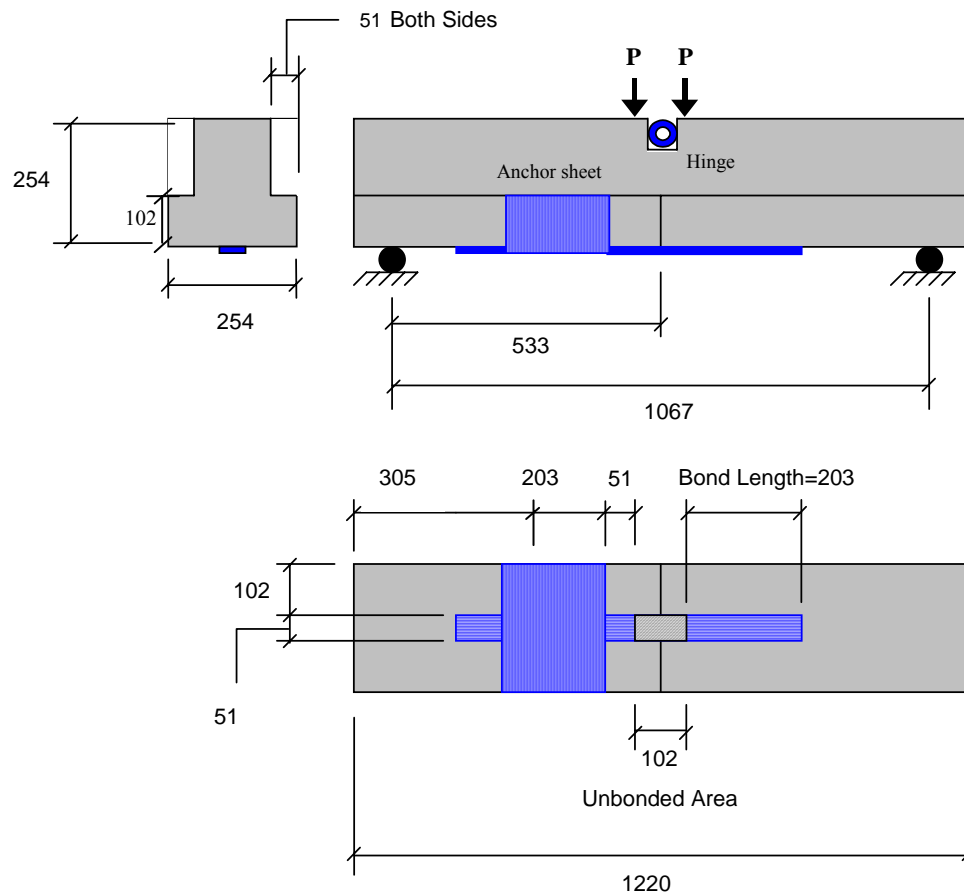


Fig. 1 Specimen and strengthening (Unit: mm)

The bond length of the CFRP laminate was 203 mm. There was an unbonded area of 51 mm at both sides of the artificial crack to prevent stress concentration at the center point. A 203 mm wide lateral anchor laminate was installed at one end of the beam to force failure of the opposite side.

The beam was tested under four-point loading. Midspan deflection and strains along the fiber directions were collected with LVDT and strain gauges, respectively. Strain gauges were attached along the fiber direction (Figure 2).

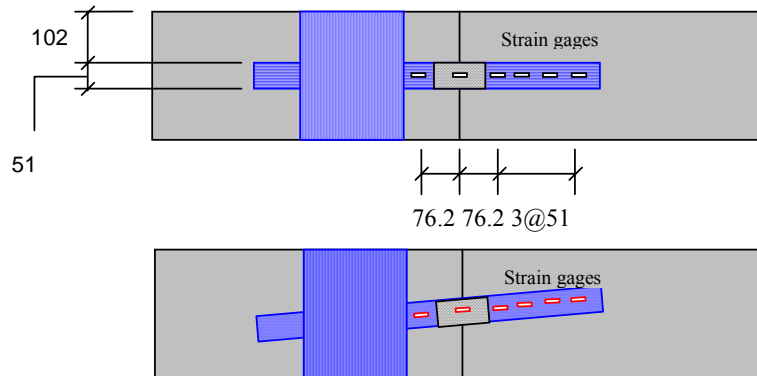


Fig. 2 Strain gage arrangement (Unit: mm)

## TEST RESULTS

### Strength and Deformation

Figure 3 shows the load versus midspan deflection for all five beams. Before cracking, beams had different stiffness and cracking loads due to the different concrete strength. At this stage, the contribution of CFRP is negligible. After cracking, the load decreased with different slopes but converged to a point with a load and deformation of 7.5 kN and 0.7 mm, respectively. The measured strain on the surface of the CFRP laminate within the central unbonded area was around 0.4%. After this point, the response of the beam entered the second stage, when only the CFRP laminate carried the tension force until failure and the compression force acted in the center of the steel hinge.

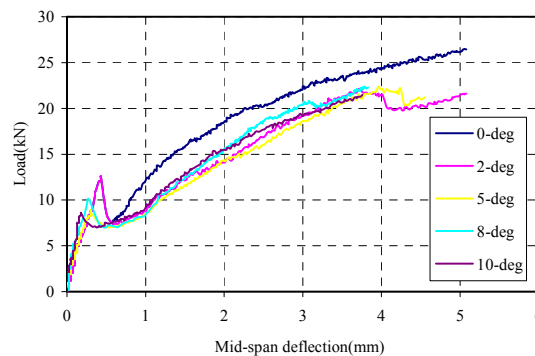


Fig. 3 Load-midspan deflection of all beams

Figure 3 shows that the beam with 0-deg CFRP laminate had a higher ultimate load from the beginning of the second stage while all other four beams did not show much difference in ultimate load and response. The individual ultimate load and midspan deflection are listed in Table 3 and plotted in Figures 4 and 5 versus the misalignment angle. Except for the ultimate load of the 2-deg beam that decreased by 18.2% compared with that of the 0-deg beam, all of the other four beams had a negligible difference in ultimate load. The change of midspan deflection shows a little difference from that of ultimate load. The 0-deg and 2-deg beams had the same maximum deflection. The deflection of the 5-deg beam was only 10.0% less than that of the 0-deg beam. For misalignment angles larger than 5 degree, the midspan deflection decreased significantly. The deflection of 8-deg and 10-deg beams decreased 25.0% compared with the 0-deg beam.

The change of midspan deflection actually reflects the trend of the stiffness degradation of misaligned CFRP laminates from the tensile coupon tests (Yang *et al.* 2000). The modulus of elasticity of 0, 5, and 10-deg coupons and the normalized average modulus of laminates from these beam tests is depicted in Figure 6. When the misalignment angle is less than 5 degree, the modulus of elasticity does not degrade. After the angle exceeds 5 degree, the modulus degrades rapidly. The modulus degradation of CFRP laminates shows the same trend of the coupon tests.

Table 3 Ultimate load and deflection of all beams

Angle (deg)	Ultimate load (kN)	Maximum midspan deflection (mm)
0	26.43	5.10
2	21.62	5.10
5	21.23	4.55
8	22.27	3.84
10	21.48	3.76

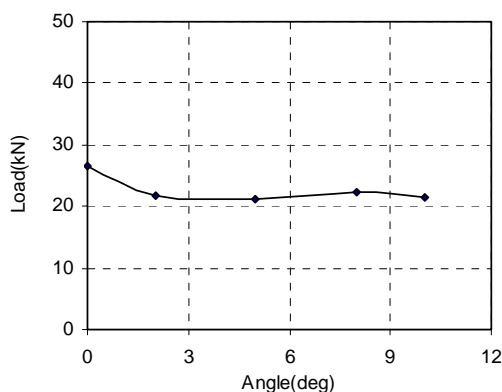


Fig. 4 Degradation of ultimate load deflection

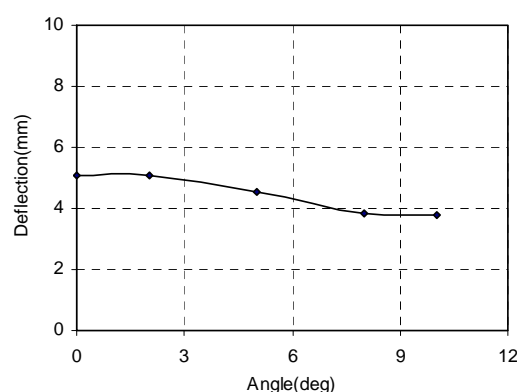


Fig. 5 Degradation of midspan

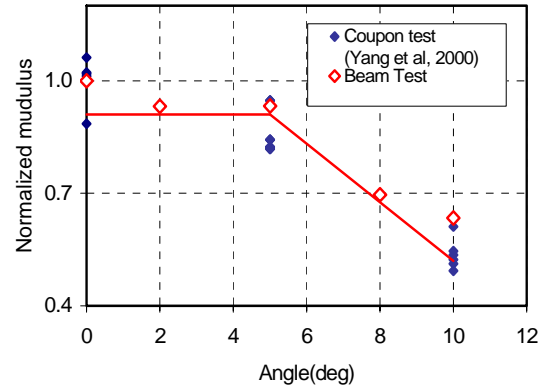


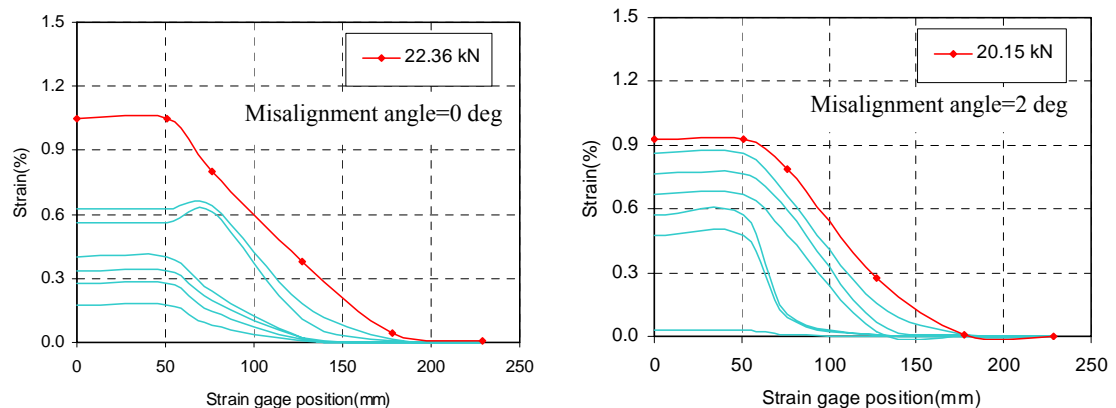
Fig. 6 Modulus degradation of tensile coupons and beams

### Strain Distribution and Failure Modes of CFRP Laminates

Figure 7 shows the typical strain distribution for CFRP laminates along the fiber direction. The strain gage positions were measured from the center of the beam, which is also the center of the unbonded area. It is assumed that the strain in the laminates within the unbonded area is constant.

Figure 7 also shows that the effective bond length of CFRP laminate when delamination first occurred is independent of other parameters such as concrete strength and surface condition. All five beams have an effective bond length of 127 mm.

All beams failed with rupture of CFRP laminate within the delaminated area. Figure 8 shows that the CFRP laminate of the 0-deg beam pulled off less concrete and had a smoother surface than that of the CFRP laminate of 10-deg beam.



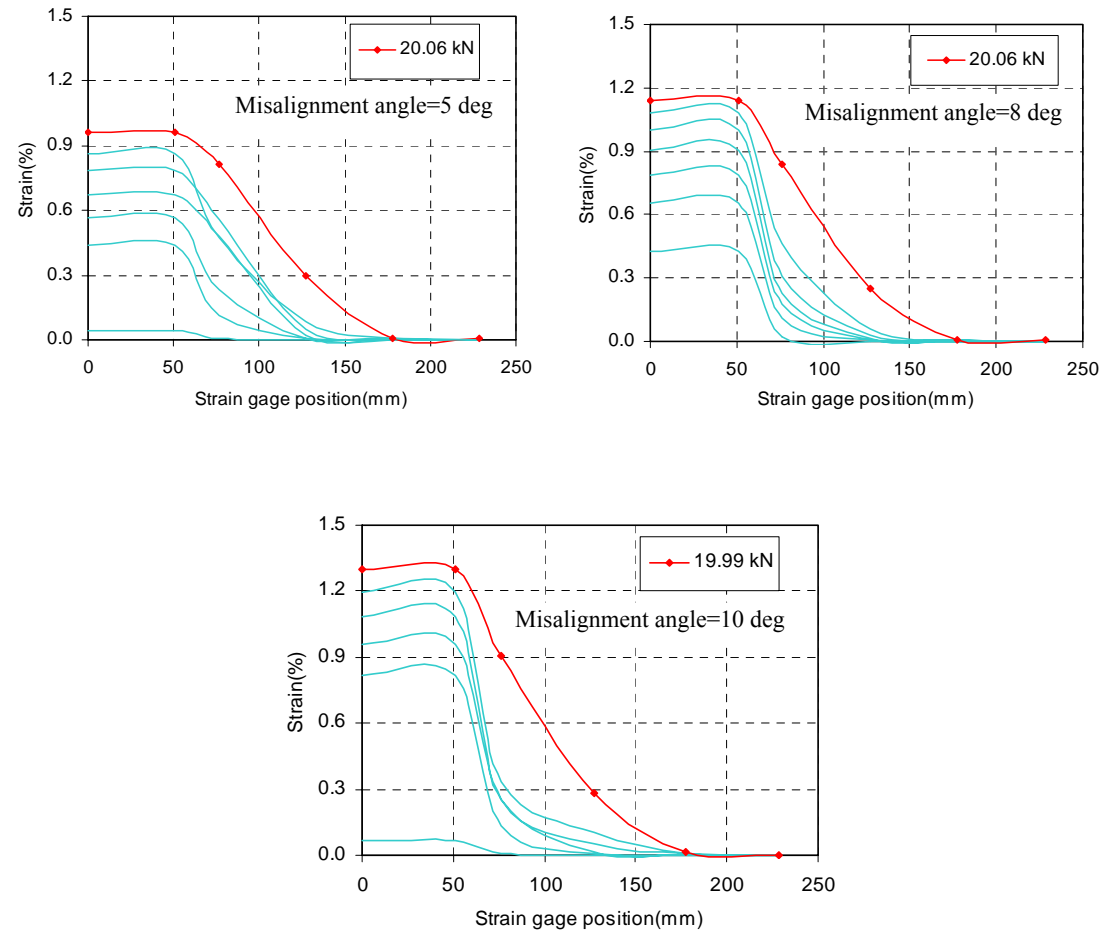


Fig. 7 Strain distribution of all beams

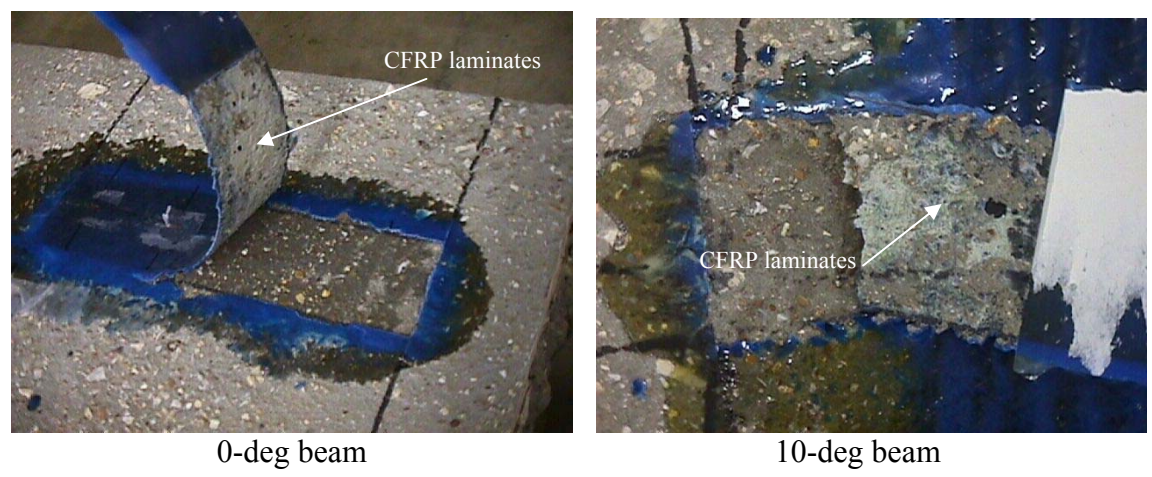


Fig. 8 Delamination of CFRP laminates

## CONCLUSIONS

Based on the experimental investigation of concrete beams strengthened with misaligned CFRP laminate, the following conclusions can be reached.

- The change of strength and deformation with misalignment shows different trends. When the misalignment angle is small (less than 5 degree), the strength of the beam is not affected. The deformation decreases very slowly at first, and then more rapidly with increasing misalignment, which agrees with the stiffness degradation of CFRP laminate with misalignment.
- Rupture of CFRP laminates is the controlling failure mode if the concrete surface is properly prepared. Delamination occurs in the CFRP laminates but it is not the controlling failure mode.

## ACKNOWLEDGEMENT

The Federal Highway Administration is gratefully acknowledged for financially supporting this research. The research was undertaken in the Center for Infrastructure Engineering Studies at University of Missouri-Rolla. The authors want to thank Jeff Bradshaw and Steve Haug for their contributions to the experimental work.

## REFERENCES

1. M'Bazza, I., Missihoun, M. and Labossiere, P. (1996), "Strengthening of Reinforced Concrete Beams with CFRP Sheets". *Proc. 1<sup>st</sup> Conference on Composites in Infrastructure*; Ed., Saadatmanesh, H. and Ehsani, M. R., Tucson, AR, USA, pp 746-759.
2. MBrace<sup>TM</sup> (1998), Composite Strengthening System, Engineering Design Guidelines, 2<sup>nd</sup> Edition, Master Builders, Inc., Cleveland, OH, pp 109.
3. Miller, B. D. (1999), Bond Between Carbon Fiber Reinforced Polymer Sheets and Concrete, MS thesis, Department of Civil Engineering, University of Missouri-Rolla.
4. Yang, X. B, Nanni, A., Haug, S. and Sun C. L. (2000), "Strength and Modulus Degradation of CFRP Laminates from Fiber Misalignment", *J. Mat. Civil Engrg*, ASCE.(accepted)

## **EFFECT OF FIBER MISALIGNMENT ON FRP LAMINATES AND STRENGTHENED CONCRETE BEAMS**

Xinbao Yang  
Research Assistant, Department of Civil  
Engineering, University of Missouri-Rolla  
Rolla, MO 65409, USA

Antonio Nanni  
V. & M. Jones Professor, Department of  
Civil Engineering, University of Missouri-  
Rolla  
Rolla, MO 65409, USA

Lokesh Dharani  
Associate Dean of Engineering School  
Professor of Engineering Mechanics  
University of Missouri-Rolla  
Rolla, MO 65409, USA

**KEYWORDS:** FRP laminates, concrete beams, fiber misalignment, modulus of elasticity, strength

### **ABSTRACT**

Fiber misalignment can be accidentally introduced during lay-up installation when fiber reinforced polymer (FRP) materials are employed to strengthen structures. In this paper, the effect of misalignment on the performance of concrete beams is investigated. First, tension tests were performed on coupon type specimens to address the degradation of strength and stiffness as a function of fiber misalignment and specimen size. Then, verification tests were conducted on concrete beams strengthened with CFRP laminates on the tension surface with an off-axis angle of 0, 2, 5, 8, and 10° to the longitudinal axis of the beams. The beams were tested to failure under four point loading. The objectives of this research were to investigate: (1) the strength and stiffness degradation of CFRP laminates with fiber misalignment. (2) the performance of beams externally reinforced with misaligned CFRP laminates. As for the tensile coupon tests, it was found that the capacity of the beams does not show much degradation when the misalignment is less than 10°. The stiffness showed significant degradation when the misalignment angle exceeds 5°. Rupture of the CFRP laminate was experienced by all beams.

### **INTRODUCTION**

Fiber reinforced polymer (FRP) laminates have been used extensively in the past decade as externally bonded reinforcement for the upgrade of reinforced concrete (RC) and prestressed concrete (PC) structures (Nanni and Dolan 1993, Taerwe 1995, Ueda et al. 1997, Dolan et al. 1999). The majority of this work has been conducted with composites installed by the manual lay-up technique. Experimental investigations of RC and PC members strengthened with FRP have shown satisfactory performance in both strength and ductility or other special requirements. When FRP laminates are intended for strengthening, the analysis and design of the member can be performed under the conventional principles of RC and PC theory based on assumed material properties (Saadatmanesh and Malek 1998, Nanni et al. 1998). Typically, the material properties used for FRP are those provided by manufacturers and are based on tensile tests of

“perfect” coupons (Hamada et al. 1997). Obviously, there are concerns about the performance of a structural member when errors in installation may result in fiber misalignment. Depending on the severity of the fiber misalignment, the difference between actual strength and stiffness of the FRP from the assumed nominal values may become unacceptable or, at least, warrant a reduction of performance expectations.

An experimental investigation on the effect of fiber misalignment on strength and stiffness degradation is crucial for the successful use of FRP in the upgrade of the concrete built infrastructure. The results of such an investigation should be implemented into corresponding construction and design specifications for guidance in field practice. In this paper, experimental results of coupon tests for misaligned carbon FRP laminates and concrete beams strengthened with misaligned CFRP laminates are reported. Two issues were addressed by the tests, namely: the degradation of strength and stiffness as a function of the misalignment angle for one-ply CFRP laminates and its effect on flexural members.

## TEST SPECIMENS

### Material Properties

High tensile strength, unidirectional carbon tow sheets (MBrace 1998) were used for the tensile coupon specimens and to strengthen the scaled concrete beams. The carbon tow sheets were impregnated using the two-part epoxy polymer saturant provided by the manufacturer. The guaranteed mechanical properties of the CFRP laminate as per manufacturer’s literature are listed in Table 1. It is to be noted that in this table, as for the rest of the paper, the FRP mechanical properties are based on fiber cross sectional area rather than composite area. The carbon fiber thickness for one ply,  $t$ , is 0.165 mm. This is due to the following reasons: a) in manual lay-up fabrication, it is rather difficult to control the amount of resin being used; b) small variations in the amount of resin, provided that the fibers are fully impregnated, do not affect the composite mechanical performance; and c) resin mechanical properties are significantly lower than those of fibers.

Table 1: Manufacturer provided CFRP properties

Ultimate strength (MPa)	4275
Design strength (MPa)	3790
Tensile modulus (GPa)	228
Ultimate strain (mm/mm)	0.017

### Coupon Specimens

Coupon specimens used were cut from CFRP laminate panels. Two series of coupon specimens were made and all specimens had the same width of 38.1 mm. To provide appropriate anchorage during testing, rectangular aluminum tabs were used at both ends of each specimen (Figure 1). During testing, only the initial 38.1 mm in the longitudinal direction of the tabs was held by the grips of the testing machine. This was intended to further reduce the stress concentration at the onset of the specimen gage length as compared to the case of tabs totally clamped by the grips (Figure 2). For coupon specimens Series I, six misalignment angles were investigated in addition to perfectly

aligned fibers; the angles were 5, 10, 15, 20, 30, and 40°. Five identical specimens were tested for each case and the aspect ratio for these specimens was 4.0.

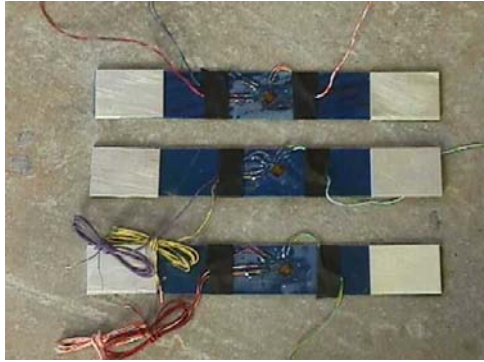


Figure 1 CFRP coupon specimens



Figure 2 Specimen in the testing machine

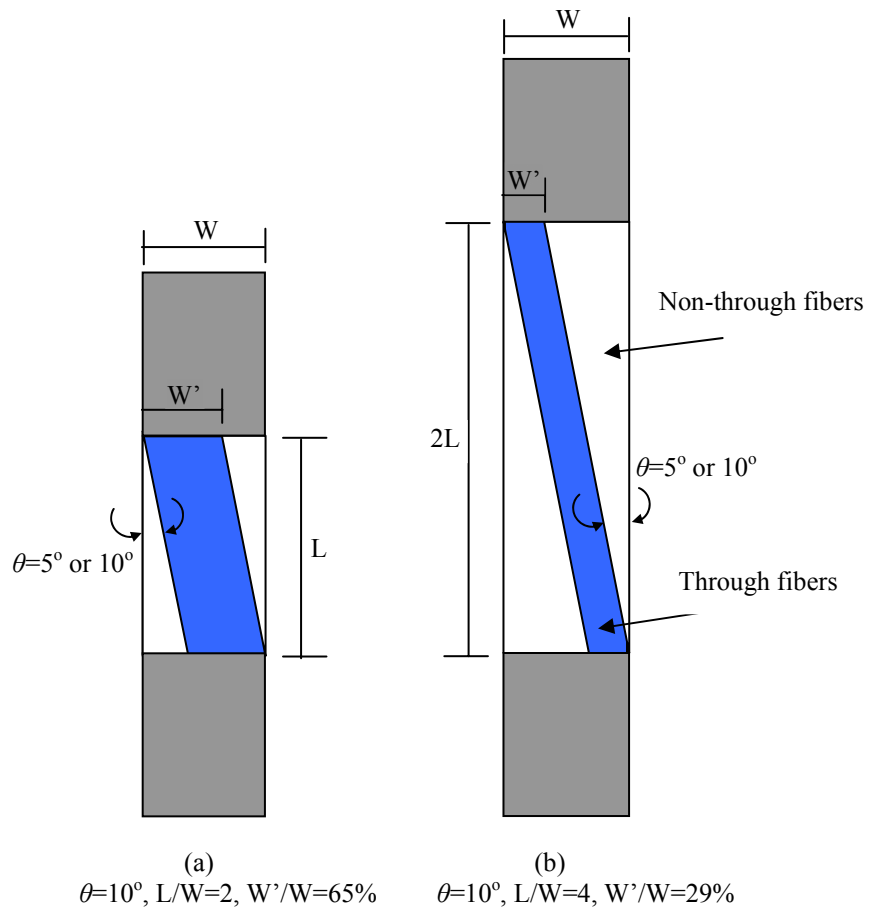


Figure 3 Width of through fibers of misaligned CFRP laminates  
( $\theta=10^\circ$ ,  $L/W=2$  or  $L/W=4$ )

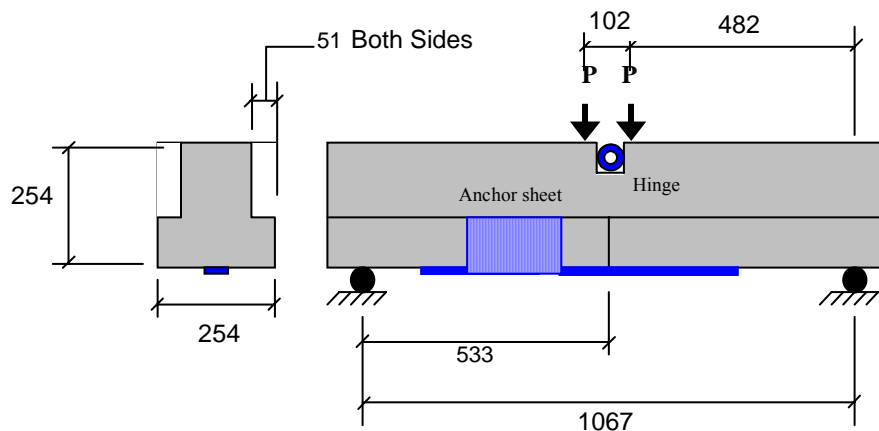
In real cases, even though some misalignment exists in FRP laminates, all fibers are continuous. But for coupon specimens with finite width,  $W$ , length,  $L$ , and misalignment angle,  $\theta$ , not all fibers can be continuous from end to end of the specimen. The width of continuous or “through” fibers,  $W'$ , is clearly shown in Figure 3. This figure shows the relevance of the specimen aspect ratio for the case of  $\theta = 10^\circ$ . When  $L/W = 2$  only 65% of the fiber area is continuous from end to end; if  $L/W = 4$ , then that area becomes 29%. Obviously, the larger the aspect ratio (and the misalignment angle), the smaller is the percentage of the through fibers. For specimens Series II, the misalignment angle was  $\theta = 5^\circ$  or  $10^\circ$ , with aspect ratios ranging from 2 to 8.

Strain gages were attached to the surface of the specimens of Series I and II to record strain in the longitudinal and transverse directions. In this paper, only the strain measurements recorded by gages applied along the centerline of the coupon in the direction of the load application are reported. For Series I readings, the gage of reference was that applied at mid height (center point, CP). For Series II readings, one additional gage located at quarter length (quarter point, QP) is monitored.

### Scaled Concrete Beams

To verify the testing results and findings from the coupon tests, five plain concrete inverted Tee beams were constructed with dimensions given in Figure 4. An artificial crack of 51 mm in depth was cut at the center of the tension face. A steel hinge was installed into a 51 mm-deep molded groove at the center point of the top compression surface (Figure 4). After cracking of the beam at the center span, a constant moment arm of 222 mm was produced from the center of the steel hinge to the CFRP laminate.

The bonded length of the CFRP laminate was 203 mm. There was an unbonded area of 51 mm at both sides of the precut to prevent stress concentration. A 203 mm wide transverse anchor laminate was installed at one end to force potential delamination to one side of the specimen.



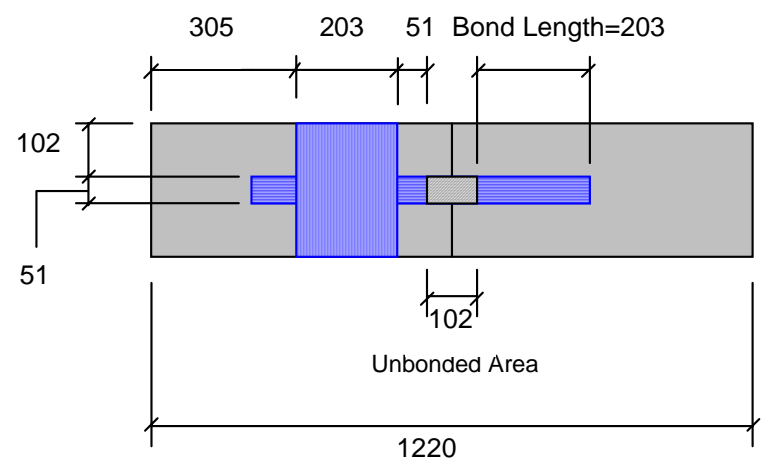


Figure 4 Design of beams and CFRP system(mm)

Concrete strength of the beams cast in different pours varied between 25.0 and 38.2 MPa. This variation only affected the cracking load but was not expected to influence the quality of the concrete-FRP bond (Miller, 1999).

Each beam was tested under four-point loading. After cracking, the specimens had constant moment arm and shear span of 222 and 483 mm, respectively. Midspan deflection and strains along the fiber directions were monitored using LVDT and strain gages, respectively. All strain gages were attached along the fiber direction for both 0-deg and misaligned CFRP laminates (Figure 5).

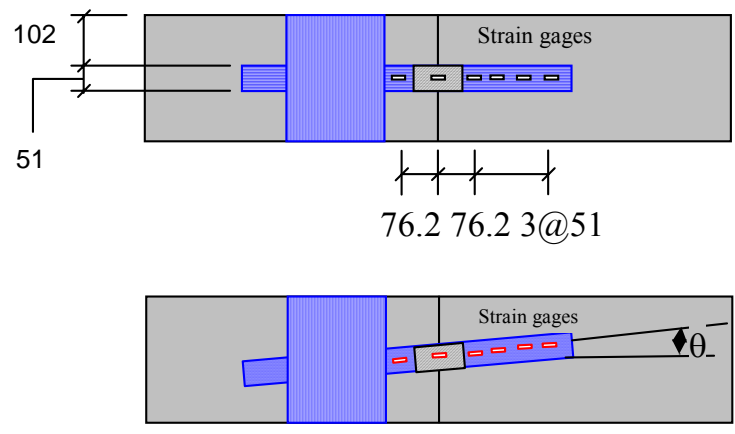


Figure 5 Strain gage arrangement(mm)

### TEST RESULTS

#### Coupon Tensile Specimens

Figure 6 shows representative stress-strain diagrams obtained from specimens of Series I. The stress of the laminate as plotted is based on the assumption that the load was solely

carried by fibers and is computed as a nominal gross value based on load divided by gross fiber area ( $t \times W$ ). The stress-strain curve is almost a perfect line for specimens with  $\theta = 0^\circ$  or  $\theta = 15^\circ$  and higher. These are the perfectly aligned fiber specimen and the ones with no through fibers. For specimens with  $\theta = 5$  and  $10^\circ$ , the diagram shows a sudden drop at a strain value of approximately 0.007 mm/mm, signaling partial failure.

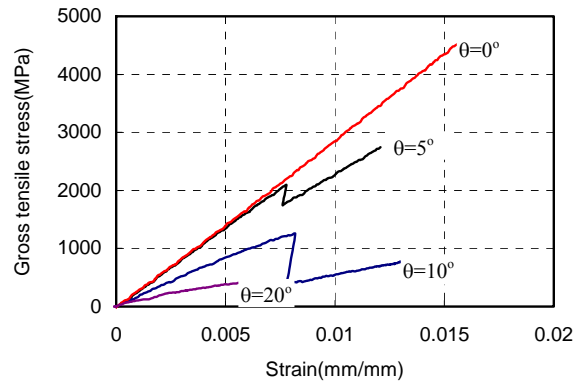


Figure 6 Stress-strain curves of one-ply specimens

A summary of strength and stiffness results for Series I is shown in Table 2. Two values of strength are reported:  $f_g$  is the gross strength based on load divided by gross fiber area ( $t \times W$ ), and  $f_t$  is the strength of through fibers based on load divided by through fiber area ( $t \times w$ ). The elastic modulus  $E_g$  is calculated from the gross stress and strain values, with the latter measured at the center point along the gage length of specimens.  $E_g$  is obtained by fitting the best straight line for given experimental data and calculating the slope of such line. It is to be noted that, for specimens with misalignment angles of  $5^\circ$  and  $10^\circ$ ,  $E_g$  refers to the slope of the first leg of the stress-strain curve prior to the stress drop.

Table 2 Strengths and moduli of specimens Series I

Angle (deg.)	W (mm)	W' (mm)	Properties based on w				Properties based on w'	
			$E_g$ (GPa) [std]*	Normalized $E_g$	$f_g$ (MPa) [std]*	Normalized $f_g$	$f_t$ (MPa) [std]*	Normalized $f_t$
0	38.1	38.1	264 [18]	1.00	4323 [172]	1.00	4323 [172]	1.00
5		24.8	221 [18]	0.84	2603 [254]	0.60	4004 [391]	0.93
10		11.2	142 [11]	0.54	1210 [80]	0.28	4106 [272]	0.95
15		0	88 [7]	0.33	586 [117]	0.14	-	-
20		0	58 [7]	0.22	396 [57]	0.09	-	-
30		0	33 [6]	0.12	261 [21]	0.06	-	-
40		0	27 [2]	0.10	116 [8]	0.03	-	-

Note \* = Standard deviation based on 5 repetitions

Average gross and through strengths, and elastic modulus of all specimens in Series I are normalized with respect to the values of the specimens with perfectly aligned fibers (i.e.  $0^\circ$ ) and reported in Table 2. Normalized individual (not average) specimen strengths and moduli are plotted in Figures 7 and 8 for all specimens of Series I as a function of the misalignment angle. In this paper, no specific consideration is made with respect to the statistical significance of the experimental work; however, the data plotted in these figures show a remarkable repeatability as also indicated by the standard deviation values on strength and stiffness shown in Table 2.

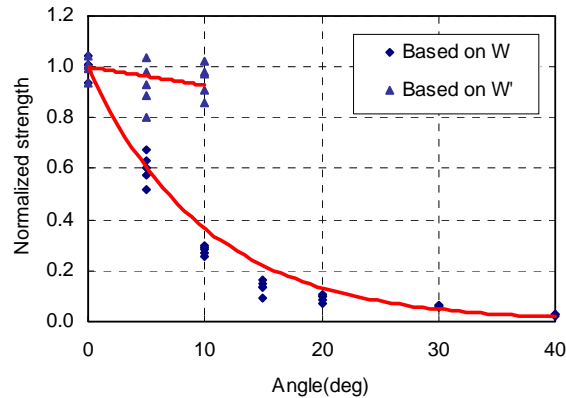


Figure 7 Normalized strength of one-ply specimens

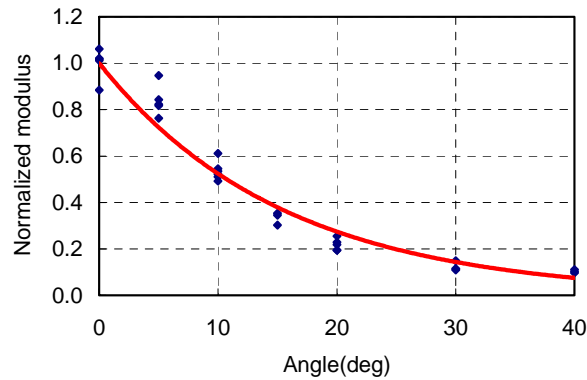


Figure 8 Normalized modulus of one-ply specimens

The gross strength,  $f_g$ , and elastic modulus,  $E_g$ , for specimens of Series II are calculated as described previously and reported in Tables 3 and 4. Two specimens were tested for each aspect ratio. The aspect ratios ranged from 2 to 8. All individual strengths and moduli are listed in Tables 3 and 4 including the modulus calculated using the strain of the quarter point of the centerline of specimen-2. The tables also report the values of through fiber width,  $W'$ , corresponding to each aspect ratio.

The average strength and modulus are normalized using the strength and modulus of the one-ply, perfectly aligned fiber specimens with an aspect ratio of 4, in order to allow for

consistent comparisons. The normalized average strength and modulus are shown as a function of the aspect ratio in Figures 9 and 10, respectively.

Table 3 Variation of strengths and moduli with aspect ratio  
(misalignment angle  $\theta = 5^\circ$ , width  $W = 38.1$  mm)

Aspect ratio L/W	2	4	6	8
W' (mm)	31.4	24.8	18.1	11.4
Strength $f_g$ (MPa)				
Specimen-1	3141	2610	1798	2039
Specimen-2	2655	2570	1961	1890
Modulus $E_g$ (GPa)				
CP of specimen-1	225	194	225	250
CP of specimen-2	252	247	187	239
QP of specimen-2	197	216	198	232

Table 4 Variation of strengths and modulus with aspect ratio  
(misalignment angle  $\theta = 10^\circ$ , width  $W = 38.1$  mm)

Aspect ratio L/W	2	4	6	8
W' (mm)	24.7	11.2	0	0
Strength $f_g$ (MPa)				
Specimen-1	1752	1132	950	727
Specimen-2	1651	-	746	758
Modulus $E_g$ (GPa)				
CP of specimen-1	144	146	137	132
CP of specimen-2	167	156	136	137
QP of specimen-2	149	177	146	129

Note: CP = center point, and QP = quarter point of the longitudinal centerline refer to the position of the strain gage

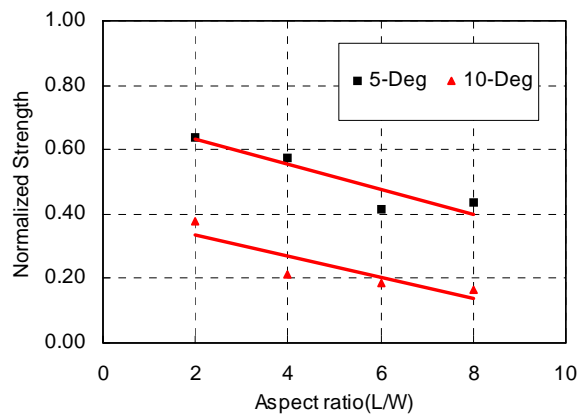


Figure 9 Size effect on strength of CFRP laminate

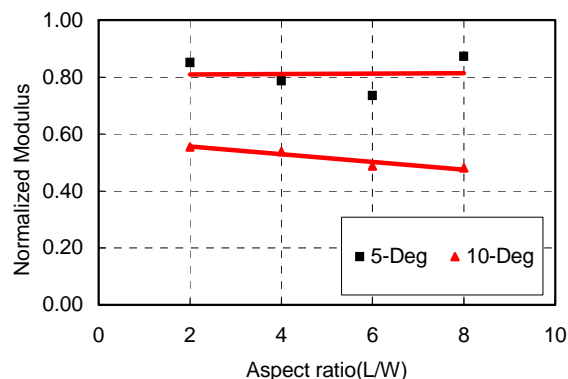


Figure 10 Size effect on tensile modulus of CFRP laminate

### Scaled Concrete Beams

#### *Strength and Deflection*

Figure 11 shows the load versus midspan deflection relationship of all five beams. It is shown that, before cracking, beams had different behavior due to the different concrete properties. After cracking, the load decreased with different slopes but converged to a point with a load and deflection of 7.5kN and 0.7 mm, respectively. The measured strain on the surface of CFRP laminate within the center unbonded area is around 0.4%. After this point, the response of beams entered the second stage, when only CFRP laminate carried the tension force until failure and the compression force acted in the center of the steel hinge.

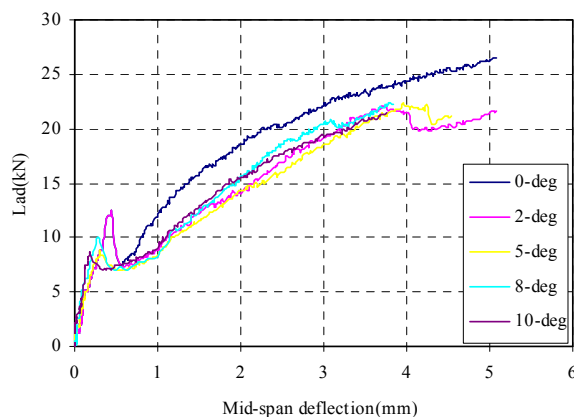


Figure 11 Load-midspan deflection of all beams

It can be seen from Figure 11 that the beam with 0° CFRP laminate shows a better response from the beginning of the second stage, while all other beams have similar behavior. The individual ultimate load and midspan deflection are listed in Table 5 and plotted in Figures 12 and 13 against the misalignment angle. The change of midspan deflection shows a little difference from that of ultimate load. The 0° and 2° beams have the same maximum deflection. The deflection of the 5° beam was 10.0% less than that of the 0° beams. For misalignment angles larger than 5°, the midspan deflection decreased

faster. The deflection of 8° and 10° beams decreased 25.0% compared with that of the 0° beam.

Table 5 Ultimate load and deflection of all beams

Angle (Deg)	Ultimate load (kN)	Maximum midspan deflection (mm)
0	26.43	5.10
2	21.62	5.10
5	21.23	4.55
8	22.27	3.84
10	21.48	3.76

The change of midspan deflection actually reflects the trend of the stiffness degradation of misaligned CFRP laminates from the coupon tensile tests (Yang et al. 2000). The modulus of elasticity of 0, 5, and 10° coupons normalized by corresponding average value and the normalized average modulus of laminates from these beam tests is depicted in Figure 14. When the misalignment angles are less than 5 degree, the modulus of elasticity of misaligned CFRP laminates does not degrade significantly. But after the angle exceeds 5 degree, the modulus degrades rapidly. The modulus degradation of CFRP laminates shows the same trend as that from coupon tests.

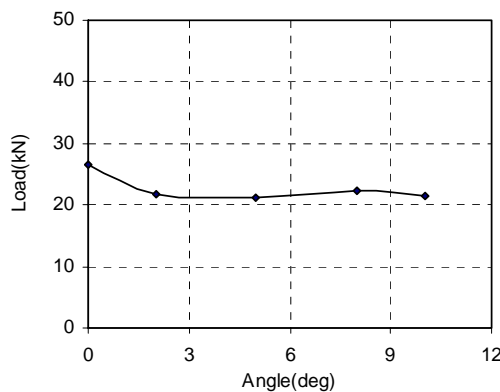


Figure 12 Change in of ultimate load

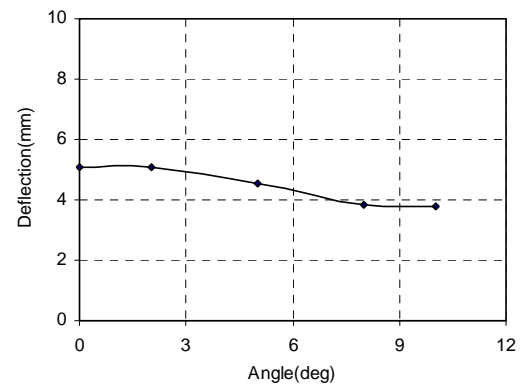


Figure 13 Change in midspan deflection

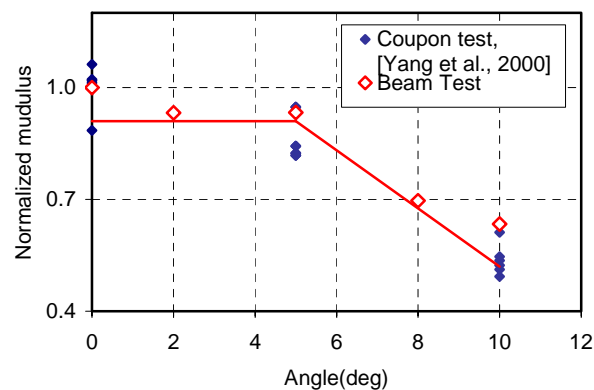


Figure 14 Modulus degradation of CFRP laminate

### Strain Distribution and Failure Mode

The strain gage positions are relative to the center of the beam, which is also the center of the unbonded area. It is assumed that the strain at any point within the unbonded area is equal. Figure 15 shows the typical strain distribution on the surface of CFRP laminates along the fiber direction for increasingly applied load levels.

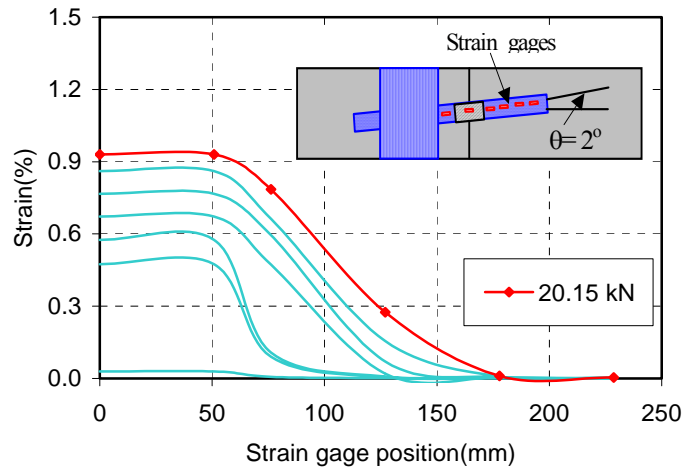


Figure 15 Strain distribution of all beams

All beams failed with rupture of CFRP laminate with some delamination from the substrate concrete surface. The delamination length varied for different beams. For  $0^\circ$  and  $2^\circ$  beam, it was 127 mm and 90 mm, respectively. The delamination length is less than 25 mm for all other beams (Figure 16).

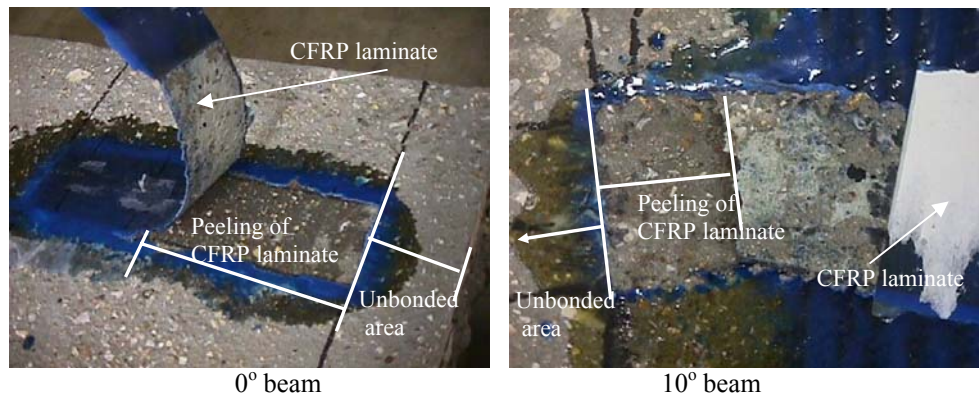


Figure 16 Delamination of CFRP laminates

### CONCLUSIONS

Based on the results of this investigation on the strength and modulus degradation of misaligned CFRP laminates and the beams strengthened with misaligned CFRP laminates, the following conclusions can be reached:

1. Strength more than elastic modulus is affected by fiber misalignment.

2. When the misalignment angle is small (less than  $5^\circ$ ), the capacity of the beams strengthened with misaligned CFRP laminates does not change significantly.
3. Flexural stiffness showed significantly degradation when the misalignment angle exceeds  $5^\circ$ .
4. Rupture of CFRP laminate was the controlling failure mode for all beams.
5. Findings from coupon tensile specimens on the properties of misaligned CFRP laminates agree with that from beam tests.

#### ACKNOWLEDGEMENT

The Federal Highway Administration is gratefully acknowledged for financially supporting this research under contract DTFH 61-00X-00017. The research was undertaken in the Center for Infrastructure Engineering Studies at University of Missouri-Rolla. The authors wish to thank Mr. Jeff Bradshaw, PE, for his contributions to the experimental work.

#### REFERENCES

1. Dolan, C.W., Rizkalla, S.H., and Nanni, A., (1999), "Fiber Reinforced Polymer Reinforcement for Reinforced Concrete Structures," FRPRCS-4, *Proc. 4<sup>th</sup> Int. Symposium*, Baltimore, MD, SP-188, American Concrete Institute, Farmington Hills, MI, 1181 pp.
2. Hamada, H., Oya, N., Yamashita, K., and Maekawa, Z.-I. (1997), "Tensile Strength and Its Scatter of Unidirectional Carbon Fiber Reinforced Composites", *Journal of Reinforced Plastics and Composites*, 16(2), pp119-130.
3. MBrace<sup>TM</sup> (1998), "Composite Strengthening System, Engineering Design Guideline", 2<sup>nd</sup> Ed., Structural Preservation Systems, Inc., Cleveland, OH, pp109.
4. Miller, B. D. (1999), Bond between Carbon Fiber Reinforced Polymer Sheets and Concrete, MS thesis, Department of Civil Engineering, University of Missouri-Rolla, pp135.
5. Nanni, A. and C.W. Dolan, Editors, (1999), Fiber Reinforced-Plastic Reinforcement of Concrete Structures - International Symposium, ACI Special Publication No. 138, American Concrete Institute, Detroit, MI, 1993, pp988.
6. Nanni, A., F. Focacci, and C.A. Cobb, (1998), "Proposed Procedure for the Design of RC Flexural Members Strengthened with FRP Sheets," *Proc., ICCI-98*, Tucson, AZ, Vol. I, pp187-201.
7. Saadamanesh, H. and Malek, A. M. (1998), "Design Guideline for Flexural Strengthening of RC Beams with FRP Plates", *Journal of Composites for Construction*, ASCE, 2(4), pp158-164.
8. Taerwe, L., ed., (1995), "Non-Metallic (FRP) Reinforcement for Concrete Structures," Proceedings of the Second International RILEM Symposium (FRPRCS-2), Ghent, Belgium, pp714.
9. Ueda, T., Nakai, H., and Tottori, S. (1997), "JCI State-of-the-Art Report on Retrofitting by CFRM-Guidelines for Design, Construction and Testing", FRPRCS-3, *Proc. 3<sup>rd</sup> Int. Symposium*, Sapporo, Japan, Vol. I, pp621-628.
10. Yang, X. B., Nanni, A., Haug, S. and Sun C. L. (2000), "Strength and Modulus Degradation of CFRP Laminates from Fiber Misalignment," *J. Mat. Civil Engrg., ASCE*. (Accepted)

# Effect of Corner Radius on the Performance of Externally Bonded FRP Reinforcement

XINBAO YANG

Research Assistant, Department of Civil Engineering, University of Missouri-Rolla, Rolla, MO 65409, USA

ANTONIO NANNI

V. & M. Jones Professor, Department of Civil Engineering, University of Missouri-Rolla, Rolla, MO 65409, USA.

GENDA CHEN

Assistant Professor, Department of Civil Engineering, University of Missouri-Rolla, Rolla, MO 65409, USA.

## ABSTRACT

Externally bonded FRP reinforcement is wrapped around concrete members in order to provide confinement and/or shear strengthening. The need for bending the fibers over the member corners affects the performance of the FRP laminate and the efficiency of its confining/strengthening action. This paper presents an experimental study focusing on the effects of corner radius on FRP mechanical properties. A unique re-usable test device was designed and used for this purpose such that plies of FRP could be applied over interchangeable corner inserts. The radius of the inserts ranged from a minimum of 0 to a maximum of 50.8 mm, and one or two plies of carbon FRP were used. The monitored parameters were strain distribution in the FRP laminate and load. It was found that only a portion of the CFRP laminate capacity was developed when failure occurred at the corner. Increasing the number of plies from one to two slightly improved the efficiency of the laminate.

## INTRODUCTION

Advanced composite materials have been extensively used in the rehabilitation of concrete structural members. One practice is to externally wrap beams and columns with fibers impregnated with a resin-based matrix to increase the strength and deformation performance of the member. For example, FRP jackets may be used to wrap the potential plastic hinge of bridge columns in seismically active regions, where fibers can be regarded as continuously distributed transverse reinforcement. The ultimate strain of concrete and its pseudo-ductility can be significantly increased with negligible cumulative damage to the composite jacket under cyclic loading.

Externally bonded laminates have to be bent when wrapped around columns and beams. Bending affects performance of the FRP laminate and the corresponding confinement action depending on the curvature radius of the corners (Rochettee et al. 2000, Restrepo et al. 2000). In this paper, an experimental investigation was conducted to study the effects of corner radius on the FRP performance. A unique reusable test device was designed for this purpose, around which FRP laminates can be wrapped. By changing its

corner inserts, different curvatures in the laminate can be simulated. A tension test was then performed until failure of the FRP laminate.

## EXPERIMENTAL PROGRAM

### Material Properties

High tensile strength carbon fiber tow sheets (MBrace, 1998) were used and impregnated using a two-part epoxy polymer saturant provided by the manufacturer. The low bound mechanical properties of the resulting CFRP laminate according to manufacturer's literature are listed in Table 1. These properties are determined and the experimental results of this project are analyzed based on the fiber cross sectional area rather than the composite area. This is due to the following reasons: (a) the laminate is fabricated using the manual lay-up technique and it is rather difficult to control the amount of resin; (b) small variations in the amount of resin, provided that the fibers are fully impregnated, do not affect the composite mechanical performance, and (c) mechanical properties of the resin are significantly lower than those of fibers.

Table 1: Manufacturer provided CFRP properties

Ultimate strength (MPa)	4275
Design strength (MPa)	3790
Tensile modulus (GPa)	228
Ultimate strain (mm/mm)	0.017

### Design of Test Specimen

In order to simulate the force transfer mechanism of FRP wrapping a cross section via running tension test, a unique reusable test device is designed and manufactured based on the following considerations: (a) the mechanical interaction between FRP laminate and device should be similar to that of wrapped concrete members for a meaningful correlation; (b) the device should be suitable for different corner radii; and (c) failure should occur in the test zone. A detailed drawing of the two-part steel device is illustrated in Figure 1.

The upper part is designed as the test zone with two interchangeable aluminum corner inserts separated by a 51 mm wide steel. It has a uniform thickness of 51 mm while the overall width and height are 254 mm and 292 mm, respectively.

The corner inserts are made of aluminum and have overall dimensions of 102 x 102 mm. The corner radii investigated in this research include: 0.00, 6.35, 12.70, 19.05, 25.40, 38.10, and 50.80 mm. The largest radius of 50.80 mm corresponding to half of the width of the corner insert can be used to simulate a circular cross section. The corner inserts are glued to the steel part to prevent any movement during testing.

The lower part of the device is designed to anchor the FRP laminate. The semi-circular bottom steel block has a radius of 127 mm under which the FRP laminate is terminated with a lap splice length of 152 mm. Because the radius of the semi-circle is considerably larger than that of all corner inserts, no failure would be expected within the anchor zone.

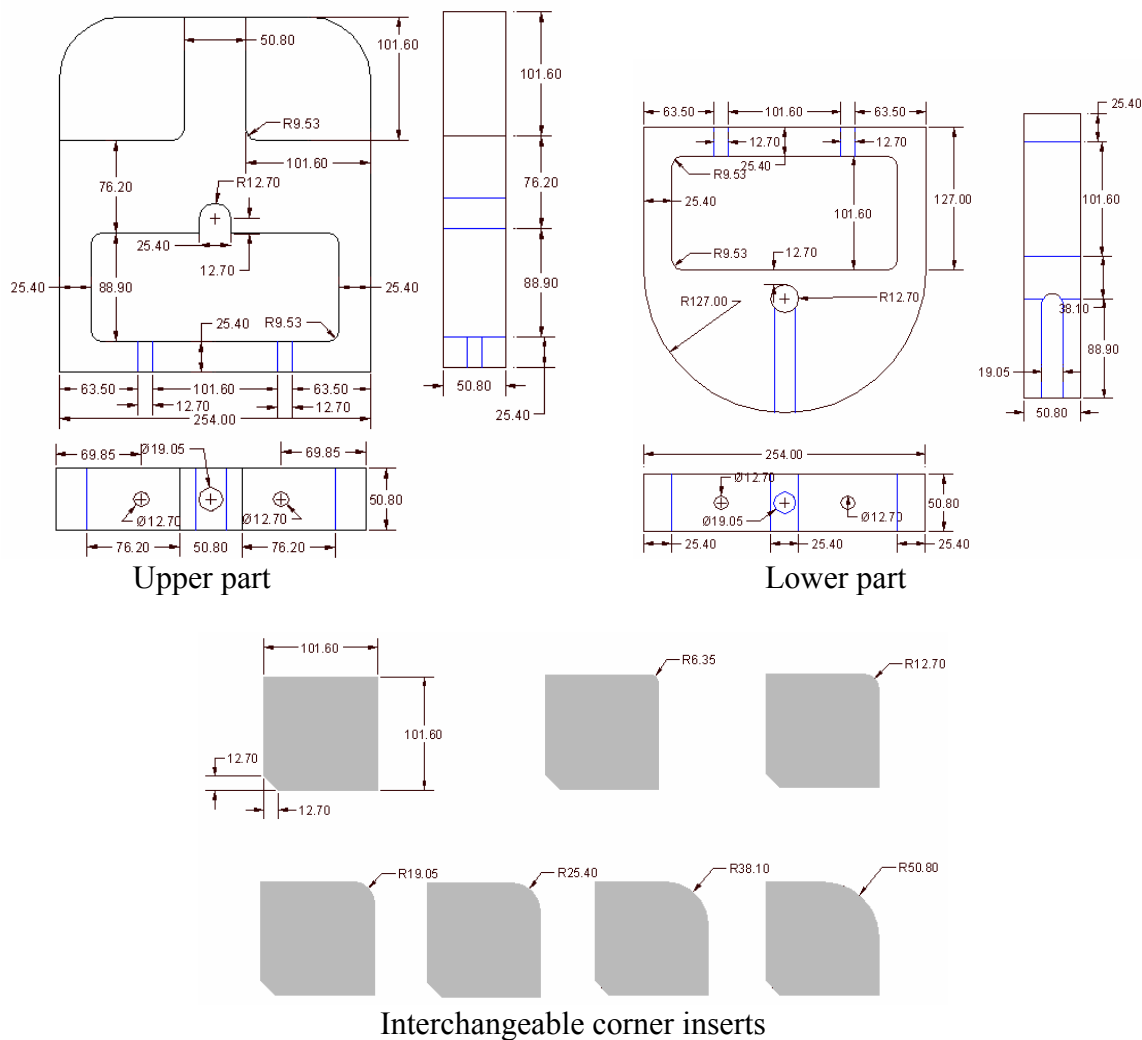


Fig. 1 Test apparatus (Unit: mm)

Prior to the installation of the FRP laminate, these two parts are joined using two through bolts. After the device is installed on the testing machine, the nuts on these bolts are loosened so that the tensile load is transferred to the FRP laminate. The loose bolts were also used as safety feature to hold the device after rupture of the laminate.

### Installation of Laminate

After placing two identical aluminum corner inserts, the side surface of the device was covered with polyethylene tapes. The polyethylene tape was used as the release film to facilitate detaching of the FRP laminate from the steel surface after completion of the test. A strip of FRP laminate was 38.1 mm wide and 1.68 m long. The laminate was applied by the manual lay-up procedure. The two-part saturant was thoroughly mixed and a thin layer was applied on both the polyethylene tape and the carbon fiber sheet using a sponge brush. Through careful handling, the carbon fiber ply was wrapped around the specimen and lap-spliced at the bottom. Then, the backing paper was removed after application of gentle pressure. A plastic roller was used to remove the air

entrapped between fiber ply and saturant. After approximately 30 minutes, a second layer of saturant was applied and the plastic roller was used again to work the resin into the fibers. The wet laminate was left to cure for three days and then strain gages were attached. Two or three identical specimens were manufactured for each set of corner inserts.

### Instrumentation

Strain gages were used to measure the strains at multiple points around each corner. The first gage was placed 38.10 mm away from the root of the corner on the flat part of the upper and side surfaces. Another two gages were positioned with one end exactly at the curvature changing point of the upper and side surfaces, respectively. For those laminates with corner radius larger than 19.05 mm, a fifth strain gage was attached at the center of the corner arc. Load was monitored by the built-in load cell in the testing machine. The strain gage arrangements for laminates with different corner radius are shown in Figure 2 and an instrumented specimen ready for testing is shown in Figure 3.

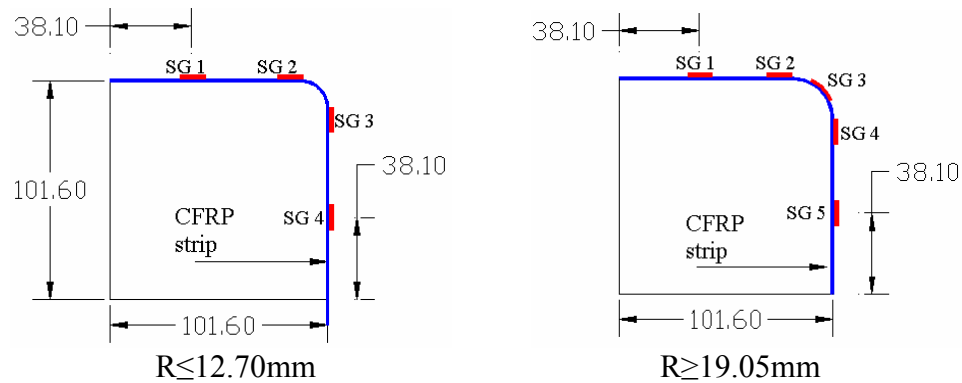


Fig. 2 Strain gage arrangement

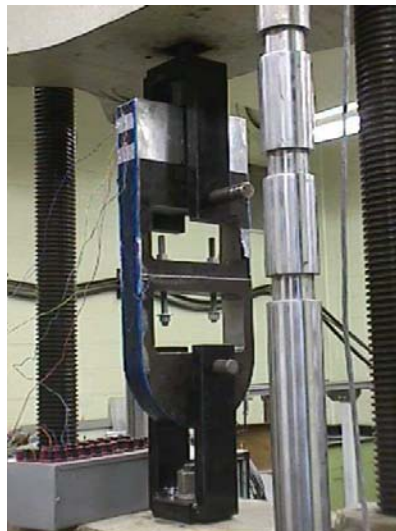


Fig. 3 Test setup

## TEST RESULTS

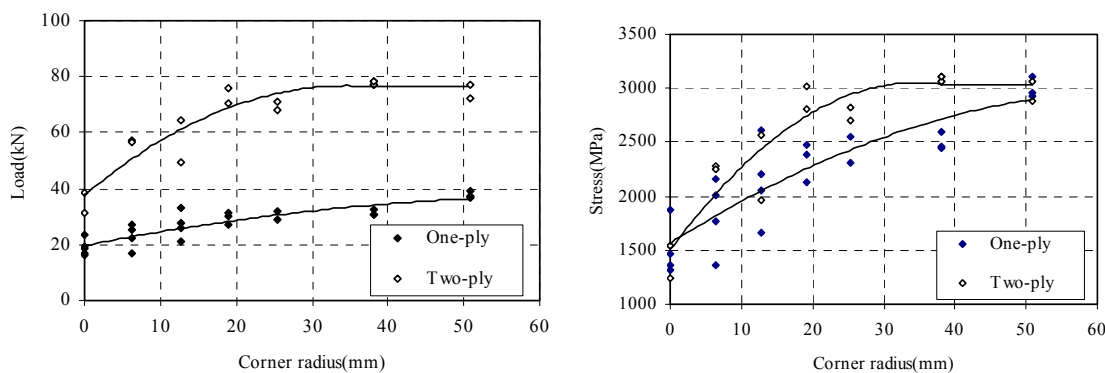
### Strength of CFRP laminates

The average ultimate load carried by CFRP laminates for different corner radii is shown in Table 2. The individual data points of load and stress versus corner radius are depicted in Figures 4(a) and (b). The average ultimate load increases with corner radius for both one and two-ply laminates. The ultimate load capacity of two-ply specimens is more than twice that of the corresponding one-ply specimen with two exceptions: corner radii of 0 and 50.80 mm, which represent the square and circular section, respectively.

Table 2 Average ultimate results

One-ply							
R (mm)	0	6.35	12.70	19.05	25.4	38.10	50.80
Load (kN)	19.03	22.92	26.86	29.39	30.56	31.46	37.72
Stress (MPa)	1513	1822	2135	2336	2429	2501	2999
Percentage of reference strength*	33	40	47	52	54	55	66
Strain(%)**	0.65	0.96	1.05	1.01	1.00	0.98	1.10
Elastic Modulus (GPa)	233	188	203	234	243	255	273
Failure mode***	I	I	I	I or II	II	II	II
Two-ply							
R (mm)	0	6.35	12.70	19.05	25.4	38.10	50.80
Load kN)	34.92	57.00	56.94	73.24	69.62	77.62	74.73
Stress (MPa)	1388	2266	2263	2911	2767	3086	2970
Percentage of reference strength*	31	50	50	64	61	68	66
Strain(%)**	0.50	0.96	0.92	1.12	1.18	1.25	1.25
Elastic Modulus (GPa)	278	236	246	260	234	247	238
Failure Mode***	I	I	I	I	II	II	II

\* 4525MPa, \*\* average from all gages, \*\*\* I: at corner, II: at flat portion



(a) Ultimate load

(b) Stress

Fig. 4 Ultimate load and stress vs. corner radius

The performance of the laminate is analyzed by comparing the stress-strain relationships with the reference one obtained through direct tension testing of CFRP coupons (Yang et al. 2000). The strain values reported in Figure 5 are those measured on the flat part of the

side surface. It can be seen that even though the diagrams (with the exception of two-ply  $R = 50.80$  mm) are almost the same for all specimens, only 67% of the reference strength (or strain) can be attained. When  $R$  is equal to 6.35 mm, only half the strength was developed, corresponding to a strain of less than 1%. The laminate stiffness (modulus of elasticity) when wrapped is less than that of the straight form.

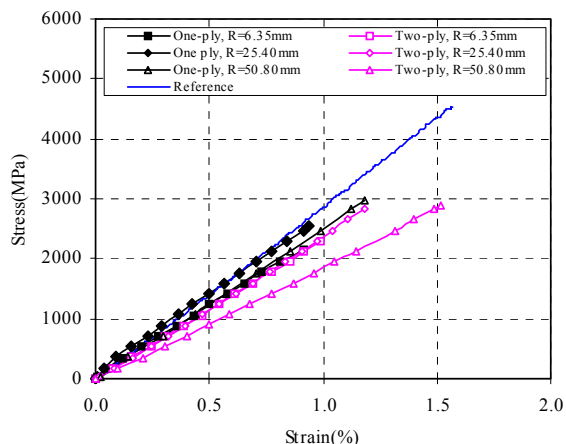
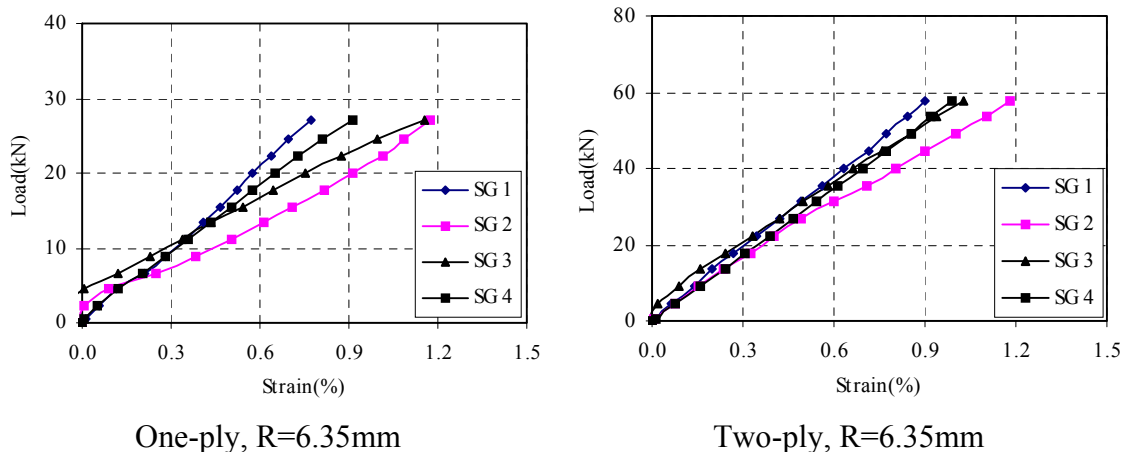


Fig. 5 Stress-strain curves of CFRP laminates

### Strain Distribution

The strain at various locations around the corner is presented in Figure 6 for different corner radii of 6.35, 25.4, and 50.80 mm and different numbers of plies. Generally, the difference in strain values is insignificant and the ultimate strains are between 0.9% and 1.2%, which is smaller than the design value of 1.7% (MBrace 1998). For the small corner radius ( $R=6.35$  mm), the largest strain occurs at the corner indicating the occurrence of stress concentration. As radius of the corner inserts increases, the location of the maximum strain shifts from the center of the corner ( $R=25.4$  mm) to the flat portion of the side surface ( $R=50.80$  mm). The strain difference at various locations is smaller for larger corner radii. One possible reason for this phenomenon is the presence of the release agent, which made the friction between CFRP laminates and the steel surface small and created a relatively smooth force transfer.



One-ply,  $R=6.35$ mm

Two-ply,  $R=6.35$ mm

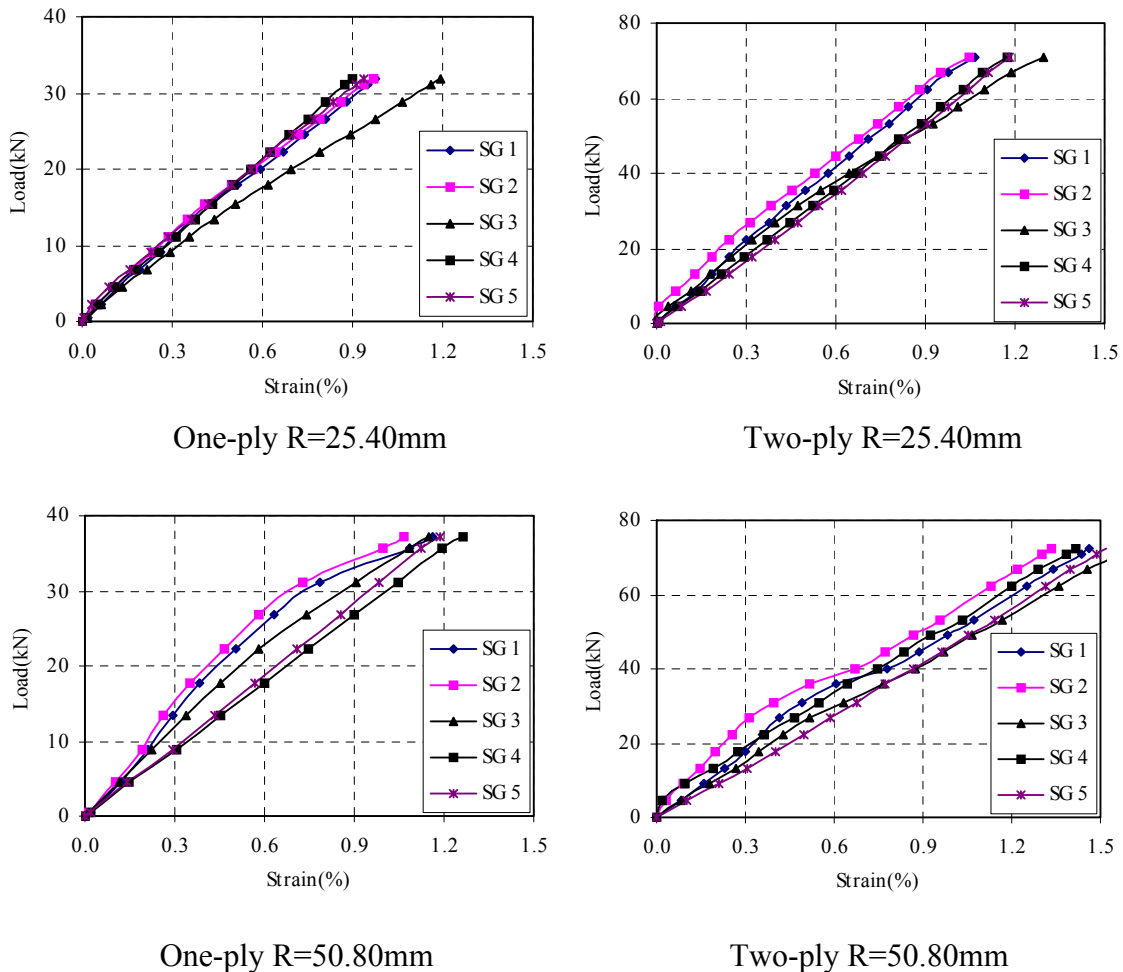


Fig. 6 Strain distribution around a corner

**Failure Modes**

One- and two-ply CFRP strips failed in a brittle manner. Three different failure modes were identified: fracture at one corner; simultaneous fracture at both corners; and fracture at the flat portion of the surface. The first failure mode mainly happened in cases of small corner radius. The other modes were typical in laminates bent around larger radii. The fractured laminates for different corner radius are illustrated in Figure 7.



R=0.0 mm

R=6.35 mm

R=19.05 mm



Fig. 7 Failure modes of CFRP laminates

## CONCLUSIONS

The experimental investigation on the effect of corner radius on the performance of CFRP laminates yielded the following conclusions:

- Corner radius plays an important role on the mechanical properties of CFRP laminates. Test results indicate that at best only 67% of the ultimate laminate strength can be developed when wrapped around a circular section. As the corner radius decreases, the efficiency of FRP wrapping further reduces.
- Multiple placement of FRP plies can slightly increase the strength of bent CFRP laminates and improve the overall strengthening performance except for the square or rectangular sections.

## ACKNOWLEDGEMENT

Financial supports from the Federal Highway Administration (FHWA) and the University Transportation Center based at UMR are gratefully acknowledged. The authors wish to thank J. Bradshaw and S. Haug for their generous help during lab testing.

## REFERENCES

- MBrace<sup>TM</sup> (1998), “Composite Strengthening System, Engineering Design Guideline”, 2<sup>nd</sup> Ed., Master Builders Technologies, Inc., Cleveland, OH.
- Restrepo, J. I, Wang, Y. C., Wymer, P. A. and Irwin, R. W. (2000), “Recent Developments in the Use of Advanced Composite Materials for Seismic Retrofitting”, *Proc. 12<sup>th</sup> WCEE*, Paper number 1593(CD-ROM).
- Rochettee, P. and Labossiere, P. (2000), “Axial Testing of Rectangular Column Models Confined with Composites”, *Journal of Composites for Construction*, ASCE, 4(3), pp.129-136.
- Yang, X. B, Nanni, A., Haug, S. and Sun, C. L. (2000), “Strength and Modulus Degradation of CFRP Laminates from Fiber Misalignment”, Submitted to *J. Mat. Civil Engrg*, ASCE.

## STRESSES IN FRP LAMINATES WRAPPED AROUND CORNERS

Xinbao Yang<sup>1</sup>, Jun Wei<sup>2</sup>, Antonio Nanni<sup>3</sup>, and Lokesh R. Dharani<sup>4</sup>

### ABSTRACT

At present, fiber reinforced polymers (FRP) composite materials are extensively used to strengthen the infrastructure and a main application is wrapping members such as building and bridge columns for improved strength and ductility. In this case, FRP laminates provide confinement to concrete and the cross section shape plays an important role on their effectiveness. In this paper, a unique device is introduced to determine the effect of corner radius on the strength development of FRP laminates and the distribution of resulting radial stress. Different geometries are investigated ranging from sharp corner to circular section, which can be realized by using different interchangeable inserts in the device. Failure load, strain distribution around corner areas, radial stress, and failure modes of the FRP laminates were monitored. The relationship between radial stress distribution and corner radius, and the stress concentration in the laminates are analyzed numerically using the finite element method and compared with experiments.

### INTRODUCTION

Advanced composite materials have been recognized as a promising repair technology for reinforced or prestressed concrete structures [1]. One of the applications involves the use of externally bonded FRP laminates for both flexural and shear strengthening where the laminates are either applied with fiber parallel to the member longitudinal axis or wrapped around a member for improved shear strength [2, 3] or confinement [4, 5]. In the latter case, the need to bend the laminates over the corners of the strengthened member affects the performance and efficiency of the FRP laminate [6]. Circular or elliptical cross sections were recommended in seismic retrofit of bridge columns using steel or FRP jackets [7].

In this paper, the effect of corner radius on the performance and efficiency of carbon FRP laminates was investigated using a unique testing device, which is reusable and can simulate the interaction mechanism between the FRP laminate and substrate concrete. By replacing the interchangeable corner inserts, member cross sections with different curvature radii can be simulated. The radius of the corner inserts ranged from 0 to 50.8 mm. The device has a symmetric configuration and the FRP laminates are wrapped around the side surface of the device and anchored by lap splicing.

- 
1. Research assistant, School of Engineering, University of Missouri-Rolla, Rolla, MO 65409
  2. Research assistant, School of Engineering, University of Missouri-Rolla, Rolla, MO 65409
  3. V & M Jones Professor, School of Engineering, University of Missouri-Rolla, Rolla, MO 65409
  4. Professor, School of Engineering, University of Missouri-Rolla, Rolla, MO 65409

To investigate the radial stress generated by the FRP laminate, a pressure film is installed at the interface. After completion of the test, the pressure films are sent to the manufacturer for image processing. During the test, the load, strain distribution around the corner area is also recorded and fiber stress derived. Finite element analysis is performed to predict the radial stress, stress distribution in the fiber direction of the laminate at the curvature changing points. The finite element analysis results are compared with experiments.

## TEST PROGRAM

### Materials

Carbon FRP laminate strips were fabricated using high tensile strength carbon tow sheets and a two-part epoxy polymer saturant [8]. The ultimate strength and modulus of the composite are 4275 MPa and 228 GPa, respectively. The ultimate strain is 0.017. In this study, these properties are calculated based on the pure fiber area because:

1. With manual lay-up, it is hard to properly control the resin volume and make the cross section of the laminate uniform.
2. As long as the fibers are fully impregnated, small variations in the amount of resin do not significantly change the mechanical performance of the composite.

### Test Specimen Design

In order to simulate the force transfer mechanism of FRP wrapping a cross section via tension test, a unique reusable test device is designed and manufactured based on the following considerations: (a) the mechanical interaction between FRP laminate and device should be similar to that of wrapped concrete members; (b) the device should be suitable for different corner radii; and (c) failure should occur in the test zone. A detailed drawing of the two-part device is illustrated in Figure 1.

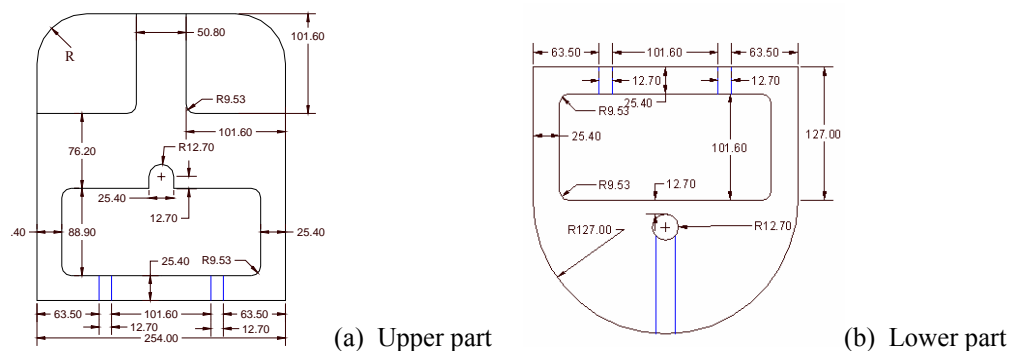


Figure 1. Test apparatus (Unit: mm)

The upper part (a) is designed as the test zone with two interchangeable aluminum corner inserts separated by a 51 mm wide steel block. It has a uniform thickness of 51

mm while the overall width and height are 254 and 292 mm, respectively. The corner inserts have overall dimensions of 102x102 mm. The corner radii investigated in this research include: 0.00, 6.35, 12.70, 19.05, 25.40, 38.10, and 50.80 mm. The largest radius of 50.80 mm corresponding to half of the width of the corner insert and can be used to simulate a circular cross section. The corner inserts are glued to the steel part to prevent any movement during testing.

The lower part (b) of the device is designed to anchor the FRP laminate. The semi-circular bottom steel block has a radius of 127 mm under which the FRP laminate is terminated with a lap splice length of 152 mm. Because the radius of the semi-circle is considerably larger than that of all corner inserts, no failure is expected within the anchor zone.

Prior to the installation of the FRP laminate, these two parts are joined using two through bolts. After the device is installed on the testing machine, the nuts on these bolts are loosened so that the tensile load is transferred to the FRP laminate. The loose bolts were also used as safety feature to hold the device after rupture of the laminate.

### **Installation of Laminate**

After placing two identical aluminum corner inserts, the side surface of the device is covered with polyethylene tape. The polyethylene tape is used as the release film to facilitate detaching of the FRP laminate from the device after completion of the test. A strip of FRP laminate is 38.1 mm wide and 1.68 m long. The laminate is applied by the manual lay-up procedure. The two-part saturant is thoroughly mixed and a thin layer is applied on both the polyethylene tape and the carbon fiber sheet using a sponge brush. Through careful handling, the carbon fiber ply is wrapped around the specimen and lap-spliced at the bottom. Then, the backing paper is removed after application of gentle pressure. A plastic roller is used to remove the air entrapped between fiber ply and saturant. After approximately 30 minutes, a second layer of saturant is applied and the plastic roller is used again to work the resin into the fibers. The wet laminate is left to cure for three days and then strain gages are attached. Two or three identical specimens are manufactured for each set of corner inserts.

### **Instrumentation**

Strain gages are used to measure the strains at multiple points around each corner. The first gage is placed 38.10 mm away from the root of the corner on the flat part of the upper and side surfaces. Two gages are positioned with one end exactly at the curvature changing point of the upper and side surfaces, respectively. For those laminates with corner radius larger than 19.05 mm, a fifth strain gage is attached at the center of the corner arc. Load is monitored by the built-in load cell in the testing machine.

Pressure films are attached on both corners. The width of the pressure films is 10 mm and the length is dependent on the corner radius. The film should cross both curvature changing points at both corners. For each corner, two films are attached with a sensitivity range of 10~49 MPa and 49~128 MPa, respectively. The pressure films at one corner after testing and an instrumented specimen ready for testing are shown in Figures 2 (a) and (b), respectively.

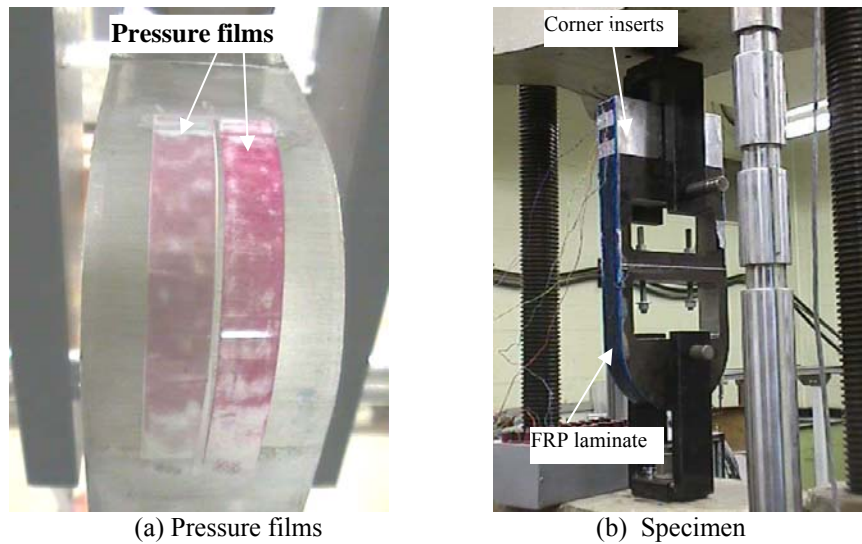


Figure 2. Test setup

## ANALYSIS OF EXPERIMENTAL RESULTS

### Strength of CFRP Laminates

The trend for the ultimate stress carried by CFRP laminates, the individual data points for different corner radii, and the failure modes are shown in Figures 3. It is to be noted that the stress was calculated based on cross section area of fibers, which have a width of 38.10 mm a thickness of 0.165 mm. It is shown that the average ultimate stress increases with corner radius.

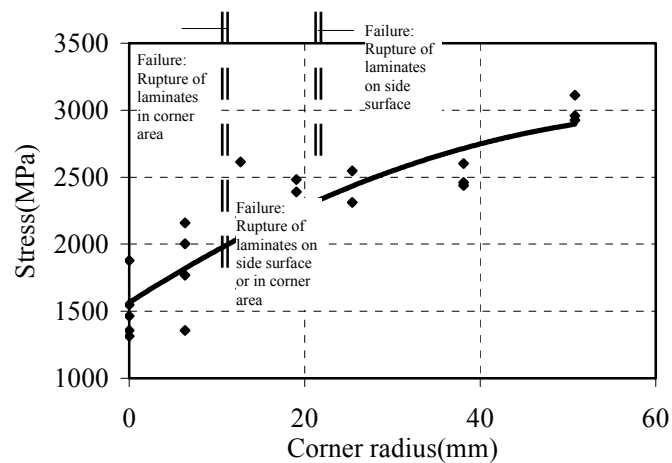


Figure 3. Ultimate stress vs. corner radius

Yang et al. [9] run tension tests and found that the average ultimate strength of this kind of CFRP sheets is 4525 MPa. Compared with this reference value, it can be seen that corner radius has a significant effect on the development of CFRP strength. With  $R=0$

mm, the ultimate strength is 1513 MPa which is significantly lower than the reference value. To show this effect, the average ultimate strength was normalized by the reference value and depicted in Figure 4. It can be seen that only 67% of the unidirectional ultimate strength can be developed even for a radius of 50.8 mm.

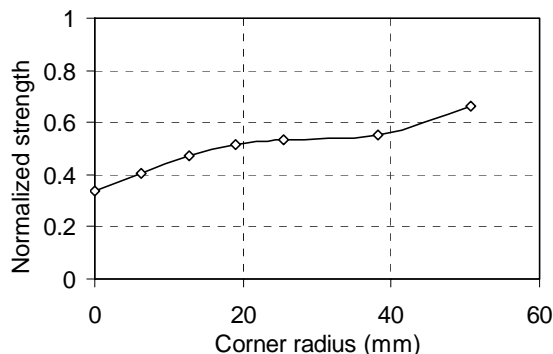


Figure 4. Normalized ultimate stress of CFRP laminate

### Radial Stress Distribution

After completion of the tests, the pressure films were analyzed using an image process technique. The films were meshed with small cells with a dimension of around 0.7 and 1.5 mm in the transverse and longitudinal direction, respectively. Therefore a typical pressure film with a radius of 25.4 mm had at least 405 cells. The total force and average stress in a cell were extracted by specially developed software. A meshed pressure film of  $R=6.35$  mm is shown in Figure 5.

For each pressure film, only one curve was extracted by taking the average of the stresses in the thickness direction of the corner insert. This is due to the fact that the stress in this direction is uniformly distributed. In the longitudinal direction, in order to clearly show the ordinates and make it consistent for different corner radius, the origin is chosen in the middle of the pressure film and the angles measured from any point of the film centerline to the origin are used as the abscissa, e.g.  $45^\circ$  and  $-45^\circ$  correspond to the two curvature changing points on the upper and side portion of the pressure film. Usually one corner broke first and the laminate flow away leaving the other corner unbroken. Figure 6 lists the radial stress distribution of the unbroken corners for  $R=6.35$  and 25.4 mm. It is noted that only the radial stress between  $-20^\circ$  and  $20^\circ$  is indicated in the figure because the radial stress distribution outside this range showed more data scattering especially for smaller corner radius.

Even though different failure modes were observed at the two corners, the radial stress distribution does not show too much variation under failure load, especially for larger corner radius. The supposed radial stress concentration at the curvature changing points was not identified from radial stress distribution diagrams but can be found from the pressure films where the color obviously exceeded the range of the films and was omitted by the data analysis system.

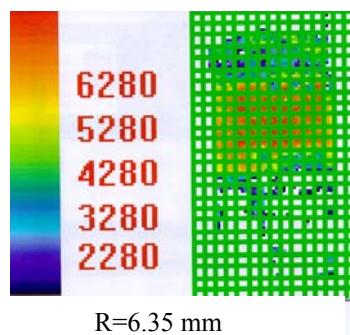


Figure 5. Pressure film

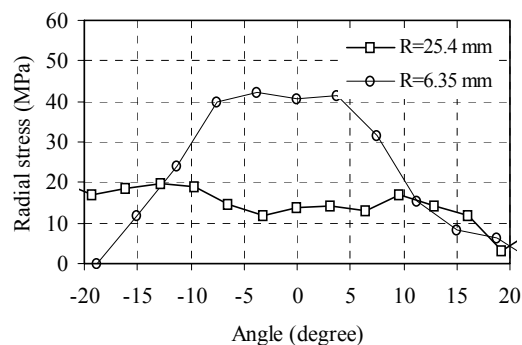


Figure 6. Radial stress distribution

## FINITE ELEMENT ANALYSIS

### Analytical Model

During construction of the numerical model, the symmetry of the specimen and the laminate were taken into consideration. Half of the upper part of the test specimen is shown in Figure 7 (a), which has a height and width of  $a=127$  mm and a thickness of  $h=50.8$  mm. The thickness of CFRP laminate is  $t=0.165$  mm. Due to the uniform distribution in the thickness direction of the corner insert, it is further simplified as shown in Figure 7(b) for the numerical model of this problem. The symmetric conditions of the entire specimen were applied on the boundaries with  $X=0$  or  $Y=0$ . A load,  $F$ , was applied at the end of FRP laminate at  $X=a$  and  $Y=0$  as shown in Figure 7 (b).

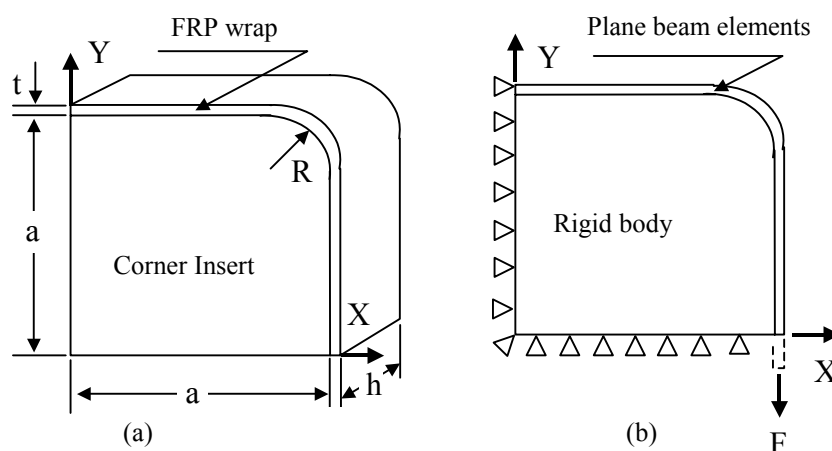


Figure 7. (a) A quarter of the test apparatus, (b) Finite element analytical model.

The displacements in the  $X$ -direction of all nodes along the line of  $Y$ -axis were constrained for both corner insert and FRP laminate elements, while the displacements in the  $Y$ -direction of all nodes along the line of  $X$ -axis were constrained only for the corner insert. After these simplifications, the analysis is actually a plane problem.

A commercial finite element codes, ABAQUS [10], was used to perform the static analysis. Because the thickness,  $t$ , of the FRP laminate is very small compared to the length, plane beam elements were used to simulate the CFRP laminate. The corner insert was modeled as a rigid body so that a contact problem was assumed between the corner insert and the CFRP laminate. In this model, a finite motion along the interface between the corner insert and the CFRP laminate is allowed but no separation is tolerated between the two parts. Linear elastic material properties were used to these beam elements.

## Results and Discussions

Figure 8 shows the FEA and experimental results of ultimate radial stress versus radii of the corner inserts. It is shown from the figure that there is a good agreement between the FEA and average test measurements. The ultimate radial stress decreases with increasing the corner radius in a non-linear manner. Figure 9 shows the radial stress distribution at the curved segment of the corner insert for both FEA and experimental results for  $R=25.4$  mm.

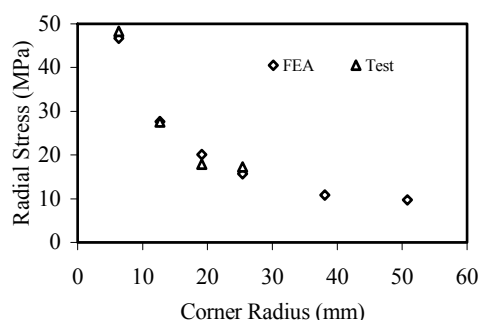


Figure 8. Ultimate radial stress by FEA and test

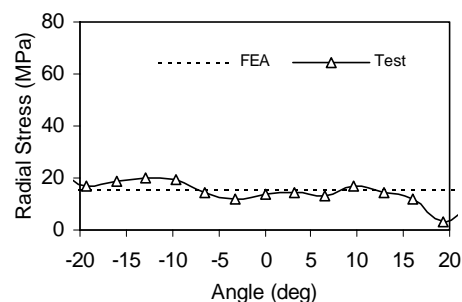


Figure 9. Radial stress distribution in corner area for  $R=25.4$  mm

It can be seen from Figure 7 that the curvature radius changes from infinity in the straight portion of the corner insert to a finite value  $R$  in the curved segment of the insert. It means that there is a geometrical discontinuity at the conjunction points between the straight and curved segments. Therefore, a stress concentration will occur around the conjunction points and CFRP laminate. The stress concentration factor versus ratio of radius of the corner insert to its width ( $R/a$ ) is shown in Figure 10 for both FEA and experimental results. In FEA, the stress concentration factor is defined as the ratio of the maximum fiber stress at the curvature changing point to that at the load application point. For the test results, they are obtained by using the reference strength 4525 MPa divided by the average ultimate stress for different corner radii. It is indicated from the figure that the FEA results agree well with experiments. When the radius of the corner insert decreases, the factor increases sharply. Figure 11 shows the stress concentration factor distributions near the conjunction points between the straight and curved segment for three typical cases with  $R=6.35$ , 19.1 and 50.8 mm.

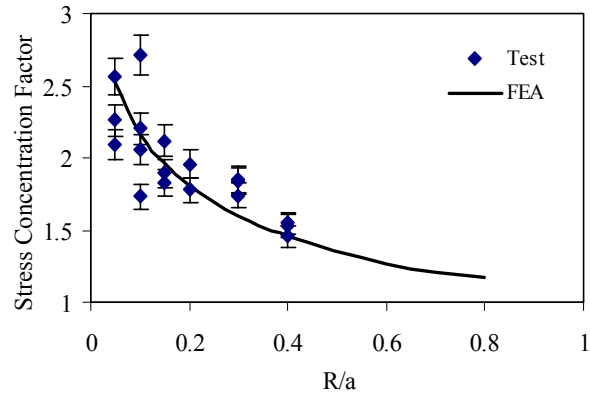


Figure 10. Stress concentration factor

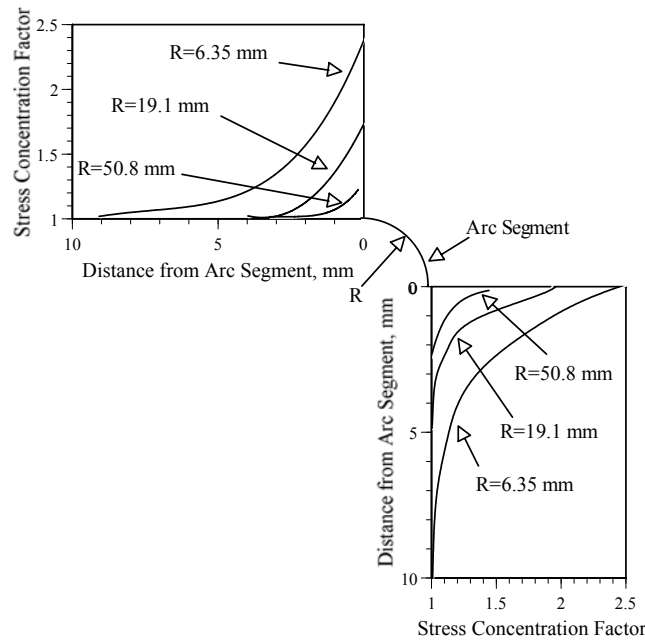


Figure 11. Stress concentration factor distribution

## CONCLUSIONS

Based on the investigations of both experiments and numerical analysis, the following conclusions can be reached:

1. The testing method and the reusable device are reliable for the investigation on the effect of corner radius on the performance of FRP laminates when wrapping structural cross sections.
2. A smaller corner radius can significantly reduce the ultimate strength of the FRP laminate due to stress concentration around the corner area. The stress concentration factor increases when the corner radius decreases. Conversely, the radial stress decreases with increasing corner radius.

3. The finite element method can predict the stress concentration in the fiber direction and the radial stress distribution. The numerical results agree well with the experiments.

## ACKNOWLEDGEMENT

The financial support from the Federal Highway Administration (FHWA) under contract number DTFH 61-00X-00017 is greatly appreciated.

## REFERENCES

1. Nanni, A. 2000. "Carbon Fibers in Civil Structures: Rehabilitation and New Construction," Proc., the Global Outlook for Carbon Fiber 2000, Intertech, San Antonio, TX.
2. Khalifa, A and Nanni, A. 2000. "Improving Shear Capacity of Existing RC T-Section Beams Using CFRP Composites," *Cement and Concrete Composites*, 22(2), pp165-174
3. Khalifa, A., De Lorenzis, L., and Nanni, A. 2000. "FRP Composites for Shear Strengthening of RC Beams," Proc., 3<sup>rd</sup> Inter. Conf. On Advanced Composites Materials in Bridges and Structures, Ottawa, Canada, Humar, J. and Razaqpur, A. G. (Editors), pp137-144.
4. Restrepo, J. I, Wang, Y. C., Wymer, P. A. and Irwin, R. W. 2000. "Recent Developments in the Use of Advanced Composite Materials for Seismic Retrofitting", *Proc. 12<sup>th</sup> WCEE*, Paper number 1593(CD-ROM).
5. Rochettee, P. and Labossiere, P. 2000. "Axial Testing of Rectangular Column Models Confined with Composites", *Journal of Composites for Construction*, ASCE, 4(3), pp.129-136.
6. Xiao, Y. and Wu, H. 2000. "Compressive Behavior of Concrete Confined by Carbon Fiber Composite Jackets," *J. Mat. Civil Engrg*, ASCE, 12(2):139-146.
7. Priestley, M.J. N., Seible, F., and Calvi, M. 1995. *Seismic Design and Retrofit of Bridges*, John Wiley and Sons, Inc., New York, 672 pp.
8. MBrace<sup>TM</sup> 1998. "Composite Strengthening System, Engineering Design Guideline", 2<sup>nd</sup> Ed., Master Builders Technologies, Inc., Cleveland, OH.
9. Yang, X. B, Nanni, A., Haug, S. and Sun, C. L. 2000. "Strength and Modulus Degradation of CFRP Laminates from Fiber Misalignment", accepted for publication in *J. Mat. Civil Engrg*, ASCE.
10. ABAQUS/Standard User's Manual. 1998, Version 5.8, Hibbitt, Karlsson & Sorensoen, Inc.

## LAP SPLICE LENGTH AND FATIGUE PERFORMANCE OF FRP LAMINATES

Xinbao Yang and Antonio Nanni  
Center for Infrastructure Engineering Studies  
University of Missouri-Rolla  
Rolla, MO 65401

### ABSTRACT

In this paper, the lap splice length and the long-term (fatigue) performance of lap-spliced carbon FRP laminates were investigated. Lap-spliced CFRP coupon specimens were fabricated with a splice length of 12.7, 25.4, 38.1, 50.8, 76.2, and 101.6 mm. To eliminate the bending on the lap splice joint, a symmetric specimen configuration was adopted. The width of the specimens was 38.1 mm. These specimens were tested to failure under tension. The ultimate load, failure mode, and strain distribution on the surface of both the non-lapped and lapped areas were monitored. It was found that a length of 38.1 mm was sufficient to develop the static ultimate strength of the CFRP laminate. Tension-tension fatigue tests were performed on 101.6-mm lap-spliced specimens to investigate the long-term performance. A stress ratio versus number of cycles curve was constructed using the test data and compared with theoretical results. It was shown that 101.6-mm lap-spliced CFRP laminates can sustain more than 2.0 million load cycles with no effect on residual strength, if the maximum applied stress does not exceed 40% of the ultimate static strength. A 101.6-mm lap splice length is recommended for field use as presently adopted in standard practice.

**Keywords:** carbon FRP laminate; fatigue; lap splice; residual strength; tensile strength; stiffness

### RESEARCH SIGNIFICANCE

When carbon fiber reinforced polymeric (CFRP) laminates are used in strengthening long structural members, lap splicing is usually adopted for the transition of forces. Determination of the effective lap splice length and its fatigue performance is of

importance. This paper shows that by conducting static and repeated tension tests on CFRP coupon specimens, the strength change and effective lap splice length can be determined. Based on the results, recommendations are made for strengthening concrete structures with lap-spliced CFRP laminates.

## **INTRODUCTION**

FRP composite materials are being used in infrastructure as a fast, effective, and durable strengthening method, and one of the main applications is to strengthen bridge structures in flexure and shear. Generally, the FRP laminates are applied externally by manual lay up. With this technique, the maximum handling length is about 7 m. When FRP laminates strengthen long members or in the presence of some geometrical restrictions, lap splicing is adopted to maintain the continuity of the laminate and allow force transition. To avoid premature failure before developing the strength of an FRP laminate, the minimum lap splice length must be determined. The main variables that influence the effective lap splice length include resin properties and installation.

In addition, the long-term performance under service loads must be assured. For FRP strengthened structures subjected to cyclic loading, fatigue performance is a limit state (Demers 1998). A considerable amount of experimental and theoretical work has been conducted in this field (Adimi *et al.* 2000, Miyano and Kudoh 1998, Tang *et al.* 2000, Caprino 2000). A typical infrastructure component, such as a bridge, will undergo several million cycles of loading during its service life. The mechanical properties change of FRP laminates under such circumstances should be assessed, especially the residual strength and the elastic modulus (Barnes and Mays 1999, Demers 1998, Shahawy and Beitelman 1999).

The emphasis of this project was to experimentally investigate the effective lap splice length of carbon FRP laminates using scaled specimens. The specimens were symmetric about the mid-plane and had lap splice lengths of 12.7, 25.4, 38.1, 50.8, 76.2, and 101.6 mm. The mid-plane consisted of a 0.5-mm thick aluminum plate which was cut in the middle to avoid its contribution to the strength of the specimen. As a result, there were two plies of laminate in the non-lapped area, and four plies of laminate in the lapped area. Direct tension tests were performed and the minimum lap splice length was determined when failure occurred outside the lap-spliced area. Tension-tension fatigue tests were

performed only on specimens with a lap splice length of 101.6 mm. Various stress ranges were adopted and the fatigue life was recorded. The measured fatigue life was also compared with that predicted by an empirical model (Caprino 2000). Even though testing was limited to the 101.6 mm lap-spliced specimen, the test protocol is generic and can be extended to other cases.

## **TEST PROGRAM**

### **Materials**

High tensile strength, unidirectional carbon fiber tow sheets (MBrace 1998) were used for the laminates. The guaranteed ultimate strength for design was 3792 MPa, the tensile modulus was 228 GPa and the ultimate strain was 0.017. The carbon fiber tow sheets were impregnated using the two-part epoxy polymer provided by the manufacturer. Yang *et al.* (2001) conducted tension tests on one-ply and two-ply CFRP unidirectional laminates made with this type of tow sheets and confirmed these specified values.

### **Test Specimens and Setup**

One concern about the specimen layout was that, for single layer lap splicing, the two opposing forces in the laminate would not be situated on the same plane causing a couple to form (Fig.1), which could initiate peeling. To avoid this phenomenon, a symmetric specimen configuration (double layer) was adopted (Fig. 2). To facilitate the construction of the CFRP panel, a 0.5-mm thick aluminum plate was inserted between the two layers of CFRP laminate. The aluminum plate was separated in the middle with a gap of about 2 mm. A strip of waxed backing paper was attached to the aluminum surface with a length of the lap splice plus 76.2 mm. The contribution to the strength from the aluminum plate could thus be eliminated. The surface of the aluminum plate was roughened with sand paper in the bonded area to improve the adhesion to the CFRP laminate. Specimens were cut from CFRP panels which were fabricated using a hand lay-up technique (MBrace 1998). Each specimen had a width of 38.1 mm and a length equal to  $305+d$  mm, where  $d$  was the lap splice length.

During each tension test, the specimen was loaded between the steel grips of the testing machine. Due to the stiffness difference between grips and specimen, effective diffusion of the stress is important to reduce stress concentrations. In this study, three layers of tabs were used. Right on the laminate were two layers of CFRP tabs applied at the same time of other plies. These tabs were 76.2 and 50.8 mm long. Before testing, the surfaces of CFRP tabs were roughened and 38.1 by 50.8 mm aluminum tabs were attached using a conventional quick-set adhesive (Fig. 2). This method was very successful and no premature failure was observed during testing. All specimens failed within the gage length. The gripping length was 38.1 mm and the gripping stress was 12.0 MPa.

Three identical specimens were tested for each case. The monitored variables included: failure load, failure mode, strain in the non-lapped area, and strain in the middle of the lapped area. For specimens with a lap splice length of 76.2 and 101.6 mm, strain at the end of the lapped area was also recorded. The various test specimens and the test setup are shown in Figures 3 (a) and (b), respectively.

Fatigue tests were conducted only on specimens with a lap splice length of 101.6 mm. The load cycle frequency was 4.0 Hz, which is acceptable for tests simulating bridge structures under traffic loading (Barnes and Mays 1999). The minimum stress was 5% of the average ultimate strength obtained from the static tests on the 101.6-mm lap-spliced specimens. Maximum stress values of 80%, 60%, and 40% of the average ultimate strength were investigated. If a specimen did not fail after 2.5 million cycles, a quasi-static test was conducted on it to determine the residual stiffness and strength. Two identical specimens were used for each case. The typical S-N curve was constructed based on the experimental data.

## **EXPERIMENTAL RESULTS AND ANALYSIS**

### **Lap Splice Length**

The relationship between failure load and lap splice length is shown in Table 1 and Figure 4. When the lap splice length  $d$  is less than or equal to 38.1 mm, the failure load is almost proportional to lap splice length. The failure load of the  $d=25.4$  mm specimens was approximately twice that of the  $d=12.7$  mm specimens, while the failure load of the

$d=38.1$  mm specimens was a little less than triple that of the  $d=12.7$  mm specimens. The trend of failure load versus lap splice length can be explained by the failure modes of the specimens. For specimens with  $d=12.7$  and  $25.4$  mm, failure occurred at the plies and sliding was observed on both sides. For specimens of  $d=38.1$  mm, rupture of the CFRP laminate outside the lap area was observed. When  $d$  was longer than  $38.1$  mm, the failure load almost remained constant and rupture of CFRP laminate was observed in all specimens. It was found from the test results that  $38.1$  mm might be sufficient to develop the static ultimate strength of CFRP laminates.

The experimental results of strength and stiffness for  $101.6$ -mm lap-spliced specimens are analyzed in more detail. The strain gage location is shown in Figure 5. The strain gages (SG 1 and SG 4) for the non-lapped zone were located  $19.0$  mm away from the end of the lap splice joint and the strain gages (SG 3 and SG 6) for the lapped zone were situated at the middle points of both sides. The load-strain relationship in both the lapped and non-lapped zones are shown in Figures 6 (a) and (b). The scatter of the data appears to be negligible. The reference line shows the results from the continuous unidirectional CFRP laminates (Yang *et al.* 2000). The reference load-strain curve of four-ply CFRP laminate was derived from the two-ply specimen. It is indicated in Figure 6(b) that the overall stiffness of the specimens in the non-lapped zone is very close to the two-ply reference specimen but the failure load is about 15% less than the reference value. The reason for the difference may be attributed to the fact that failure started at one side of the specimens followed by the immediate failure of the other side. The load-strain curve in the middle of the lapped zone is very close to that of the four-ply reference line, which means that all four plies in the lapped zone equally participated in sustaining the applied load.

To show the strain difference in both non-lapped and lapped areas, a detailed strain distribution versus strain gage position at different load levels is shown in Figure 7. The strain at both sides of each  $101.6$ -mm lap-spliced specimen is depicted in one plot. Strain gages were placed symmetrically on both sides of the specimens. It is shown that the strain distribution is symmetric except for specimen 2 under loads of  $35.6$  and  $44.8$  kN. The strain in the non-lapped area is significantly larger than that in the lapped area. The strain at the end of the lapped area is almost equal to that in the middle of the lapped area.

The jump in the strain of specimen 2 indicated that some delamination may have occurred at the end of the lapped area.

### **Fatigue Performance of Lap-spliced CFRP Laminates and Theoretical Prediction**

Fatigue tests were performed only on 101.6-mm lap-spliced specimens. The test matrix and measured fatigue life results are listed in Table 2 and plotted in Figure 8.  $S_{max}$  and  $S_{min}$  are the maximum and minimum stresses for each fatigue test, respectively.  $\bar{f}_u$  is the average ultimate strength of the 101.6-mm lap-spliced CFRP laminate obtained in this study. For all specimens,  $S_{min}$  was kept constant at 11.6 kN, which is about 5% of the average ultimate load. The stress ratio  $R=S_{min}/S_{max}$  ranged from 6 to 12 percent. For the tested values, it is shown that the log of fatigue life appears to have a linear relationship as a function of the maximum stress  $S_{max}$ . When the maximum stress is equal to 80% of  $\bar{f}_u$ , the specimens failed after about 50,000 cycles. When  $S_{max}$  is equal to 40% of  $\bar{f}_u$ , the specimens sustained two and a half million cycles without rupture. At both sides of these two specimens, some delamination developed throughout the fatigue test in a progressive manner. After two and a half million cycles, a 19.0 to 25.4 mm delamination was observed at both ends of the lapped area.

Caprino (2000) proposed an empirical model to predict the fatigue strength of FRP laminates subjected to tension-tension fatigue loading, which is used herein for the lap-spliced CFRP laminates. The model can be expressed by the following equation:

$$f_n = \bar{f}_u - \alpha S_{max} (1 - R)(n^\beta - 1) \quad (1)$$

where  $f_n$  = strength after  $n$  cycles

$\bar{f}_u$  = monotonic strength of the virgin material

$S_{max}$  = maximum stress during cyclic loading

$S_{min}$  = minimum stress during cyclic loading

$R$  = stress ratio =  $\frac{S_{min}}{S_{max}}$  (%)

$n$  = loading cycles

$\alpha, \beta$  = constants dependent on the material considered

Let  $N_f$  be the fatigue life of the specimen, if  $n=N_f, f_n=S_{max}$ , so  $N_f$  can be expressed as:

$$N_f = \left[1 + \frac{1}{\alpha(1-R)} \left(\frac{\bar{f}_u}{S_{max}} - 1\right)\right]^{\frac{1}{\beta}} \quad (2)$$

In order to find  $\alpha$ ,  $\beta$  from experimental data, Eq. (2) is rewritten as:

$$\left(\frac{\bar{f}_u}{S_{max}} - 1\right)\left(\frac{1}{1-R}\right) = \alpha(N_f^\beta - 1) \quad (3)$$

Let  $K = \left(\frac{\bar{f}_u}{S_{max}} - 1\right)\left(\frac{1}{1-R}\right)$ , then,

$$K = \alpha(N_f^\beta - 1) \quad (4)$$

If a plot of  $K$  against  $N_f^\beta - 1$  is generated, a straight line passing through the origin can be obtained using a regression technique where  $\alpha$  is the slope of the straight line. Because two variables exist in the equation, a trial-and-error technique is adopted by giving a trial value to  $\beta$  until  $\alpha$  is found. Based on the test data of this study, values of 0.004 and 0.39 were assigned to  $\alpha$  and  $\beta$ , respectively. Therefore, a possible fatigue life model for lap-spliced CFRP laminate can be expressed as:

$$N_f = \left[1 + \frac{1}{0.004(1-R)} \left(\frac{\bar{f}_u}{S_{max}} - 1\right)\right]^{\frac{1}{0.39}} \quad (5)$$

The predicted fatigue life is plotted together with the test data in Figure 8.

### Residual Strength and Stiffness

During the fatigue conditioning on specimen 1, the change in stiffness was monitored by conducting periodic static tests up to a given load of 8.9 kN every 10,000 cycles. The load 8.9 kN corresponds to 20% of the average ultimate load for the 101.6-mm lap-spliced specimens. The load strain curves for 0, 500,000, 1,000,000, 1,500,000, and 2,000,000 cycles are shown in Figures 9 (a) and (b). In addition, the specimen strain in both the non-lapped and lapped areas under a load of 8.9 kN is plotted against the number of cycles in Figure 10 where the reference strain of two-ply and four-ply CFRP laminates is also shown for comparison. It is found that the modulus change in CFRP laminates subjected to fatigue load is negligible in the non-lapped area. In the lapped area, the stiffness after 2.0 million cycles increases about 19%.

After 2.5 million cycles of fatigue loading, the fatigue test was terminated and a monotonic tension test was performed with results of specimen 2 shown in Figure 11 compared with that of corresponding two-ply and four-ply reference specimen as well as that of corresponding non-cycled specimen. It is shown that fatigue loading caused negligible change on lap-spliced CFRP laminates and the stiffness in the lapped and non-lapped zone is very close to that of the reference specimen and the corresponding non-cycled specimen. The residual failure load is 47.5 kN which is close to the average failure load of 46.8 kN obtained from the static tension tests of 101.6-mm lap-spliced specimens. By the end of the fatigue tests, some delamination was observed, but the remaining bond length was more than 50.8 mm, which still allows developing the full tensile strength of the specimen.

#### **VALIDATION OF ACI 440 GUIDE SPECIFICATION**

For a CFRP laminate used as externally bonded reinforcement, the recently approved ACI 440 Design Guide (ACI 440 2001) specifies that the service stress  $F_a$  is determined from the manufacturer guaranteed tensile strength ( $f_{fu}^*$ ) as follows:

$$f_{fu} = C_E f_{fu}^* \quad (6)$$

$$F_a = 0.55 f_{fu}^* \quad (7)$$

where  $C_E = 0.85$  in the worst case of aggressive environments. For the material used in this research,  $f_{fu}^*$  is 3792 MPa. Therefore, the allowable service stress becomes  $F_a = 0.55 \times 0.85 \times 3792 \text{ MPa} = 1773 \text{ MPa}$ . According to the empirical model (Eq. (5)), if  $S_{max} = F_a$  and  $S_{min} = 180 \text{ MPa}$ , the fatigue life is more than two million cycles and gives a satisfactory fatigue performance as shown in Figure 8. It appears that the allowable stress suggested by ACI 440 is appropriate even when a lap splice is used in construction.

## CONCLUSIONS

Based on the investigation on the performance of lap-spliced CFRP laminates, the following conclusions can be reached:

- A lap splice length of 38.1 mm is sufficient for CFRP laminates to develop the ultimate tensile strength under quasi-static loading
- 101.6-mm lap-spliced CFRP laminates showed satisfactory fatigue performance in that no fatigue failure was observed after 2.5 million cycles of fatigue loading at a maximum stress  $S_{max} = 0.4 \bar{f}_u$ , where  $\bar{f}_u$  is the static ultimate strength of the lap-spliced CFRP laminate.
- The strength and modulus of 101.6-mm lap-spliced laminate showed negligible degradation after being subjected to 2.5 million cycles of fatigue loading at  $S_{max} = 0.4 \bar{f}_u$ .
- A lap splice length of 101.6 mm is recommended if CFRP laminates are used for strengthening concrete structures.
- The allowable service stress  $F_a$  specified by ACI 440 Design Guide appears to be safe for a lap splice up to 2.0 million cycles.

## ACKNOWLEDGEMENT

The financial support of the Federal Highway Administration (FHWA) and the University Transportation Center based at UMR are gratefully acknowledged. The authors wish to thank Mr. J. Bradshaw for his generous help during testing.

## CONVERSION FACTORS

$$1 \text{ mm} = 0.039 \text{ in.}$$

$$1 \text{ MPa} = 0.145 \text{ ksi}$$

$$1 \text{ N} = 0.225 \text{ lbf}$$

## REFERENCES

- ACI 440 (2001), "Guide for the Design and Construction of Externally Bonded FRP Systems for Strengthening Concrete Structures," American Concrete Institute, Detroit, Michigan.
- Adimi, M. R., Rahman, A. H., and Benmokrane, B. (2000), "New Method for Testing Fiber-Reinforced Polymer Rods under Fatigue," *J. Composites for Construction*, ASCE, pp206-213
- Barnes, R. A. and Mays, G. C. (1999), "Fatigue Performance of Concrete Beams Strengthened with CFRP Plates," *J. Composites for Construction*, ASCE, Vol. 3, No. 2, pp63-72
- Caprino, G. (2000), "Predicting Fatigue Life of Composite Laminates Subjected to Tension-Tension Fatigue," *J. Composite Materials*, Vol. 34, pp1335-1355
- Demers, C. E. (1998), "Tension-Tension Axial Fatigue of E-glass Fiber-Reinforced Polymeric Composites: Tension Fatigue Modulus," *Construction and Building Materials*, Vol. 12, No. 1, pp51-58
- MBrace™ (1998), "Composite Strengthening System, Engineering Design Guideline", 2<sup>nd</sup> Ed., Structural Preservation Systems, Inc., Cleveland, OH, pp109.
- Miyano, Y, Nakada, and Kudoh, H. (1998), "Determination of Tension Fatigue Life of Unidirectional CFRP," *Experimental Mechanics*, Allison (ed.), Balkema, Rotterdam, pp1399-1404
- Shahawy, M. and Beitelman, T. E. (1999), "Static and Fatigue Performance of RC Beams Strengthened with CFRP Laminates," *J. Struct. Engrg.*, ASCE, pp613-621
- Tang, H. C., Nguyen, T., Chuang, T. et al (2000), "Fatigue Model for Fiber-Reinforced Polymeric Composites," *J. Mat. Civil Engrg.*, ASCE, pp97-104
- Yang, X. B., Nanni, A., Haug, S. and Sun C. L. (2001), "Strength and Modulus Degradation of CFRP Laminates from Fiber Misalignment," *J. Mat. Civil Engrg.*, ASCE. (Accepted)

**LIST OF TABLES****Table 1 Failure Load****Table 2 Fatigue Test Matrix and Results**

**TABLE OF ILLUSTRATIONS**

- Fig. 1 Couple in Single Layer Specimen**
- Fig. 2 Symmetrical Configuration of a Specimen**
- Fig. 3 Coupon Specimen and Test Setup**
- Fig. 4 Failure Load versus Lap Splice Length**
- Fig. 5 Strain Gage Distribution of 101.6-mm Lap-spliced Specimens**
- Fig. 6 Load-Strain Curves on CFRP Laminates**
- Fig. 7 Strain Distribution in Lapped and Non-lapped Areas  
(101.6-mm lap splice length)**
- Fig. 8 FRP Laminate Fatigue Life**
- Fig. 9 Load-Strain Curves after Fatigue Loading**
- Fig. 10 Strain Change with Fatigue Cycles**
- Fig. 11 Residual Strength of CFRP Laminates**

**Table 1 Failure Load**

Lap splice length $d$ (mm)		12.7	25.4	38.1	50.8	76.2	101.6
Failure Load (kN) $P_f$	Specimen 1	19.4	37.3	45.9	48.9	N/A	45.7
	Specimen 2	18.7	34.0	46.6	43.5	46.6	47.9
	Specimen 3	20.9	36.6	50.7	47.4	48.7	N/A
Average failure load (kN) $P_{af}$		19.7	36.0	47.7	46.6	47.7	46.8
$P_{af}/P_u$ (%) *		34.6	63.3	83.8	81.9	83.8	82.2

\*  $P_u$  is the average experimental failure load of continuous unidirectional CFRP laminates.

$P_u=56.9$  kN (Yang *et al.* 2001)

**Table 2 Fatigue Test Matrix and Results**

$S_{max}$ (MPa)		2882	2165	1441
$S_{max}/\bar{f}_u$ (%)		80	60	40
$S_{min}$ (MPa)		180	180	180
Stress ratio $R$ $= \frac{S_{min}}{S_{max}}$ (%)		6	8	12
Fatigue life $N_f$ ( $\log_{10} N_f$ )	Specimen 1	48,000 (4.68)	537,528 (5.73)	>2,500,000 (6.40)
	Specimen 2	56,420 (4.75)	626,684 (5.80)	>2,500,000 (6.40)

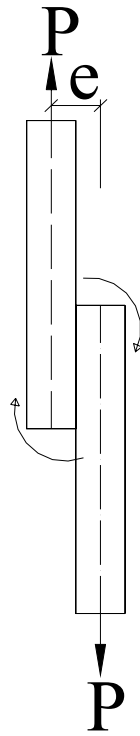


**Fig. 1 Couple in Single Layer Specimen**

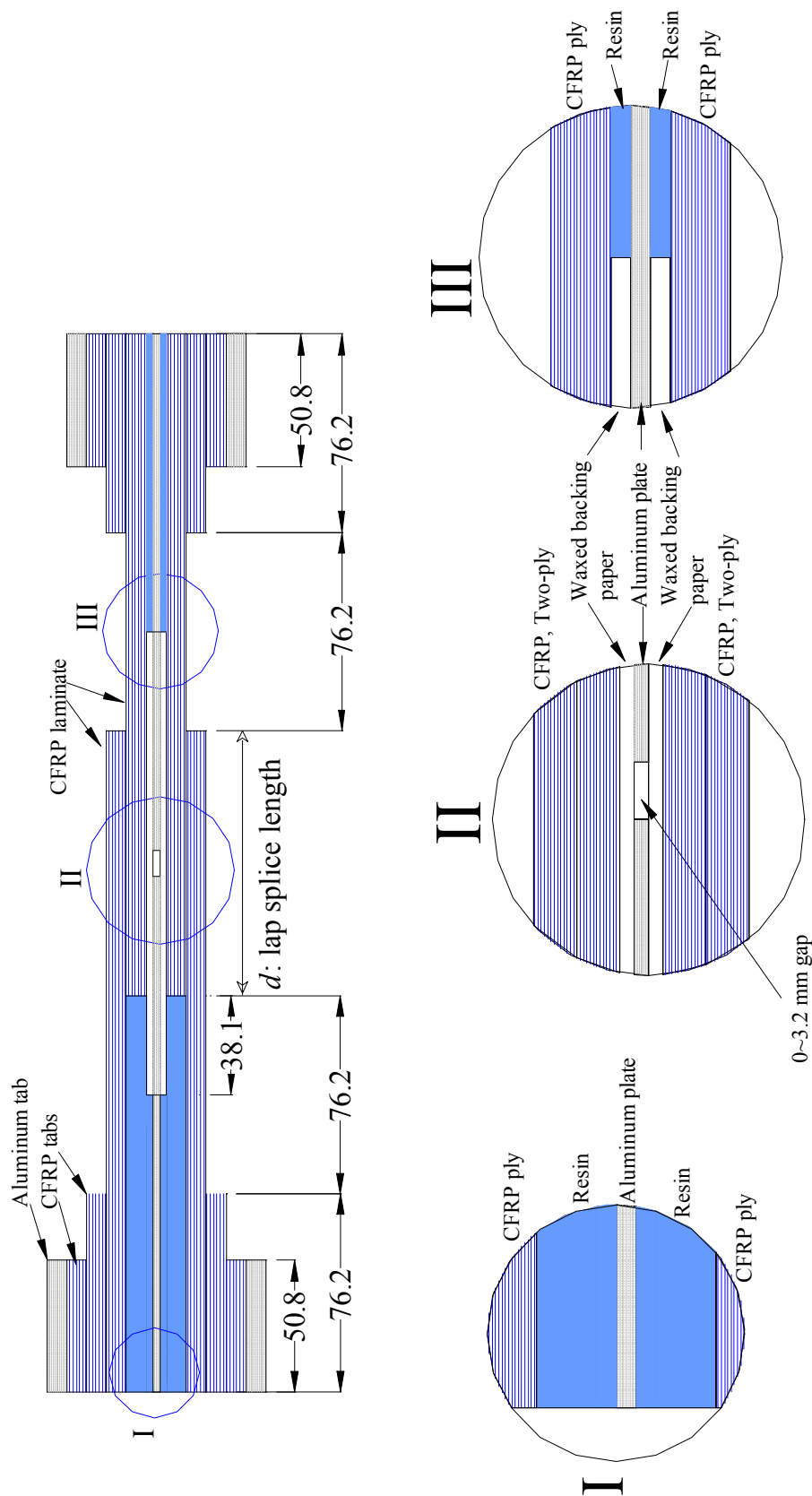
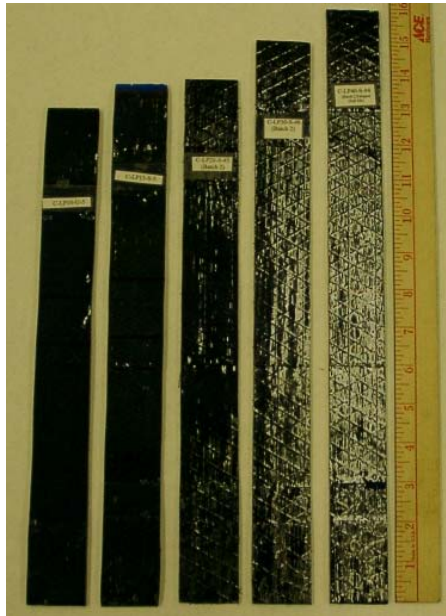
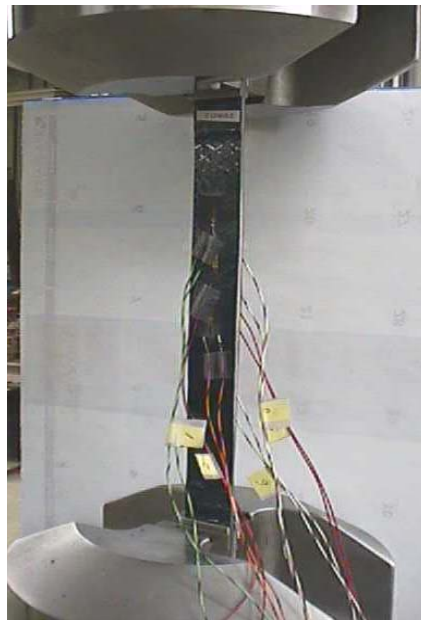


Fig. 2 Symmetrical Configuration of a Specimen (unit: mm)



(a) Test specimens



(b) Test setup

**Fig. 3 Coupon Specimen and Test Setup**

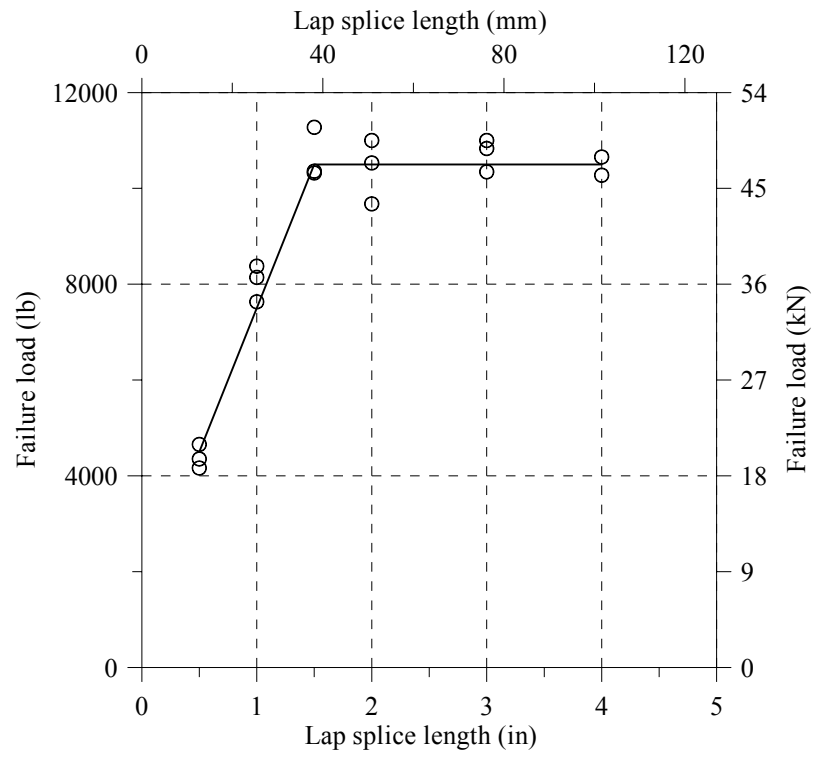


**Fig. 4 Failure Load versus Lap Splice Length**

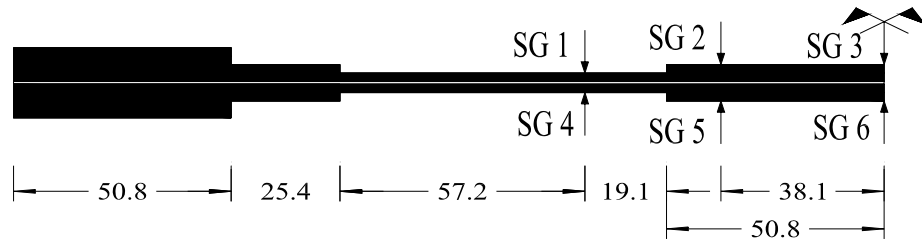
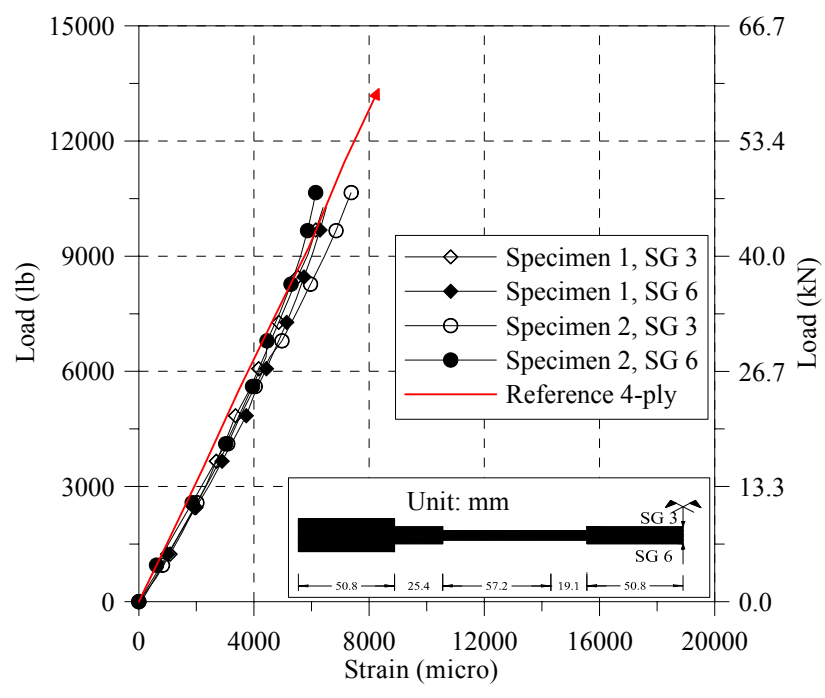
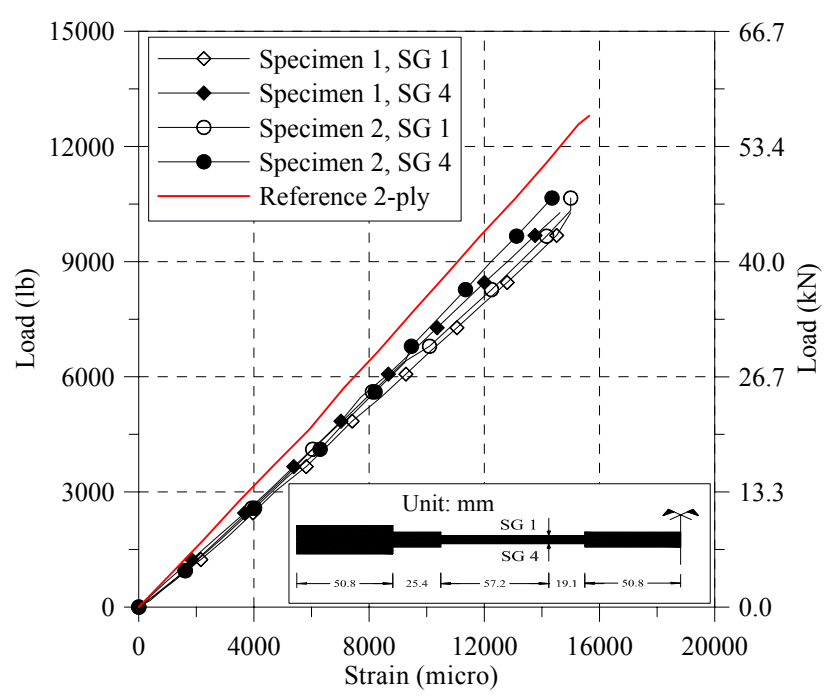


**Fig. 5 Strain Gage Distribution of 101.6 mm Lap-spliced Specimens**

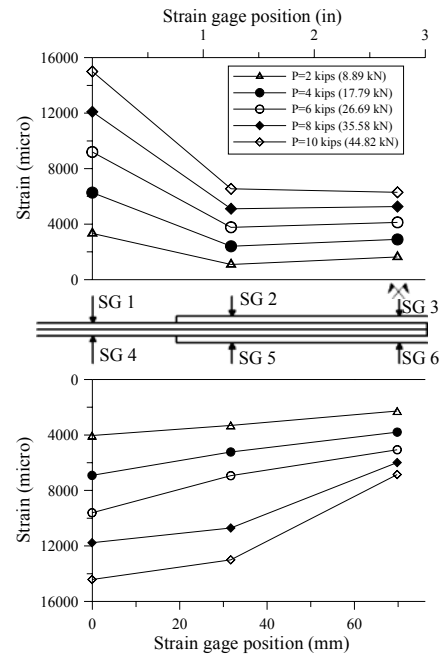
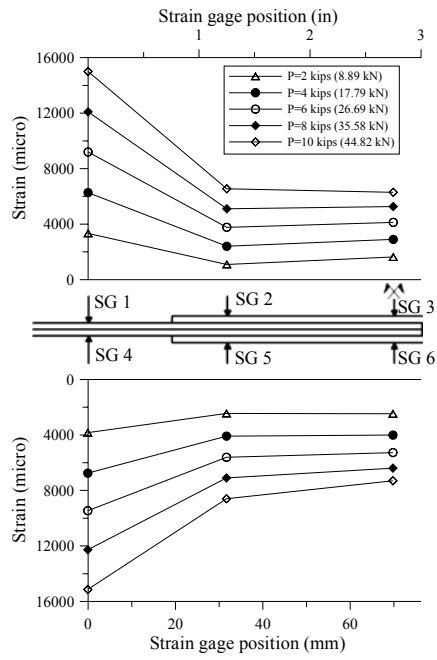


(a) Lapped area



(b) Non-lapped area

**Fig. 6 Load-Strain Curves on CFRP Laminates**



(a) Specimen 1

(b) Specimen 2

**Fig. 7 Strain Distribution in Lapped and Non-lapped Areas  
(101.6-mm lap splice length)**

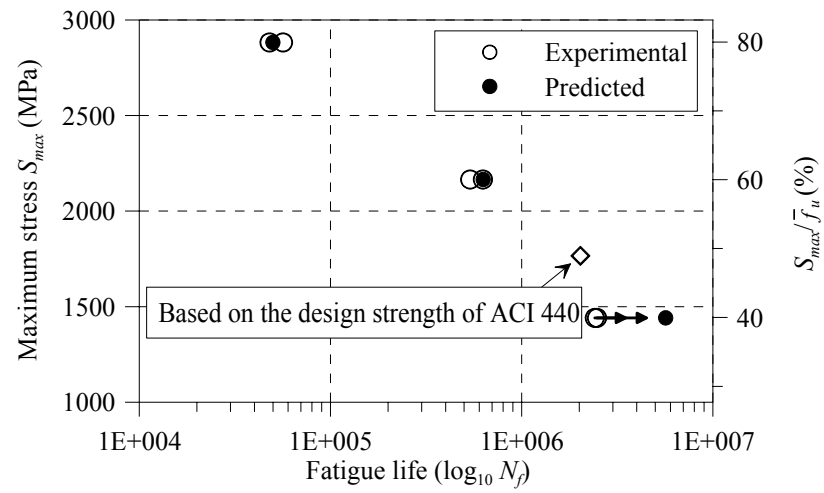
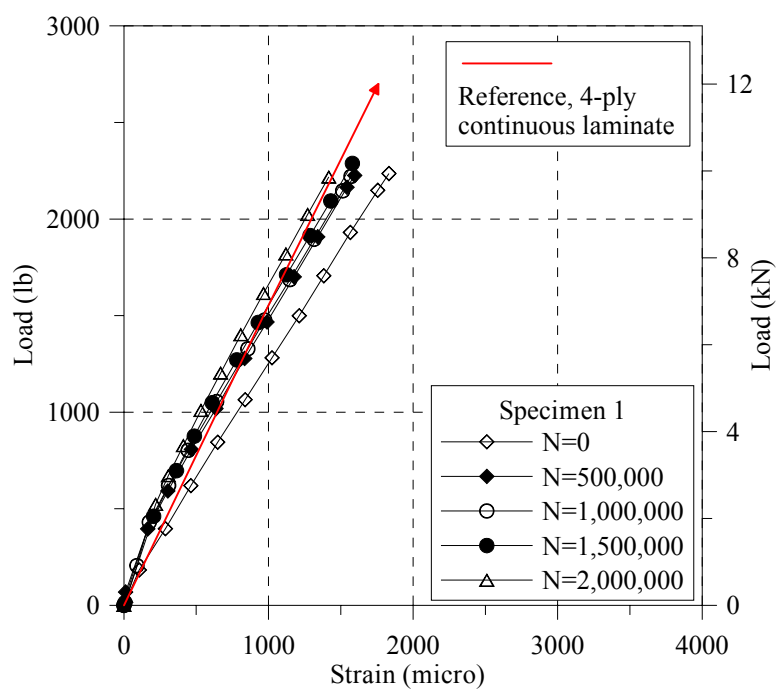
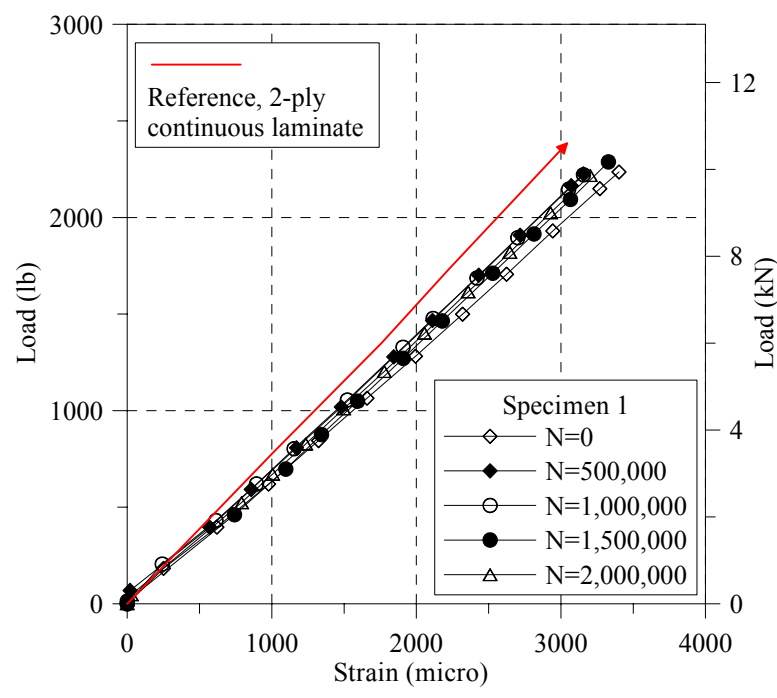


**Fig. 8 FRP Laminate Fatigue Life**



(a) Lapped area



(b) Non-lapped area

**Fig. 9 Load-Strain Curves after Fatigue Loading**

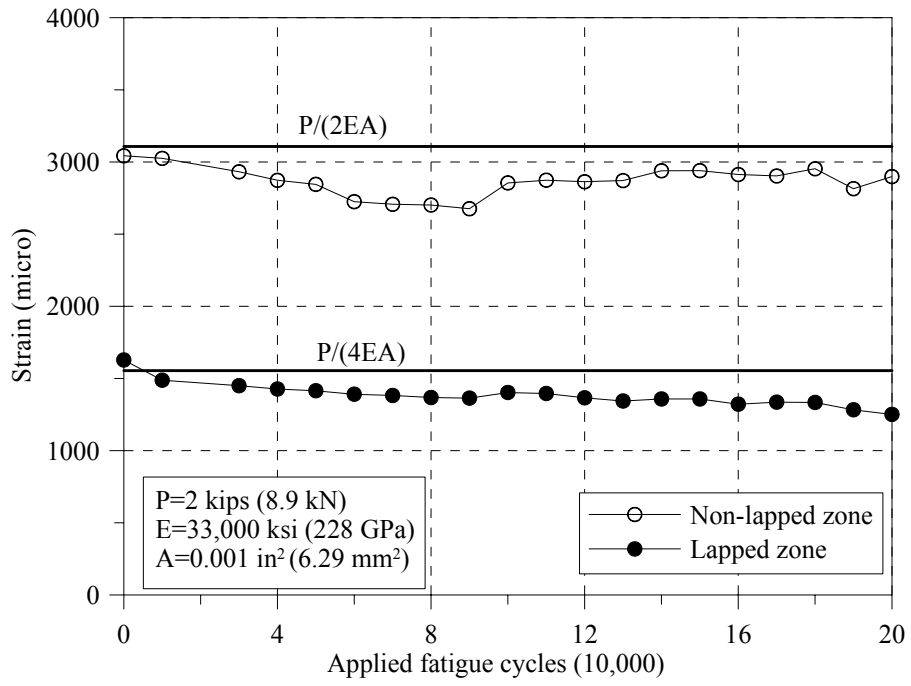


**Fig. 10 Strain Change with Fatigue Cycles**

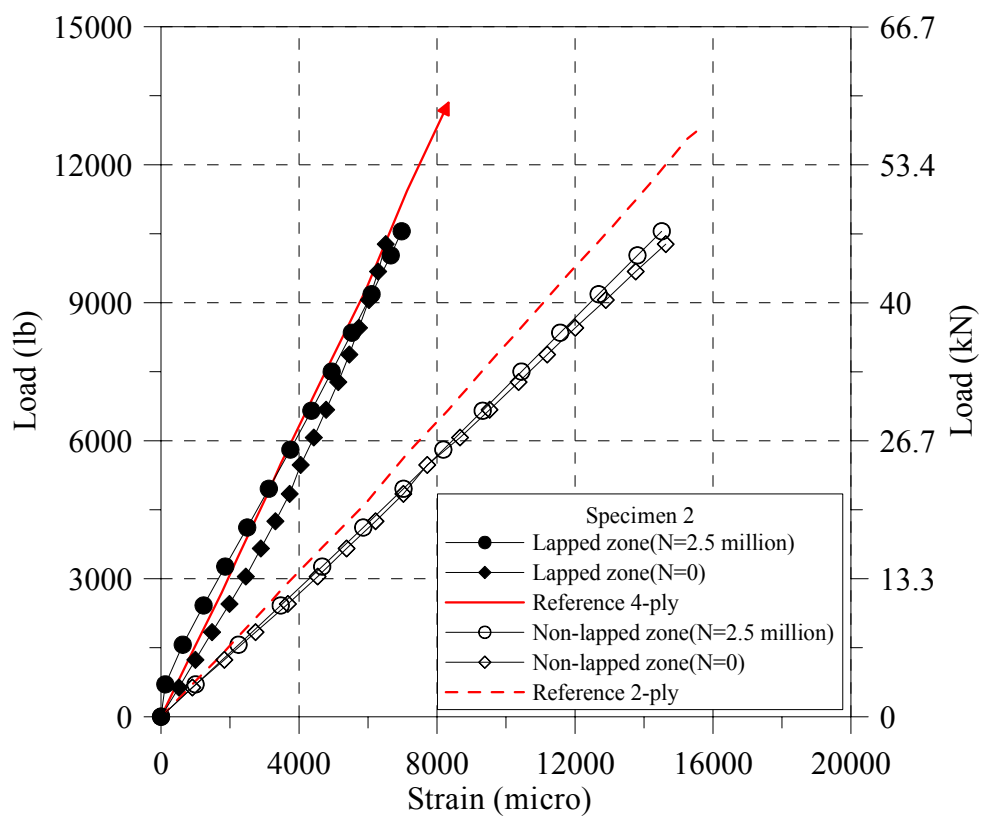


**Fig. 11 Residual Strength of CFRP Laminates**

## **Biographical Sketch of Authors**

**Xinbao Yang** is a PhD candidate in the Center for Infrastructure Engineering Studies, University of Missouri-Rolla, Rolla, MO. He holds his advanced degrees from Shanghai Institute of Railway Technology and Tongji University, Shanghai, China. His research interests include applications of FRP composite materials in reinforced concrete structures.

**Antonio Nanni**, FACI, is the V&M Jones Professor of Civil Engineering and Director of Center for Infrastructure Engineering Studies, University of Missouri-Rolla, Rolla, MO. He is a member of several ACI Technical Committees and Chair of ACI 437-strength evaluation. His research interests include the structural performance and field application of construction materials.

## CONCLUSIONS

Externally bonded FRP laminates have been developed as mainstream strengthening technology in the last decade to make concrete structures resist higher design loads. Successful implementation of FRP composites lies in many aspects in manufacturing, design, and construction, which, in general, include scientifically valid and widely accepted design specifications and strict construction quality control procedures. Three critical aspects on the performance of FRP systems have been covered in the investigation of this dissertation: fiber misalignment, corner radius, and lap splice length. Both experimental and theoretical investigations have been performed and the results have been presented in six technical papers. The main conclusions are presented herein separately on the three topics.

### **Fiber Misalignment**

- Strength more than the elastic modulus of CFRP laminates is affected by fiber misalignment.
- In practice, all misaligned fibers in a laminate can be regarded as through fibers (all fibers are anchored on both ends), it is recommended to use a reduction factor for strength and no reduction factor for stiffness to account for fiber misalignment.
- The results from testing concrete beams strengthened with misaligned CFRP laminate verified the degradation of strength and modulus.
- It is recommended that the misalignment angle of FRP laminates not exceed 5 degree to avoid any significant degradation of strength or stiffness.

### **Corner radius**

- Corner radius plays an important role on the mechanical properties of CFRP laminates. It is indicated that at best only 67% of the ultimate laminate strength can be developed when wrapped around a circular cross section. As the corner radius decreases, the efficiency of FRP wrapping further reduces.
- Multiple placements of FRP plies can slightly increase the strength of bent CFRP laminates and improve the overall strengthening performance except for rectangular sections with sharp corners.

- The testing method and the reusable device are reliable for the investigation on the effect of corner radius on the performance of FRP laminates when wrapping structural cross sections.
- A smaller corner radius can significantly reduce the ultimate strength of the FRP laminate due to stress concentration around the corner area. The stress concentration factor increases when the corner radius decreases. Conversely, the radial stress decreases with increasing corner radius.
- The finite element method can predict the stress concentration in the fiber direction and the radial stress distribution.
- It is recommended that a minimum of 1.0 in. corner radius be used when FRP laminates are used to strengthen structures.

### **Lap Splice Length**

- A lap splice length of 1.5 in. is sufficient for CFRP laminates to develop the ultimate tensile strength under quasi-static loading.
- 4-inch lap-spliced CFRP laminates showed satisfactory fatigue performance in that no fatigue failure was observed after 2.5 million cycles of fatigue loading at a maximum stress  $S_{max} = 0.4 \bar{f}_u$ , where  $\bar{f}_u$  is the static ultimate strength of the lap-spliced CFRP laminate.
- The strength and modulus of 4-inch lap-spliced laminate showed negligible degradation after being subjected to 2.5 million cycles of fatigue loading at  $S_{max} = 0.4 \bar{f}_u$ .
- A lap splice length of 4.0 in. is recommended if CFRP laminates are used for strengthening concrete structures.
- The allowable service stress  $F_a$  specified by ACI 440 Design Guide appears to be safe for a lap splice up to 2.0 million cycles.

## **APPENDIX 1**

### **Proposed Standard Test Method for Determining the Effect of Corner Radius on Tensile Strength of Fiber Reinforced Polymers**

## **Proposed Standard Test Method for Determining the Effect of Corner Radius on Tensile Strength of Fiber Reinforced Polymers**

### **1. Scope**

1.1 This method determines the effect of corner radius on the properties of fiber reinforced polymers (FRP's) used in strengthening structural cross sections where the composite laminates are subject to directional change when wrapped around corners of sections. Tension tests are conducted using a three-component test fixture. The specimen is wet wrapped and cured over the test fixture.

1.2 The SI units are to be regarded as the standard.

1.3 This guide does not purport to address all of the safety concerns, if any, associated with its use. It is the responsibility of the user of this guide to establish appropriate safety and health practices and determined the applicability of regulatory limitations prior to use.

### **2. Referenced Documents**

#### *2.1 ASTM Standards*

D 883 Terminology Relating to Plastics

D 3039/D 3039M Test Method for Tensile Properties of Polymer Matrix Composite Materials

E 4 Practices for Force Verification of Testing Machines

E 6 Terminology Relating to Methods of Mechanical Testing

E 1012 Practice for Verification of Specimen Alignment Under Tensile Loading

### **3. Summary of Test Method**

Tension tests are conducted using a unique test fixture. The testing fixture consists of three components, upper and lower parts and interchangeable aluminum corner inserts(Figure 1). Detailed dimensions are shown in Figures 2, 3, 4, 5, and 6. The FRP specimen in the form of a thin strip is wet wrapped and cured around the surface of the test fixture and lap-spliced in the lower part (semi-circular anchoring area). Instrumentation is mounted depending on the variables being monitored. If modulus and strain distribution are required, strain gages can be mounted around the corner areas. In addition, the radial stress exerted by the FRP laminate on the aluminum surface can be measured with pressure meters or pressure films. The load is applied until failure of the FRP specimen.

### **4. Significance and Use**

4.1 This tension test can provide accurate information with regard to the effect of corner radius on the tensile properties of FRP's when applied under conditions with similar interaction mechanisms to those of the test method.

4.2 This test can be used to acquire data of strength development, radial stress distribution, and failure mode when FRP is used to wrap an existing member section for strengthening.

4.3 The method can be used for testing composite materials with any fiber type. Due to the limited width and wet wrapping procedure, unidirectional laminates are preferred.

4.4 The data provided by this test can be used for research and development, design, and acceptance/rejection criteria.

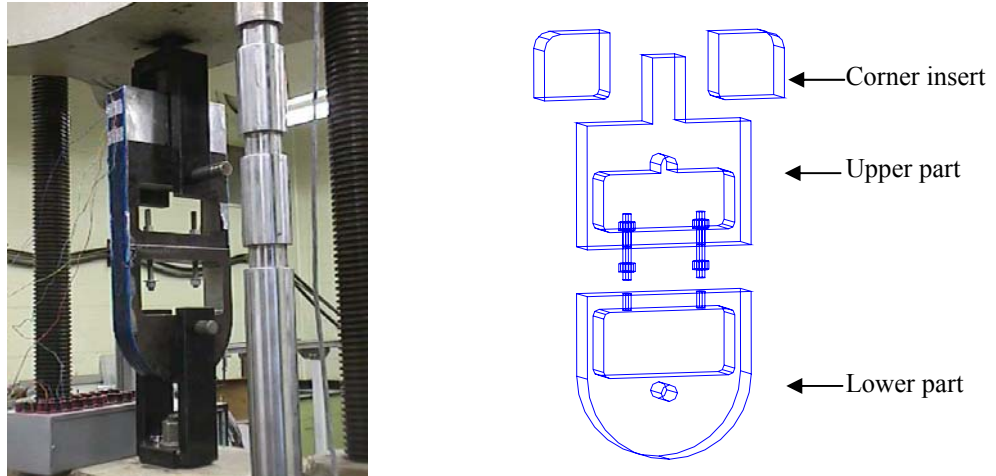


Fig. 1 Assembled Test Fixture

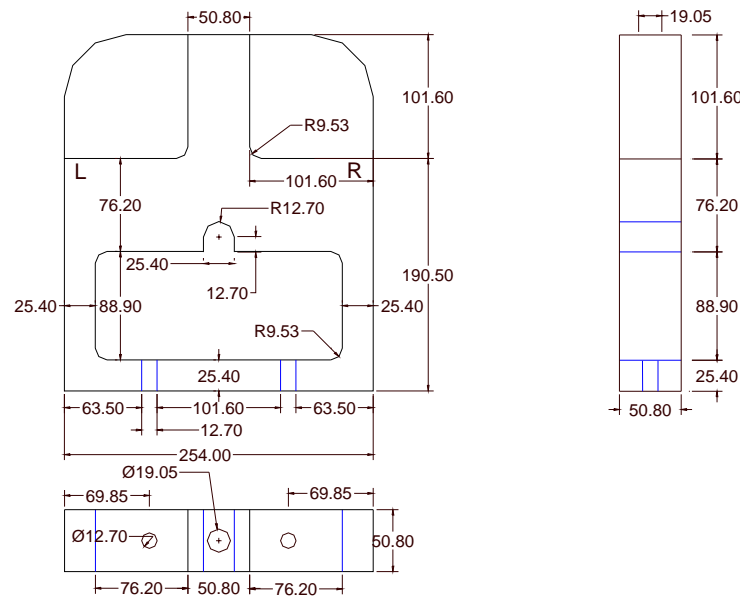


Fig. 2 Upper Part of Test Fixture(mm)

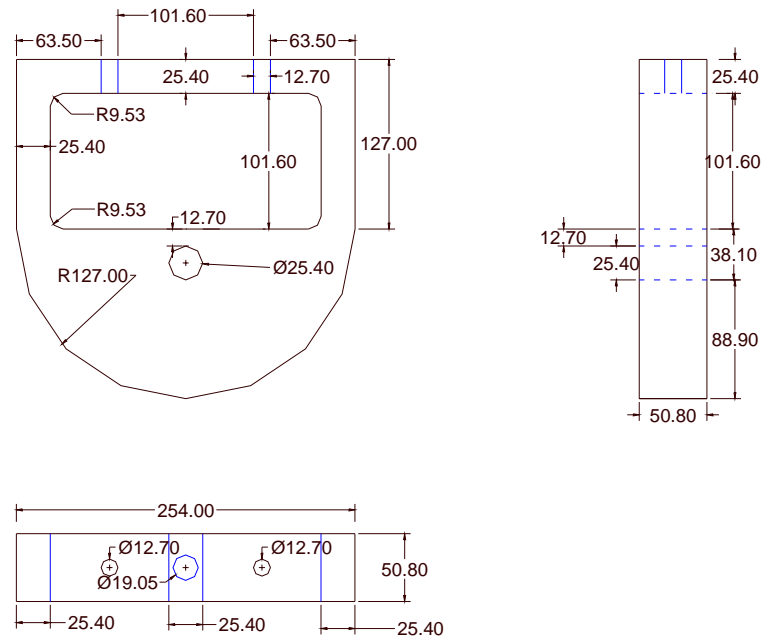


Fig. 3 Lower Part of Test Fixture(mm)

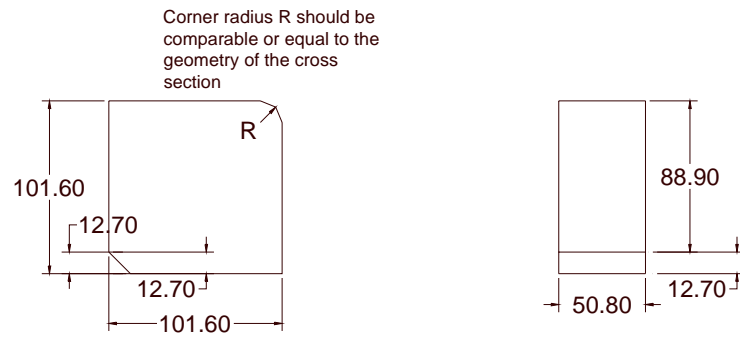


Fig. 4 Interchangeable Corner Inserts(mm)

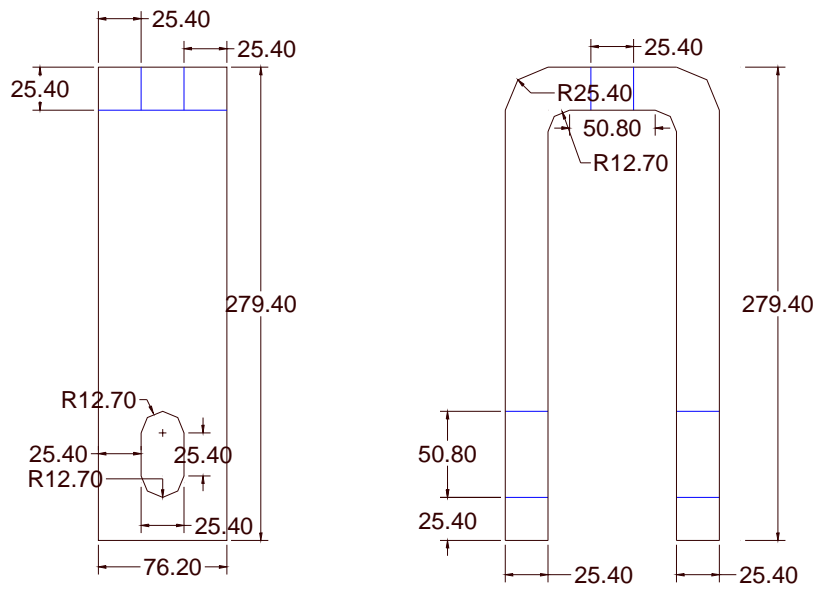


Fig. 5 Tensile Fixture(Two sets needed) (mm)

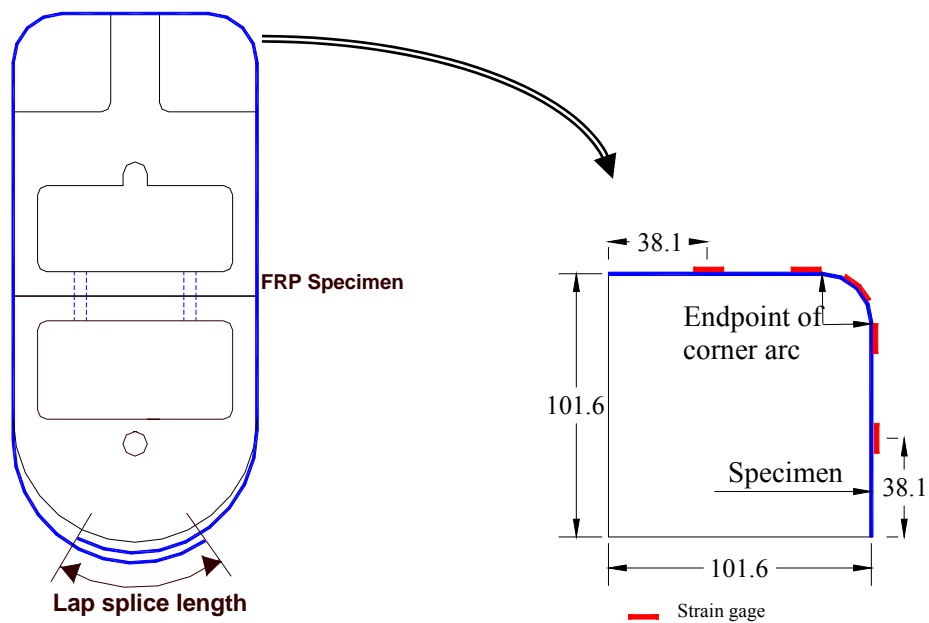


Fig. 6 Installation of Specimen and Suggested Strain Gage Arrangement(mm)

## 5: Apparatus

5.1 *Gages*, accurate to at least 0.01mm for measuring the width of the specimen.

5.2 *Testing machine*, comprised of the following:

5.2.1 *Fixed member*---A fixed or essentially stationary member supporting the load fixture.

5.2.2 *Movable member*---A member capable of applying a tensile load to the tensile loading fixture and transfer the load to the test fixture.

5.2.3 *Drive mechanism*---A drive for imparting to the movable member a controlled speed with respect to the stationary member.

5.2.4 *Load Indicator*---A suitable load-indicating mechanism capable of showing the total tensile load carried by the test fixture. This mechanism should indicate the load with an accuracy of 1% or better of the actual value. The accuracy should be verified in accordance with Practice E4 in ASTM

5.3 *Strain Recording*---A Suitable strain-recording system is required for modulus determination and strain distribution.

### 5.4 *Test Fixture*

The test fixture consists of the upper and lower parts around which the FRP laminate is wrapped. The upper part is used as the testing area because the interchangeable corner inserts are located at its two corners. The lower part is used to anchor the specimen through lap splicing. A semi-circular shape is used for better anchoring performance. Two bolts are used to hold the upper and lower fixture sections together during specimen installation.

5.5 *Tensile Loading Fixtures* are used to transfer the load from the testing machine to the test fixture (Figure 5). All drilled holes in tensile loading fixtures and test fixture should be oversized to avoid any twisting and tightening when the rods and nuts are installed. It is recommended that all holes are drilled 1.60mm larger than nominal value.

5.6 *Pressure Film* can show the pressure change by changing its color under different pressure. It may be mounted in any area where the pressure distribution measurement is desired. It is recommended that a pressure film be mounted around a corner between points of changing curvature.

## 6. Test Specimen

6.1 *Geometry*. The FRP test specimen shall conform to the dimensions of the test fixture shown in Figure 2 and 3.

6.1.1 *Width*---Specimen width must be less than the width of the side surface of testing fixture. A value of 38.1mm is recommended.

6.1.2 *Laminate Lap Splice*---The lap splice should be sufficient to guarantee that failure occurs in the upper fixture area.

6.1.3 *Alignment*, the specimen should be installed with its center-line parallel to that of the side surface of test fixture. A convenient method is to have two lines are marked on the side surface of the test fixture between which the FRP sheets is applied.

6.1.4 *Number of plies*---multiple plies of FRP laminates can be applied as long as the failure load is less than the capacity of the test fixture.

6.2 *Strain*- Where load-strain data are desired, the specimen may be instrumented with strain gages. The strain gages should be located at the center of the specimen in the width direction and parallel to the fiber direction. Strain gages should be mounted on both the flat surfaces outside the corner area and the corner area. A recommended strain gage arrangement is shown in Figure 6.

6.3 *Number of Specimen*. A minimum of three specimens is recommended for each material.

#### 6.4 Wrapping Procedure

6.4.1 *Application of Release Layer*. A release tape is first wrapped and tightened around the entire side surface of the test fixture prior to specimen wrapping. The tape is used to prevent the polymer matrix from bonding to the fixture surface. It also reduces the friction between the fixture surface and the test specimen. The following release tapes have been successfully used: Marking tape; Waxed backing paper; Plain paper, and Polyethylene tape.

6.4.2 *Wet wrapping of Specimen*. After the release type is in place, the specimen is wet wrapped around the entire side surface of the test fixture. A thin layer of saturant is applied on both the surface of release layer and the FRP sheet. After the FRP sheet is attached on the side surface of the test fixture and lap-spliced in the semi-circular lower part, a plastic roller is used to saturate the sheet and also work out the entrapped air between the FRP sheet and the release layer.

### 7. Procedure

7.1 *Assembling of Test Fixture*, the upper and lower parts of test fixture are connected and fastened using two bolts. Corner inserts with desired radius are glued at both corners of the upper part. The radii of the two corner inserts can be different if a performance comparison is expected in a single test.

7.2 *Wet wrapping of specimen*--The specimen is wet wrapped around the test fixture.

7.3 *Curing Specimen(polymerization)*--The specimen is cured under conditions specified by manufacturer before strain gages are attached when desired.

7.4 The fastened test fixture with cured specimen is placed onto the testing machine and connected to the tensile fixture using two short plain rods through the holes on the lower and upper parts. Ensure that there is no misalignment between test fixture and tensile loading fixture in order to produce a uniform stress distribution in the specimen. No twisting should be produced in the test fixture and specimen.

7.5 Loosen the nuts of the bolts that connect the upper and lower part of test fixture. The nuts should not be removed from the bolts so that after failure of the specimen, the bolts can still prevent the test fixture from separation.

7.6 Connect data recording equipment.

7.7 Apply and release a small load on the specimen (less than 5% of expected failure load) to realign the test fixture. The strain gages are zeroed in this step.

7.8 Set the recommended speed of testing. Speed of Testing shall be determined by the specifications for the material being tested or by the client. However, when the speed of testing is not specified, a speed of 1.0~2.0mm/min is recommended.

7.9 Record the strain and load values continuously.

7.10 Record the maximum load from the load indicator of the testing machine.

7.11 Record the failure mode of specimen. The failure zone is normally located around the corner.

## 8. Conditioning

8.1 *Standard Conditioning Procedure*, the test specimen shall be conditioned and tested in a room or enclosed space at  $23\pm 2^{\circ}\text{C}$  and  $50\pm 5\%$  relative humidity in accordance with Procedure A of Practice D 618.

8.2 Other conditioning protocols may be specified by client.

## 9. Calculations

9.1 *Reduced Tensile Strength*: Calculate the reduced tensile strength using the following equation. Report the results to three significant figures.

$$S=P/(2wt)$$

Where:

S=reduced tensile strength of specimen corresponding to a specific corner radius(MPa)

$P$ =Failure load of specimen(N)  
 $w$ =Width of specimen(mm)  
 $t$ =thickness of FRP sheet or its fiber(mm)

9.2 *Tensile Modulus*: Calculate the tensile modulus of different points using the following equation. Report the results to three significant figures.

$$E = \Delta P / (2wt\Delta\varepsilon)$$

Where:

$E$ =Elasticity modulus of specimen(MPa)

$\Delta P$ =Load increment(N)

$w$ =Width of specimen(mm)

$t$ =thickness of FRP sheet or its fiber(mm).

$\Delta\varepsilon$ =Strain increment

9.3 For each series of specimens, calculate the mean value,

$$\bar{x} = \frac{\sum_{i=1}^N X_i}{N}$$

Where:

$X_i$ =test value of the  $i^{\text{th}}$  test and

$N$ =number of samples.

## 10. Report

10.1 Complete identification of the material tested, including tape, source, manufacturer's code number, form, previous history, resin type, processing details, specimen quality control, description of equipment used, deviations from this standard test method, complete description of the fabrication process of the specimen compared with the specified one provided by the manufacturer.

10.2 Method of preparing test specimen and verification of quality.

10.3 Test specimen dimensions and corner radius.

10.4 Test environment and conditioning procedure.

10.5 Number of specimens tested.

10.6 Speed of testing.

10.7 Failure load.

10.8 Individual specimen strength and average values.

10.9 Individual specimen modulus and average values.

10.10 Date of tests.

## **11. Keywords**

11.1 Corner radius, fiber reinforced polymers, modulus of elasticity, strengthening, tensile strength.

## **APPENDIX 2**

### **Stress Strain Curve of Misaligned CFRP Laminates**

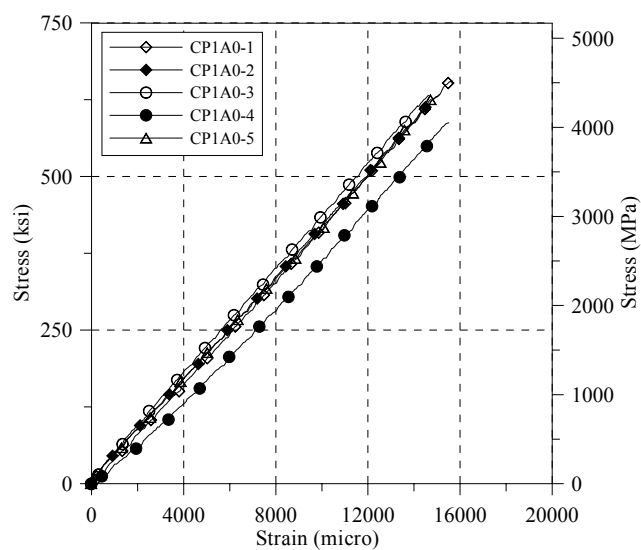


Fig. 1 Stress strain curve of one-ply CFRP laminate ( $\theta = 0^\circ$ )

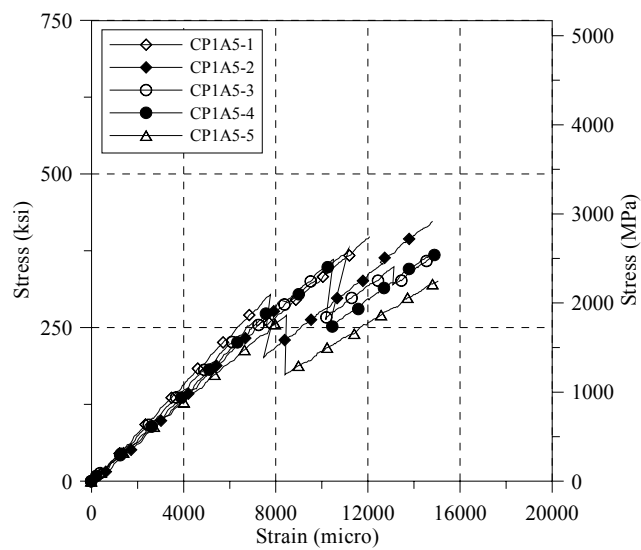


Fig. 2 Stress strain curve of one-ply CFRP laminate ( $\theta = 5^\circ$ )

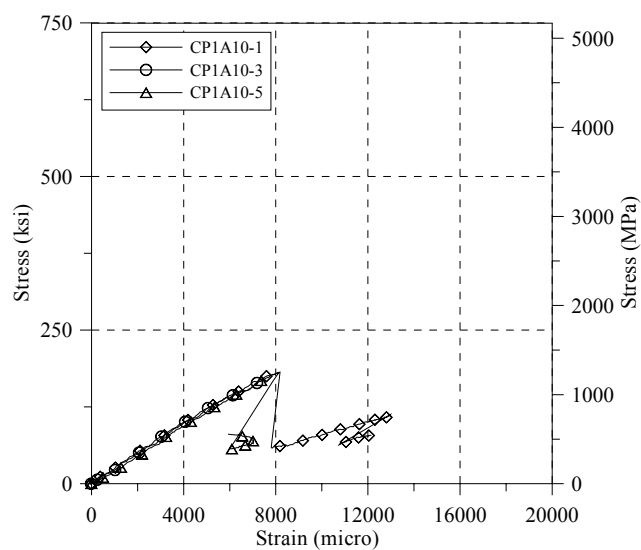


Fig. 3 Stress strain curve of one-ply CFRP laminate ( $\theta = 10^\circ$ )

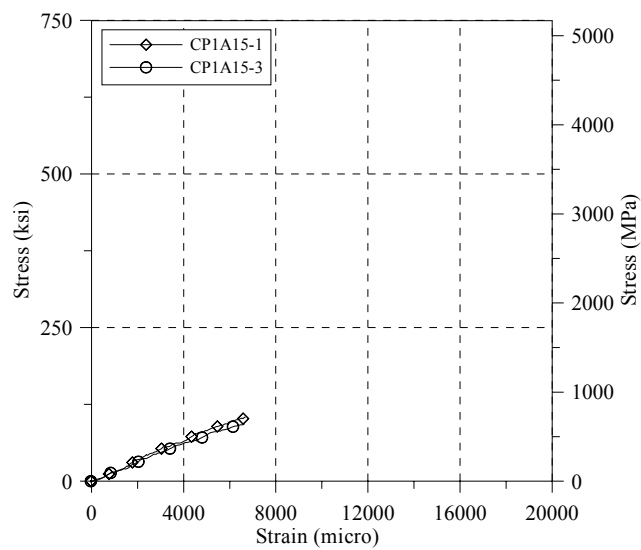


Fig. 4 Stress strain curve of one-ply CFRP laminate ( $\theta = 15^\circ$ )

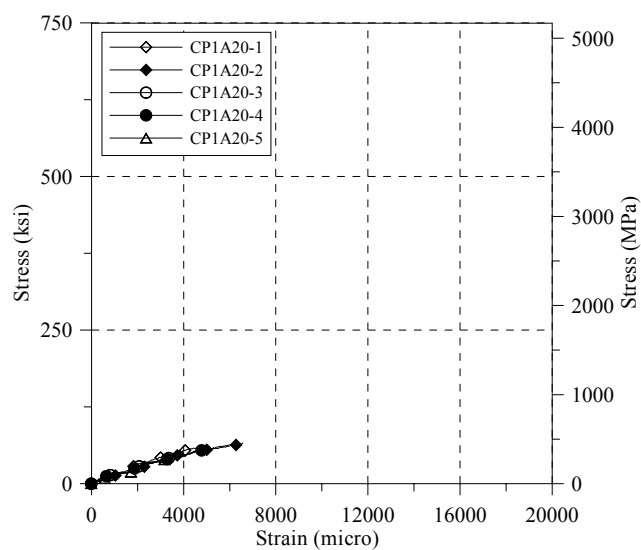


Fig. 5 Stress strain curve of one-ply CFRP laminate ( $\theta = 20^\circ$ )

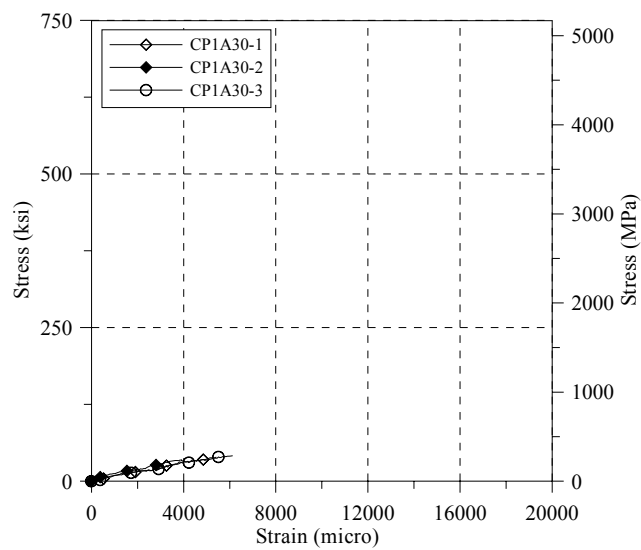


Fig. 6 Stress strain curve of one-ply CFRP laminate ( $\theta = 30^\circ$ )

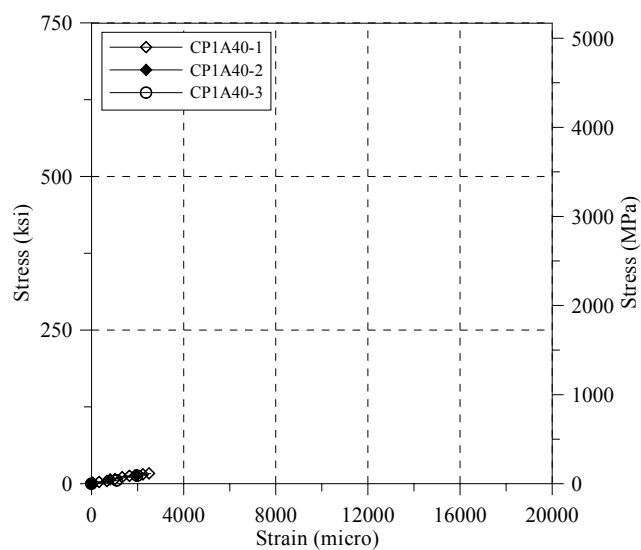


Fig. 7 Stress strain curve of one-ply CFRP laminate ( $\theta = 40^\circ$ )

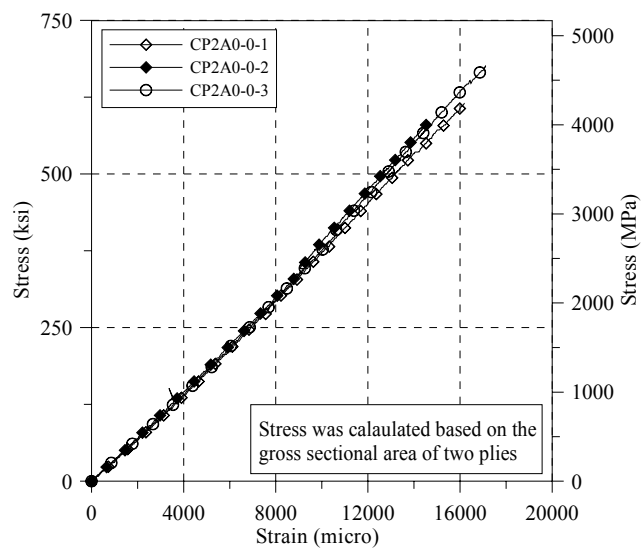


Fig. 8 Stress strain curve of two-ply CFRP laminate ( $\theta = 0^\circ \sim 0^\circ$ )  
(based on gross sectional area)

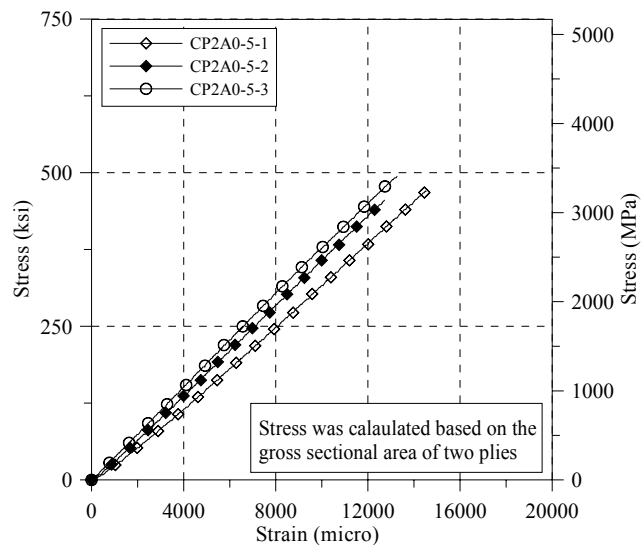


Fig. 9 Stress strain curve of two-ply CFRP laminate ( $\theta = 0^\circ \sim 5^\circ$ )  
(based on gross sectional area)

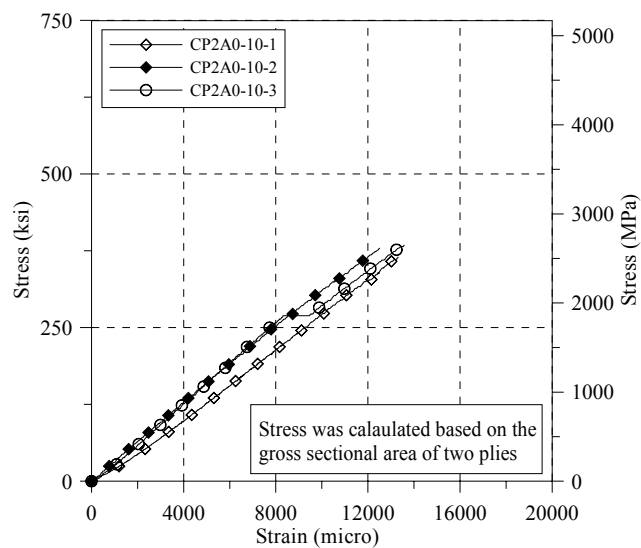


Fig. 10 Stress strain curve of two-ply CFRP laminate ( $\theta = 0^\circ \sim 10^\circ$ )  
(based on gross sectional area)

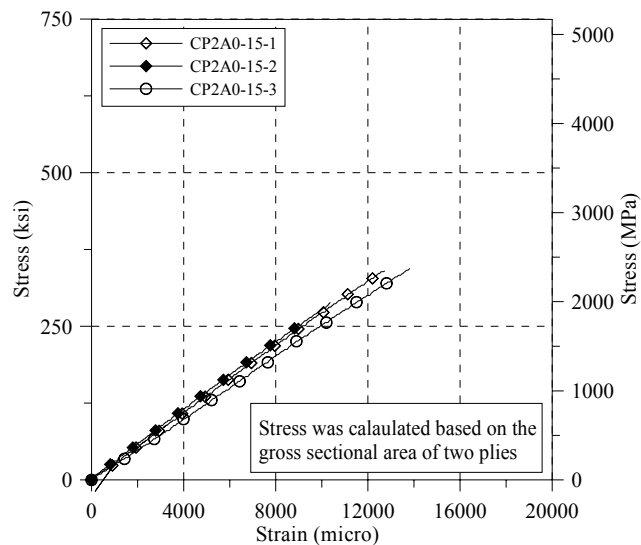


Fig. 11 Stress strain curve of two-ply CFRP laminate ( $\theta = 0^\circ \sim 15^\circ$ ) (based on gross sectional area)

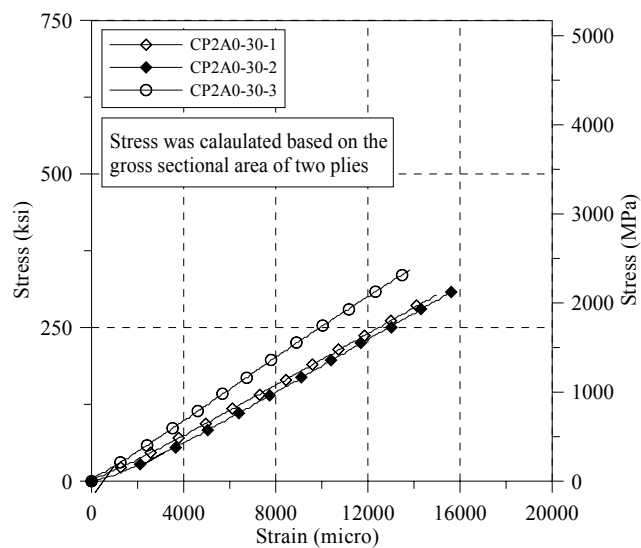


Fig. 12 Stress strain curve of two-ply CFRP laminate ( $\theta = 0^\circ \sim 30^\circ$ ) (based on gross sectional area)

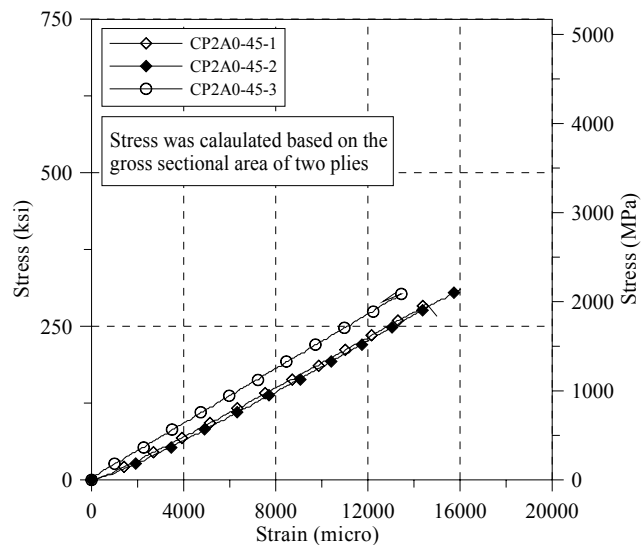


Fig. 13 Stress strain curve of two-ply CFRP laminate ( $\theta = 0^\circ \sim 45^\circ$ ) (based on gross sectional area)

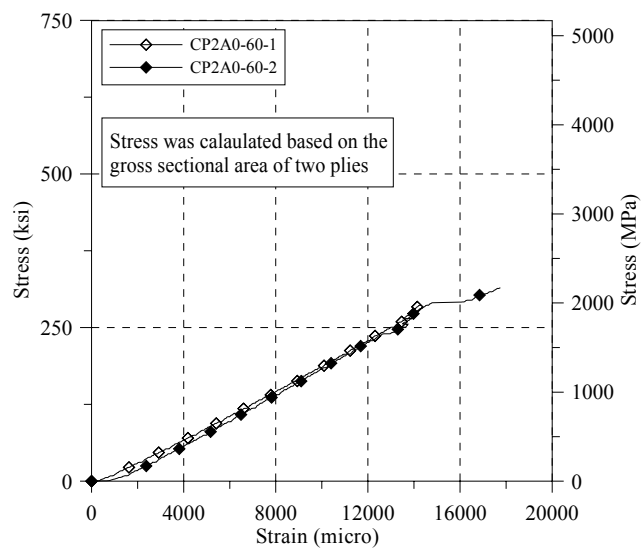


Fig. 14 Stress strain curve of two-ply CFRP laminate ( $\theta = 0^\circ \sim 60^\circ$ ) (based on gross sectional area)

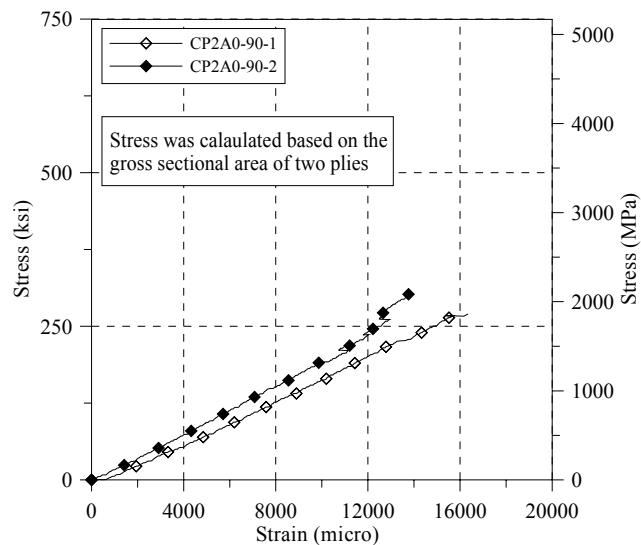


Fig. 15 Stress strain curve of two-ply CFRP laminate ( $\theta = 0^\circ \sim 90^\circ$ ) (based on gross sectional area)

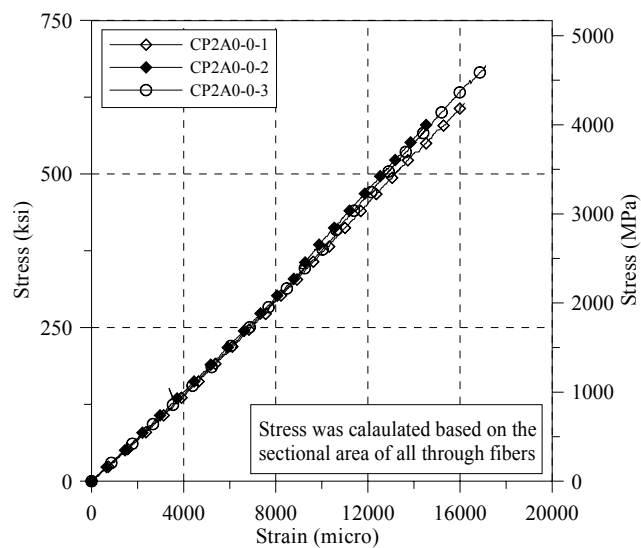


Fig. 16 Stress strain curve of two-ply CFRP laminate ( $\theta = 0^\circ \sim 0^\circ$ ) (based on sectional area of through fibers)

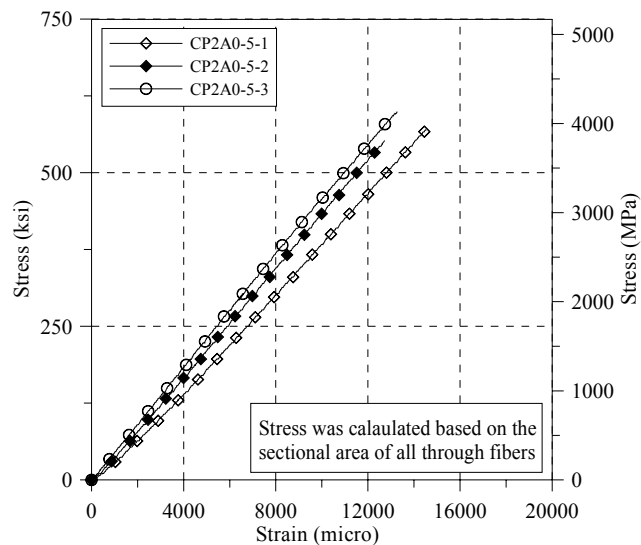


Fig. 17 Stress strain curve of two-ply CFRP laminate ( $\theta = 0^\circ \sim 5^\circ$ ) (based on sectional area of through fibers)

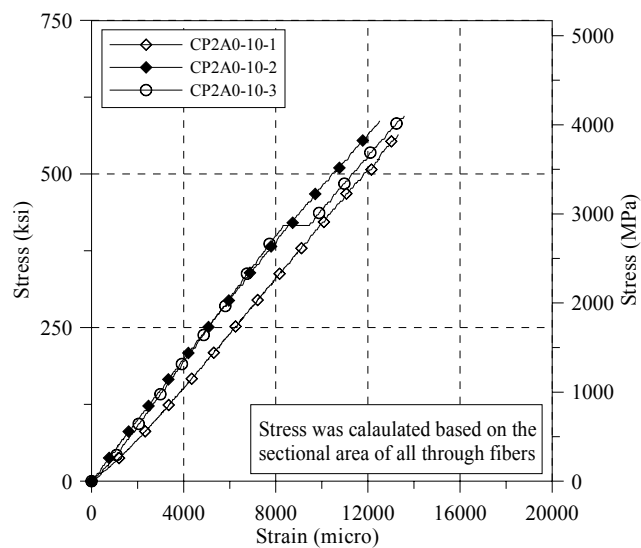


Fig. 18 Stress strain curve of two-ply CFRP laminate ( $\theta = 0^\circ \sim 10^\circ$ ) (based on sectional area of through fibers)

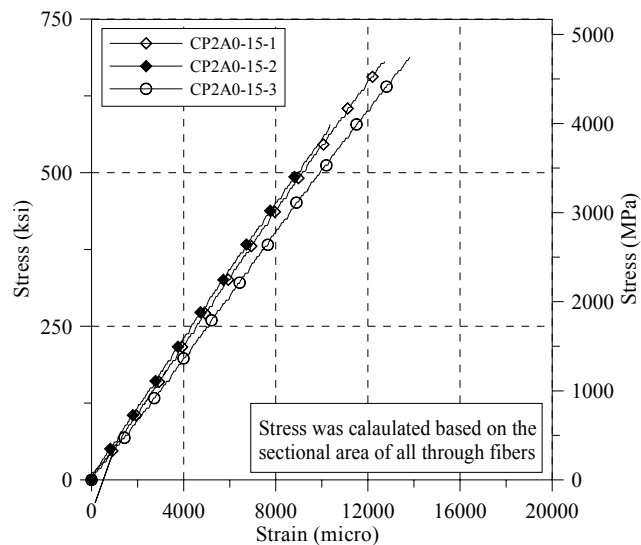


Fig. 19 Stress strain curve of two-ply CFRP laminate ( $\theta=0^{\circ}\sim 15^{\circ}$ ) (based on sectional area of through fibers)

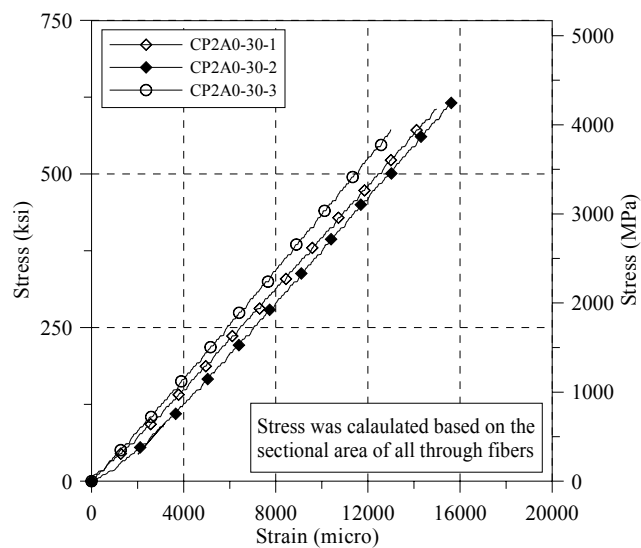


Fig. 20 Stress strain curve of two-ply CFRP laminate ( $\theta=0^{\circ}\sim 30^{\circ}$ ) (based on sectional area of through fibers)

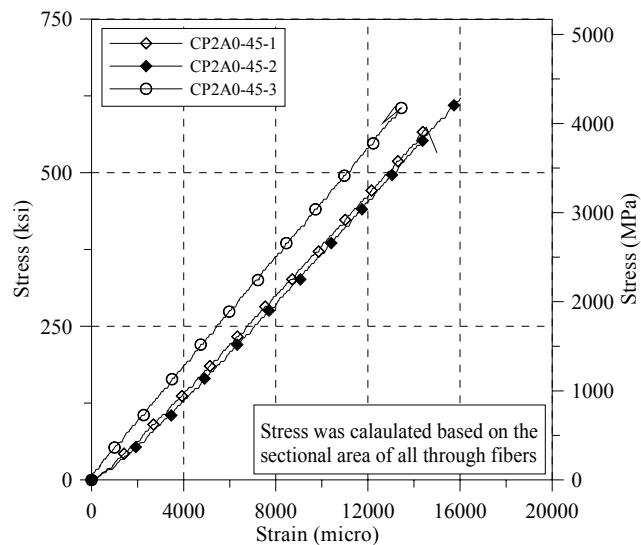


Fig. 21 Stress strain curve of two-ply CFRP laminate ( $\theta=0^{\circ}\sim 45^{\circ}$ ) (based on sectional area of through fibers)

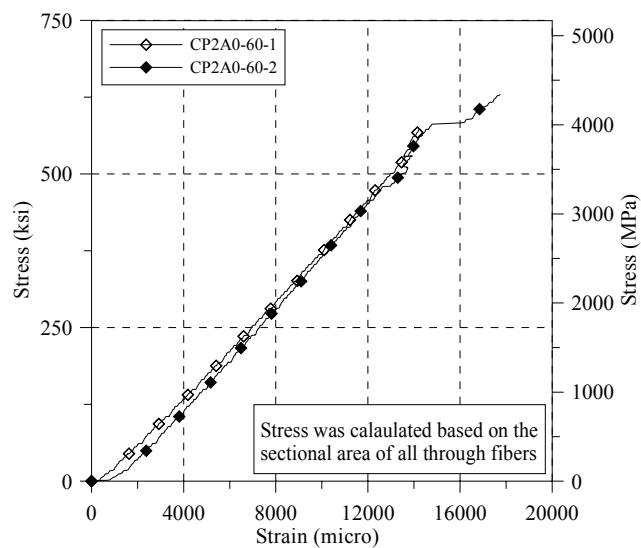


Fig. 22 Stress strain curve of two-ply CFRP laminate ( $\theta=0^{\circ}\sim 60^{\circ}$ ) (based on sectional area of through fibers)

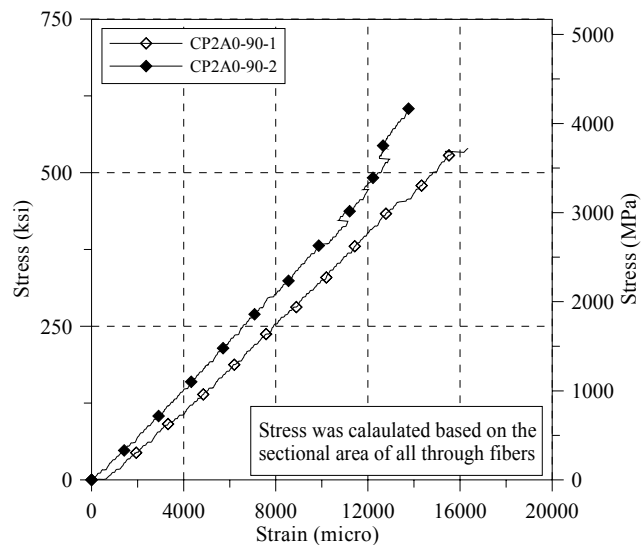


Fig. 23 Stress strain curve of two-ply CFRP laminate ( $\theta = 0^\circ \sim 90^\circ$ ) (based on sectional area of through fibers)

### **APPENDIX 3**

#### **Stress Strain Curve of FRP Laminates with Different Corner Radius and Confining Stress between Curvature Changing Points**

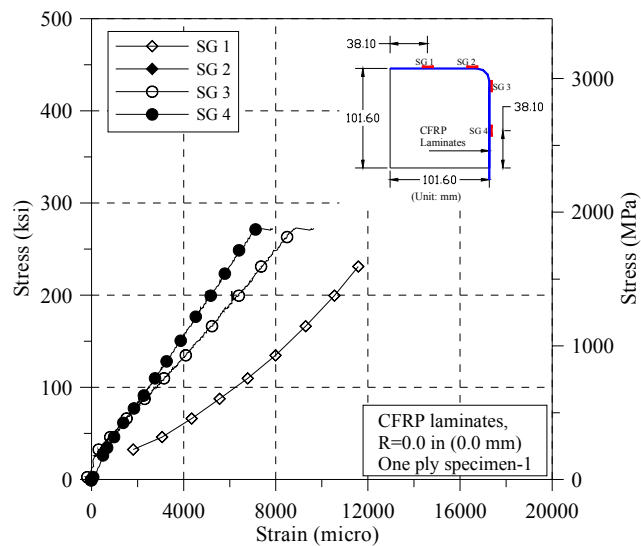


Fig. 1 Stress strain curve of one ply CFRP laminates (R=0.0 mm, Specimen 1)

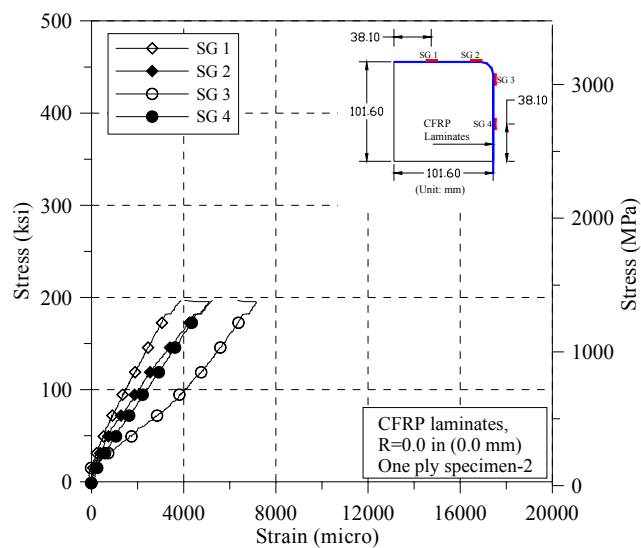


Fig. 2 Stress strain curve of one ply CFRP laminates (R=0.0 mm, Specimen 2)

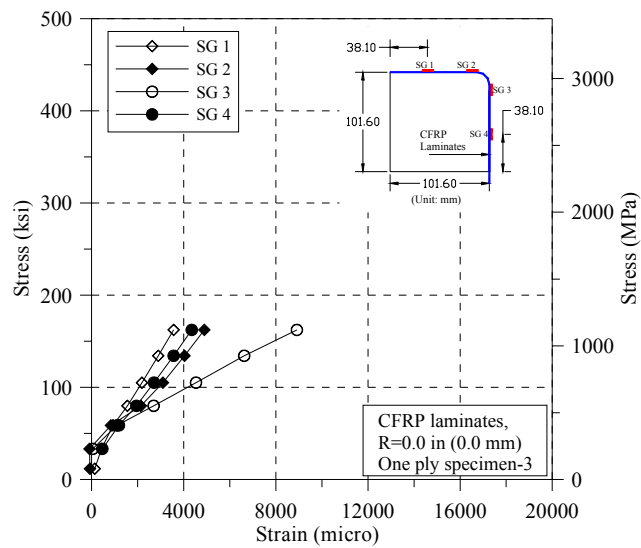


Fig. 3 Stress strain curve of one ply CFRP laminates (R=0.0 mm, Specimen 3)

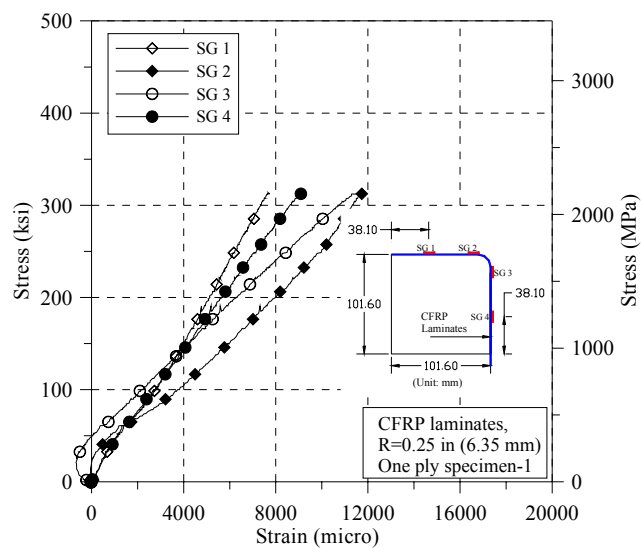


Fig. 4 Stress strain curve of one ply CFRP laminates (R=6.35 mm, Specimen 1)

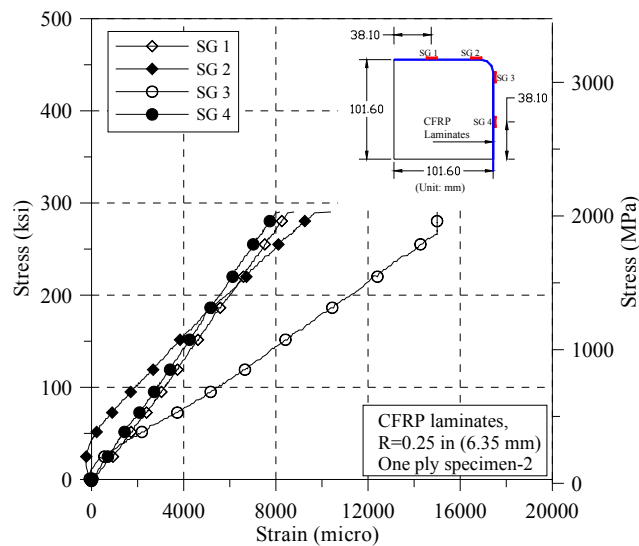


Fig. 5 Stress strain curve of one ply CFRP laminates ( $R=6.35$  mm, Specimen 2)

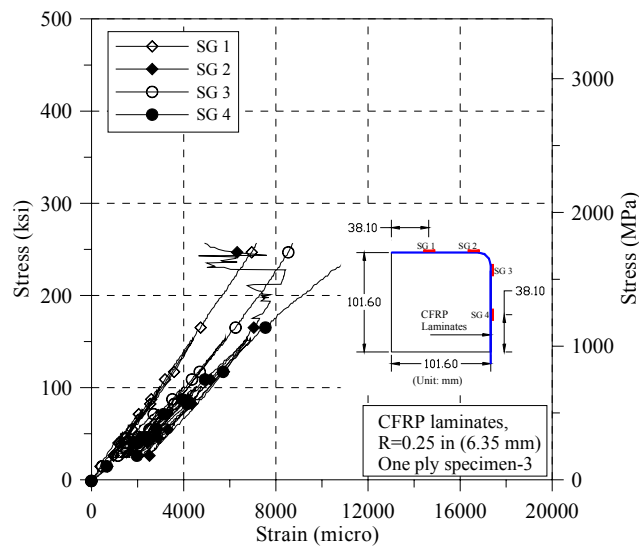


Fig. 6 Stress strain curve of one ply CFRP laminates ( $R=6.35$  mm, Specimen 3)

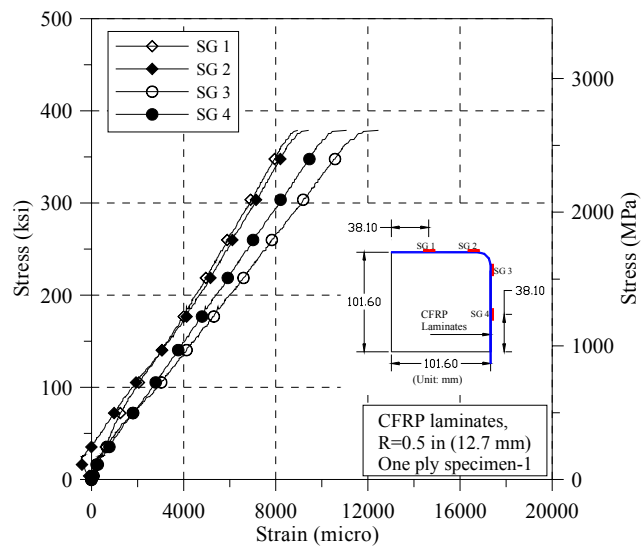


Fig. 7 Stress strain curve of one ply CFRP laminates  
( $R=12.7$  mm, Specimen 1)

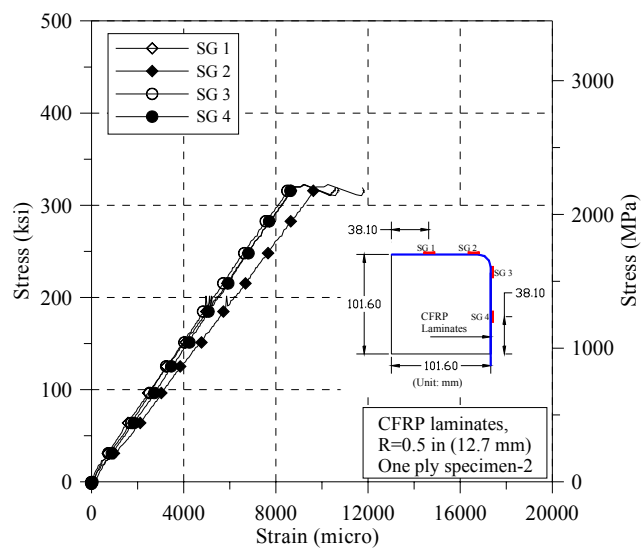


Fig. 8 Stress strain curve of one ply CFRP laminates  
( $R=12.7$  mm, Specimen 2)

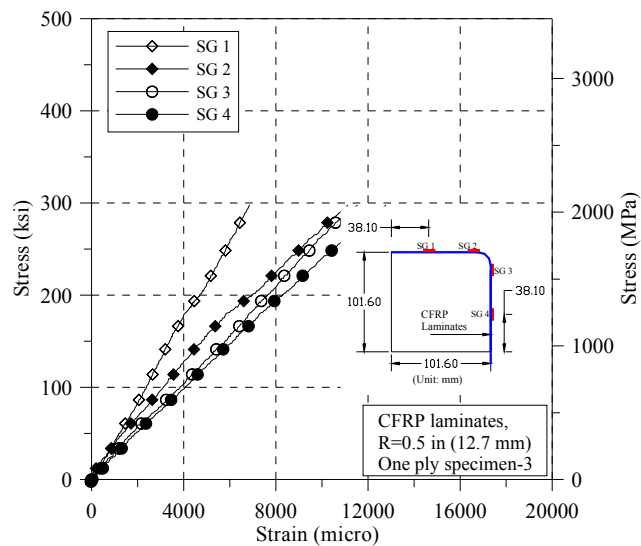


Fig. 9 Stress strain curve of one ply CFRP laminates (R=12.7 mm, Specimen 3)

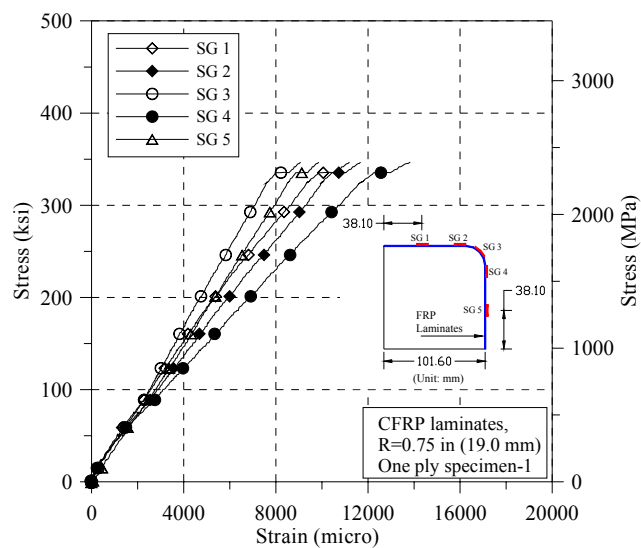


Fig. 10 Stress strain curve of one ply CFRP laminates (R=19.0 mm, Specimen 1)

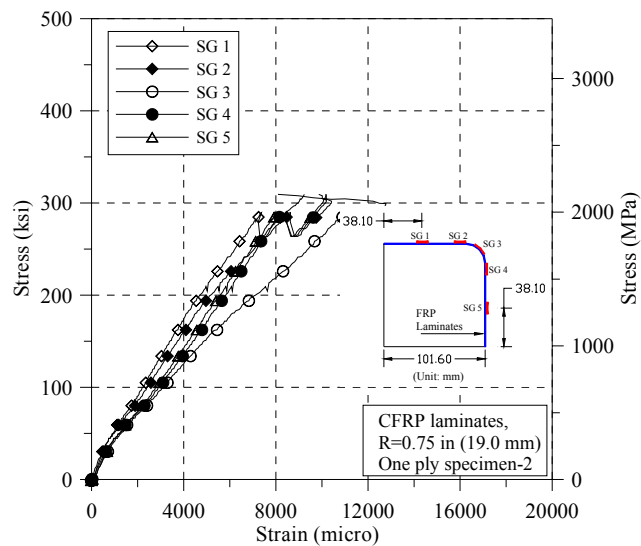


Fig. 11 Stress strain curve of one ply CFRP laminates (R=19.0 mm, Specimen 2)

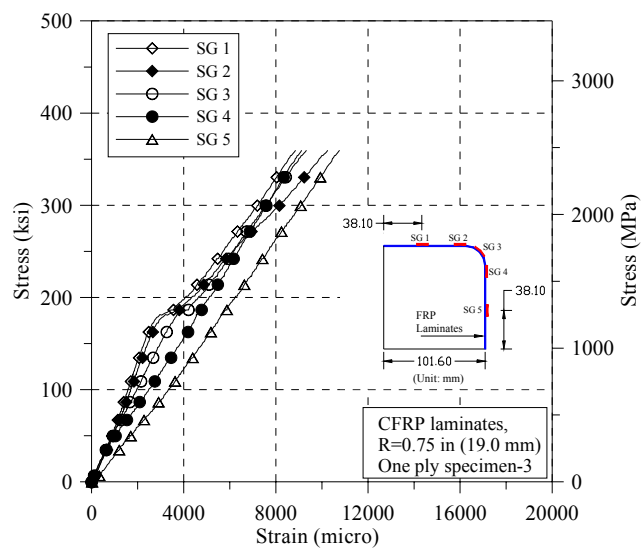


Fig. 12 Stress strain curve of one ply CFRP laminates (R=19.0 mm, Specimen 3)

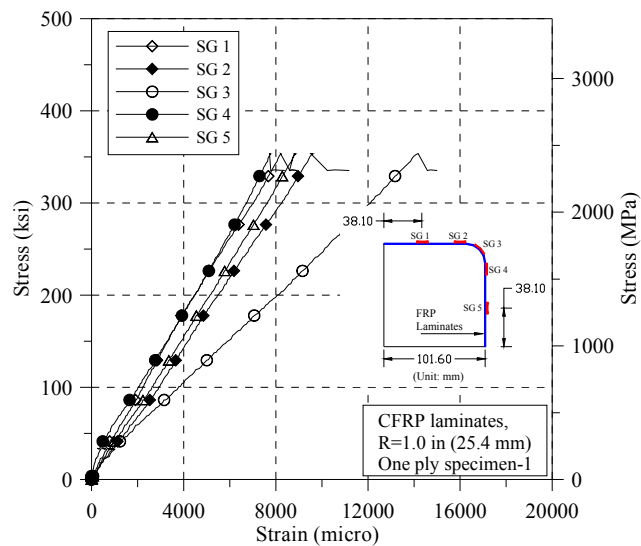


Fig. 13 Stress strain curve of one ply CFRP laminates  
(R=25.4 mm, Specimen 1)

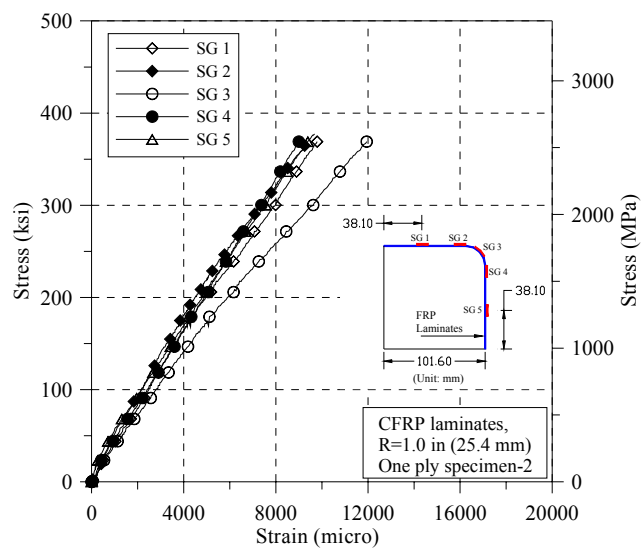


Fig. 14 Stress strain curve of one ply CFRP laminates  
(R=25.4 mm, Specimen 2)

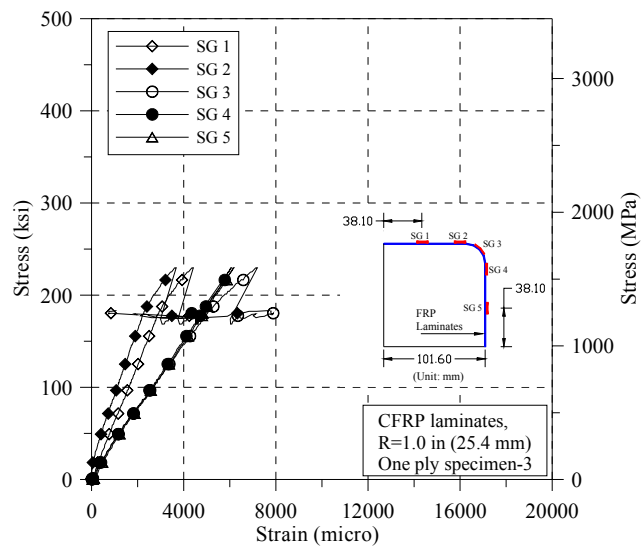


Fig. 15 Stress strain curve of one ply CFRP laminates (R=25.4 mm, Specimen 3)

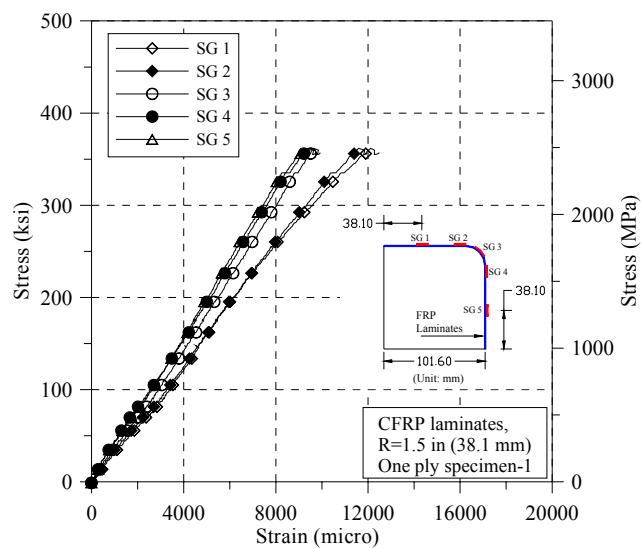


Fig. 16 Stress strain curve of one ply CFRP laminates (R=38.1 mm, Specimen 1)

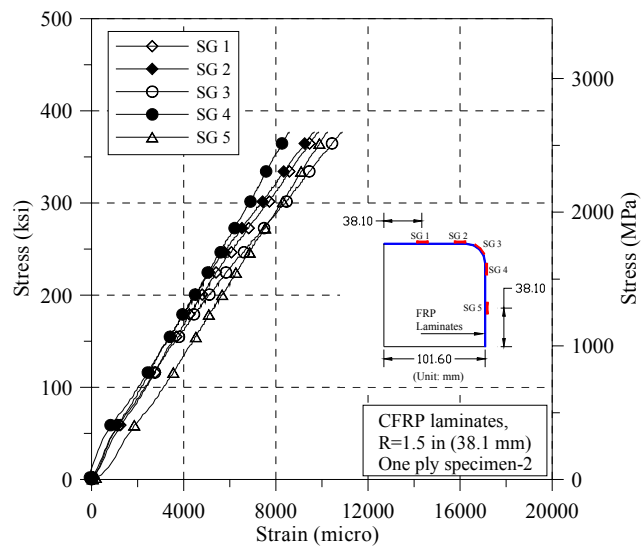


Fig. 17 Stress strain curve of one ply CFRP laminates (R=38.1 mm, Specimen 2)

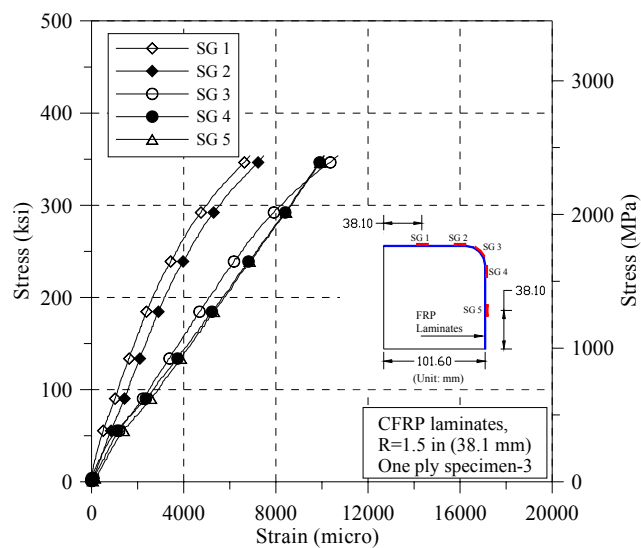


Fig. 18 Stress strain curve of one ply CFRP laminates (R=38.1 mm, Specimen 3)

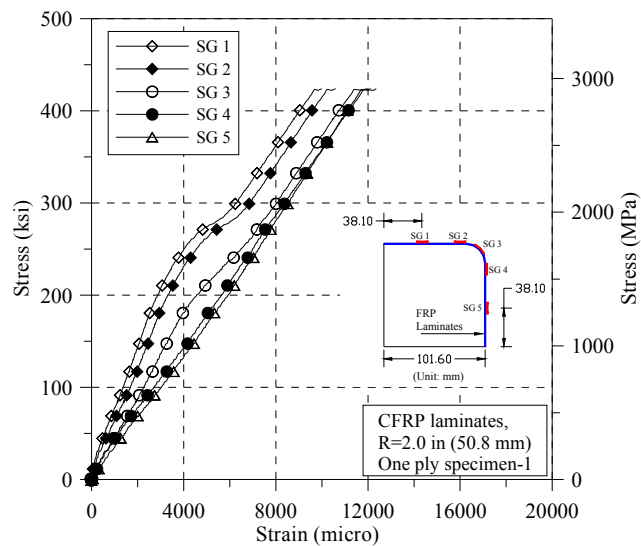


Fig. 19 Stress strain curve of one ply CFRP laminates ( $R=50.8$  mm, Specimen 1)

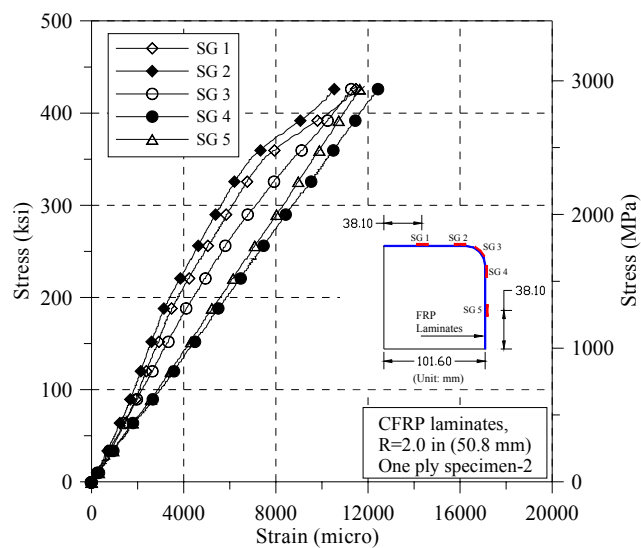


Fig. 20 Stress strain curve of one ply CFRP laminates ( $R=50.8$  mm, Specimen 2)

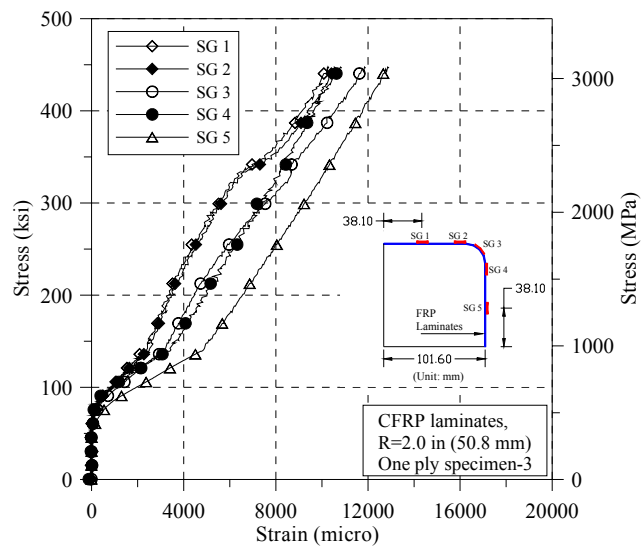


Fig. 21 Stress strain curve of one ply CFRP laminates (R=50.8 mm, Specimen 3)

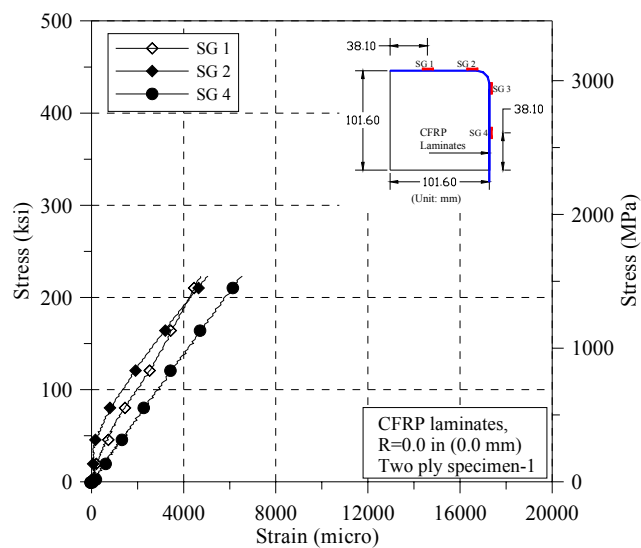


Fig. 22 Stress strain curve of two ply CFRP laminates (R=0.0 mm, Specimen 1)

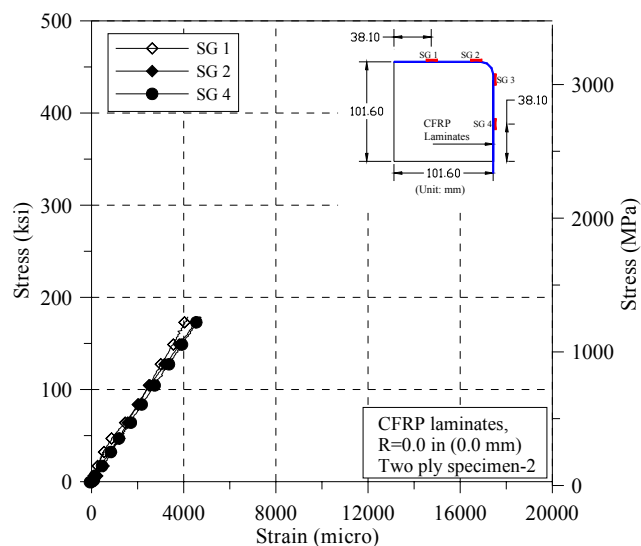


Fig. 23 Stress strain curve of two ply CFRP laminates  
( $R=0.0$  mm, Specimen 2)

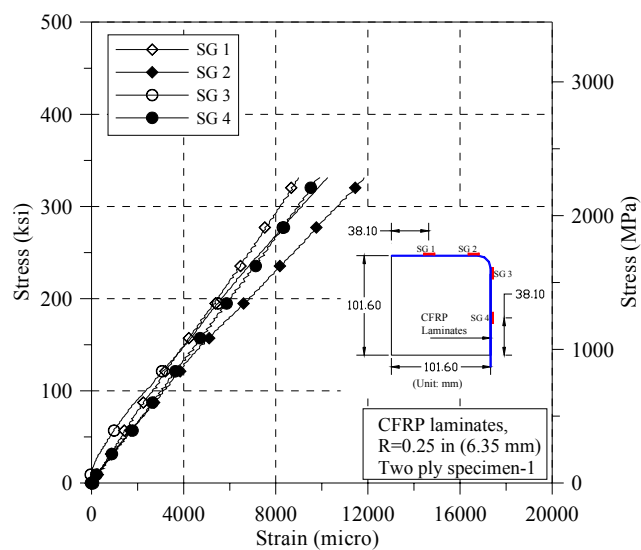


Fig. 24 Stress strain curve of two ply CFRP laminates  
( $R=6.35$  mm, Specimen 1)

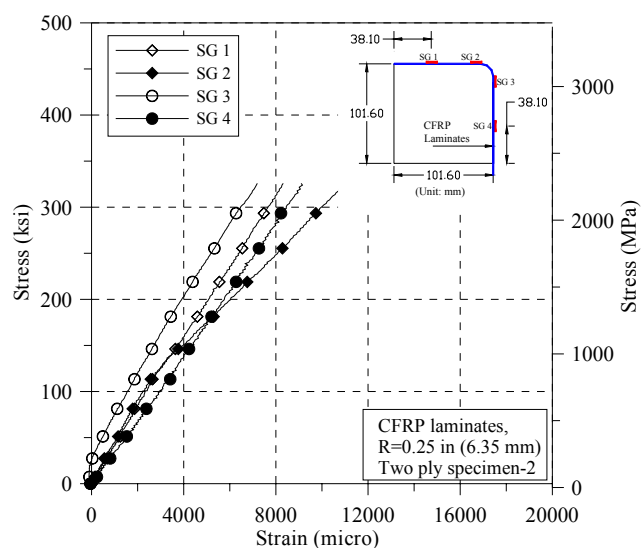


Fig. 25 Stress strain curve of two ply CFRP laminates  
(R=6.35 mm, Specimen 2)

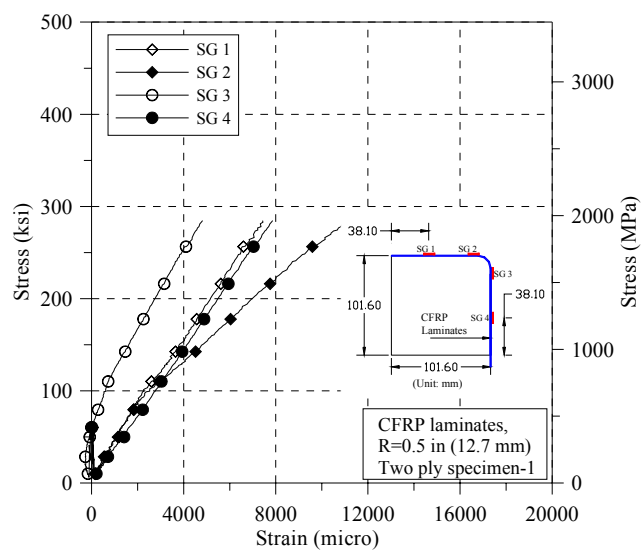


Fig. 26 Stress strain curve of two ply CFRP laminates  
(R=12.7 mm, Specimen 1)

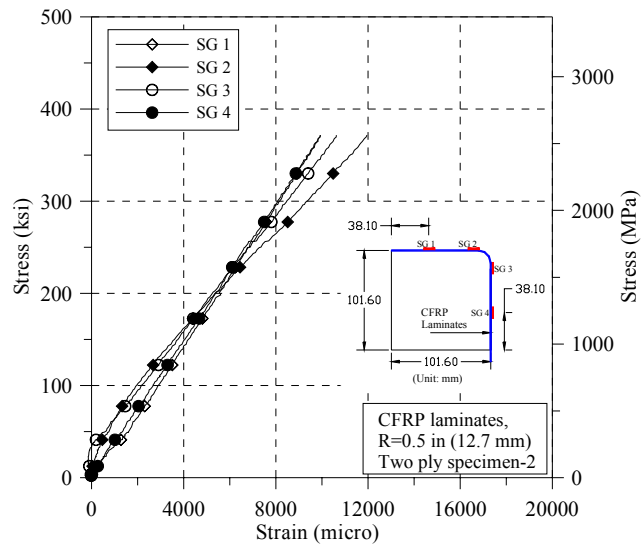


Fig. 27 Stress strain curve of two ply CFRP laminates (R=12.7 mm, Specimen 2)

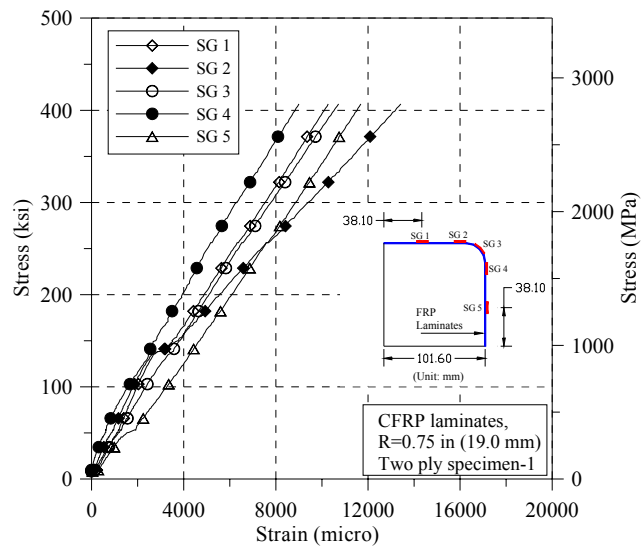


Fig. 28 Stress strain curve of two ply CFRP laminates (R=19.0 mm, Specimen 1)

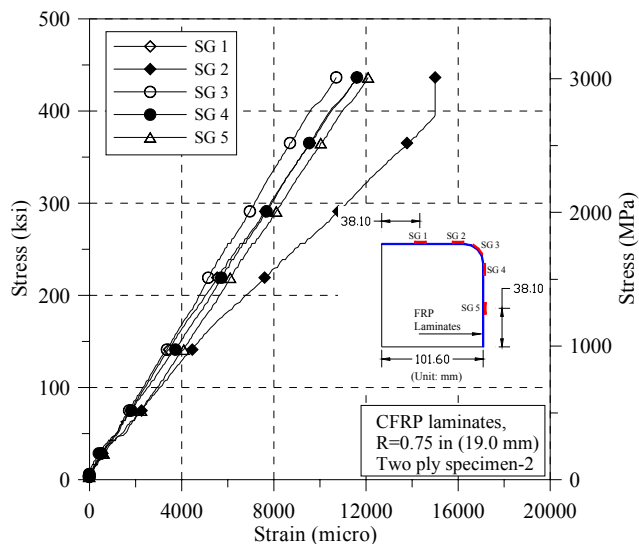


Fig. 29 Stress strain curve of two ply CFRP laminates (R=19.0 mm, Specimen 2)

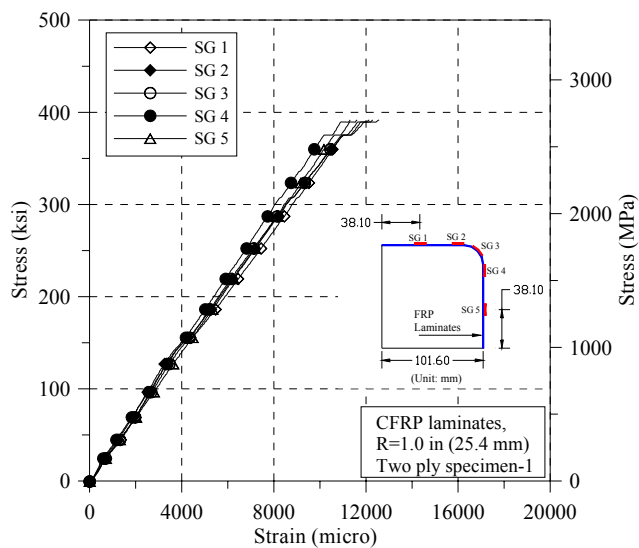


Fig. 30 Stress strain curve of two ply CFRP laminates (R=25.4 mm, Specimen 1)

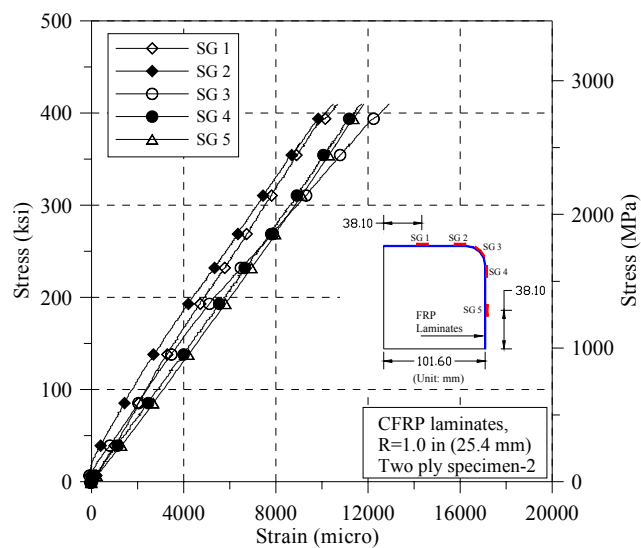


Fig. 31 Stress strain curve of two ply CFRP laminates  
(R=25.4 mm, Specimen 2)

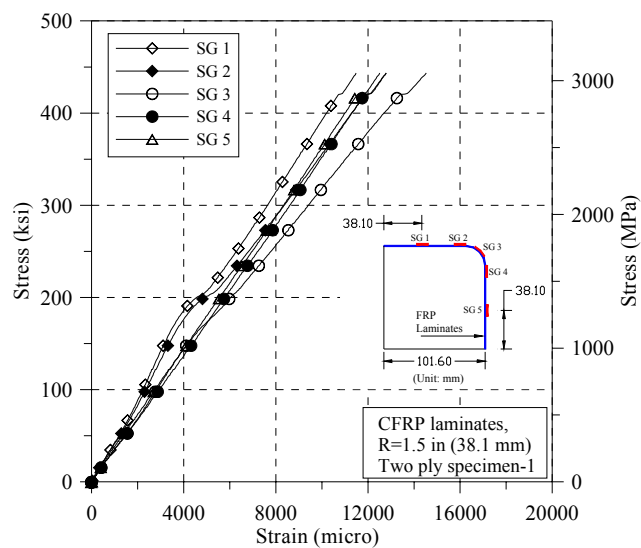


Fig. 32 Stress strain curve of two ply CFRP laminates  
(R=38.1 mm, Specimen 1)

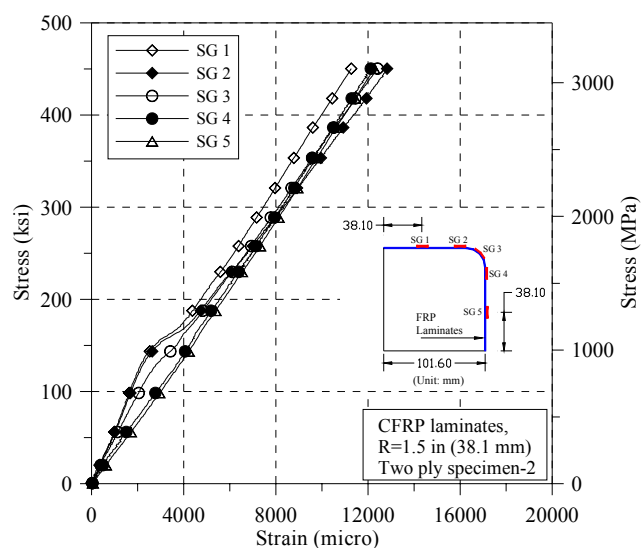


Fig. 33 Stress strain curve of two ply CFRP laminates  
(R=38.1 mm, Specimen 2)

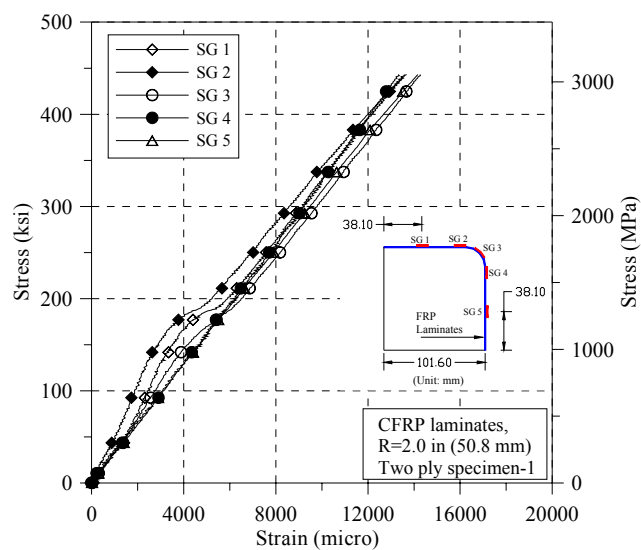


Fig. 34 Stress strain curve of two ply CFRP laminates  
(R=50.8 mm, Specimen 1)

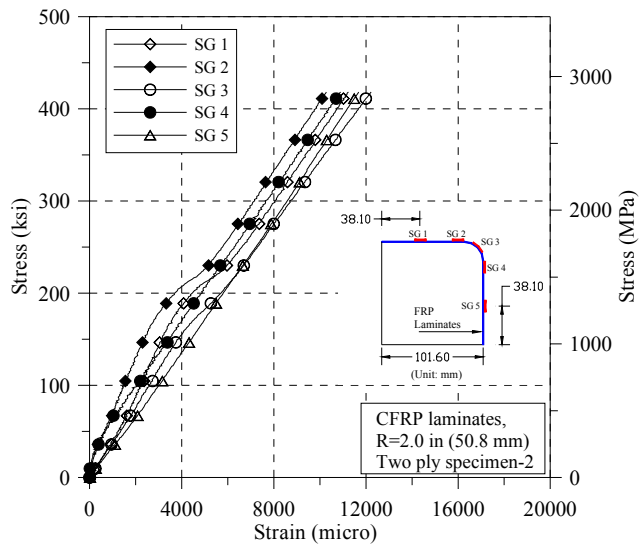


Fig. 35 Stress strain curve of two ply CFRP laminates (R=50.8 mm, Specimen 2)

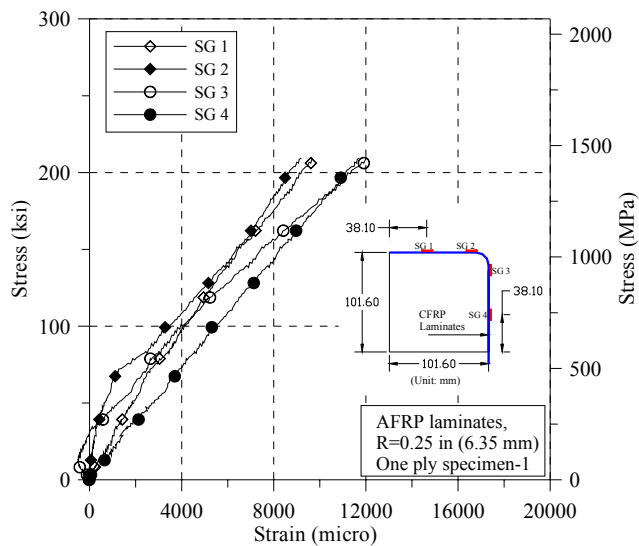


Fig. 36 Stress strain curve of one ply AFRP laminates (R=6.35 mm, Specimen 1)

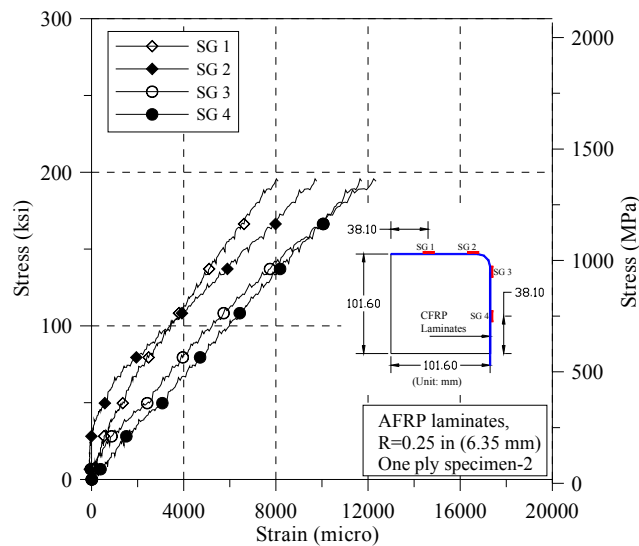


Fig. 37 Stress strain curve of one ply AFRP laminates (R=6.35 mm, Specimen 2)

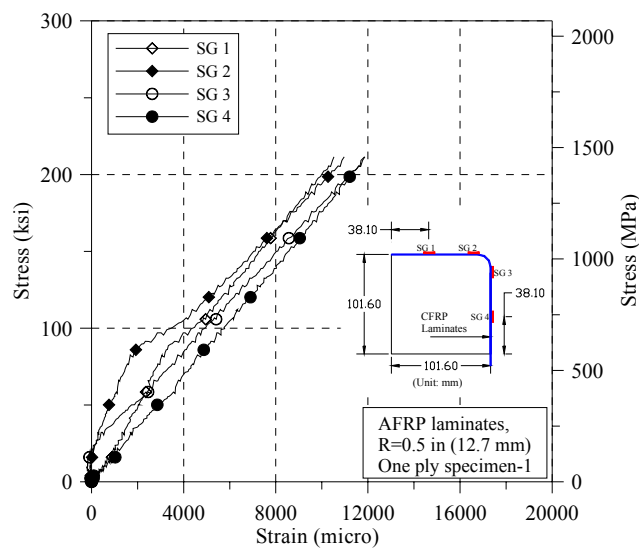


Fig. 38 Stress strain curve of one ply AFRP laminates (R=12.7 mm, Specimen 1)

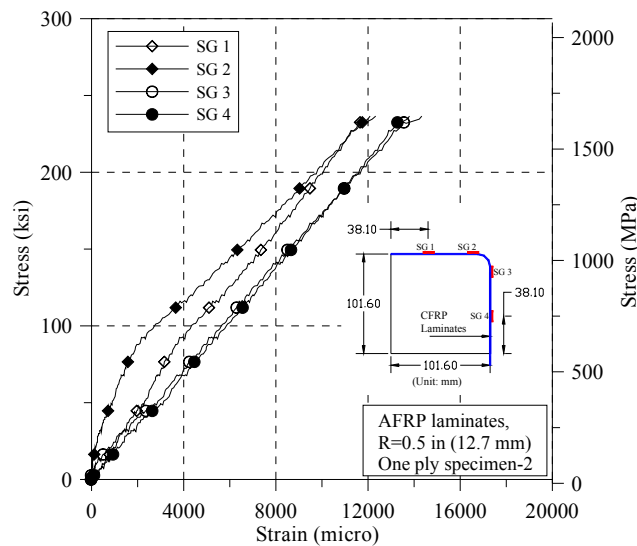


Fig. 39 Stress strain curve of one ply AFRP laminates  
( $R=12.7$  mm, Specimen 2)

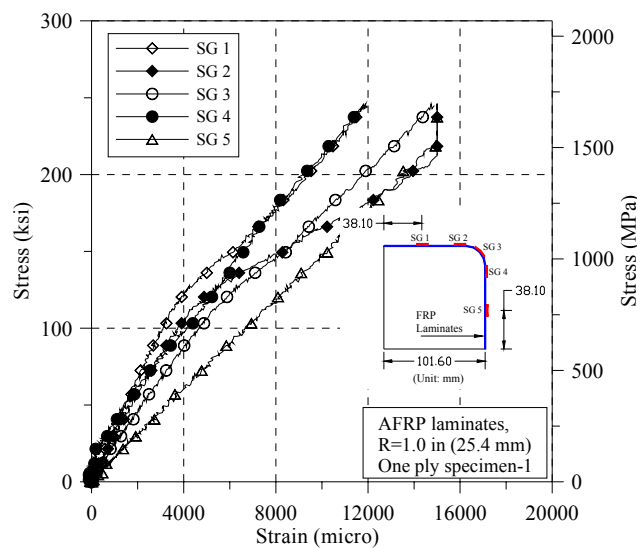


Fig. 40 Stress strain curve of one ply AFRP laminates  
( $R=25.4$  mm, Specimen 1)

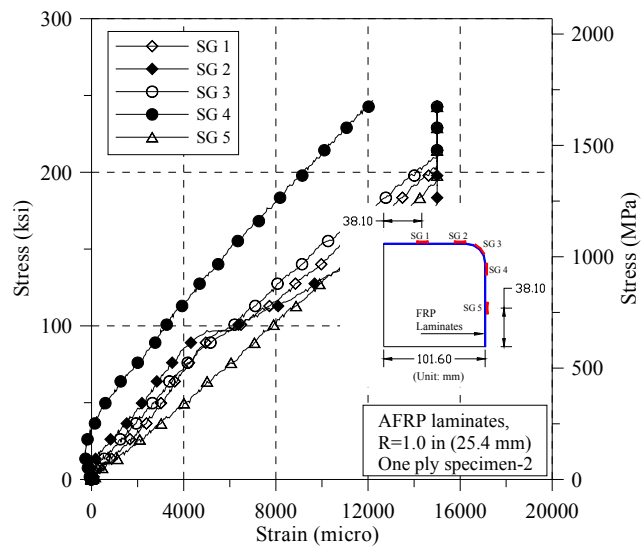


Fig. 41 Stress strain curve of one ply AFRP laminates (R=25.4 mm, Specimen 2)

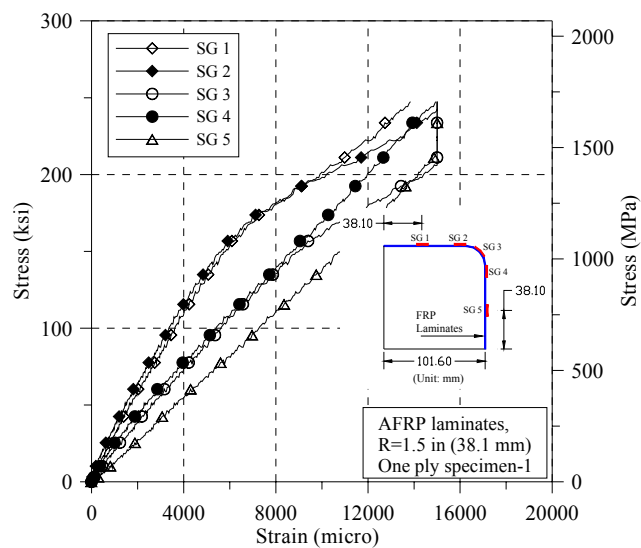


Fig. 42 Stress strain curve of one ply AFRP laminates (R=38.1 mm, Specimen 1)

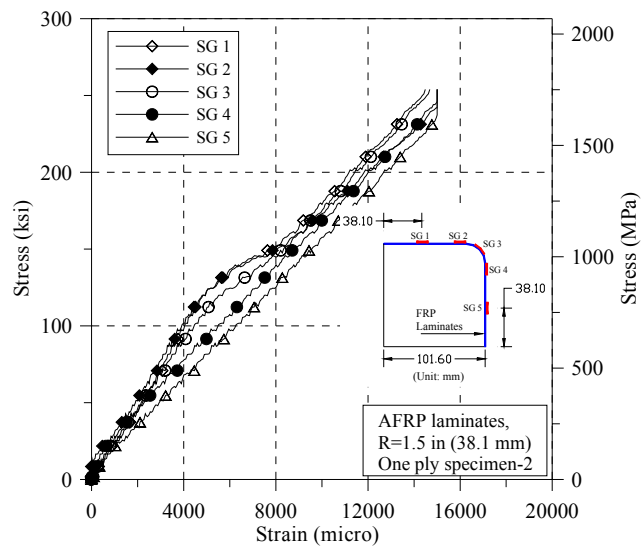


Fig. 43 Stress strain curve of one ply AFRP laminates (R=38.1 mm, Specimen 2)

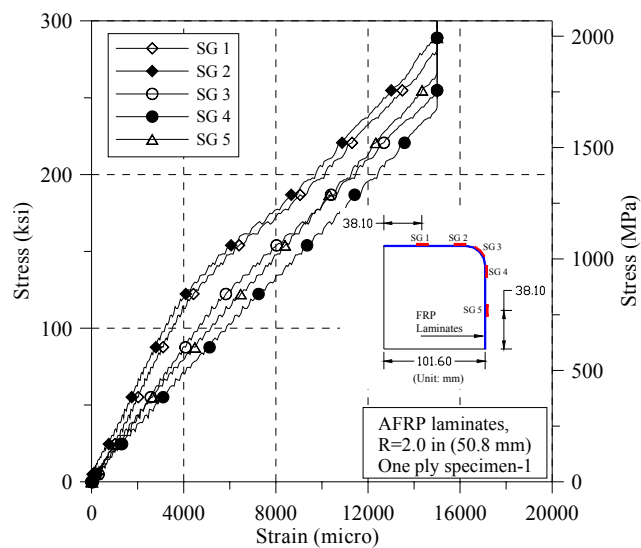


Fig. 44 Stress strain curve of one ply AFRP laminates (R=50.8 mm, Specimen 1)

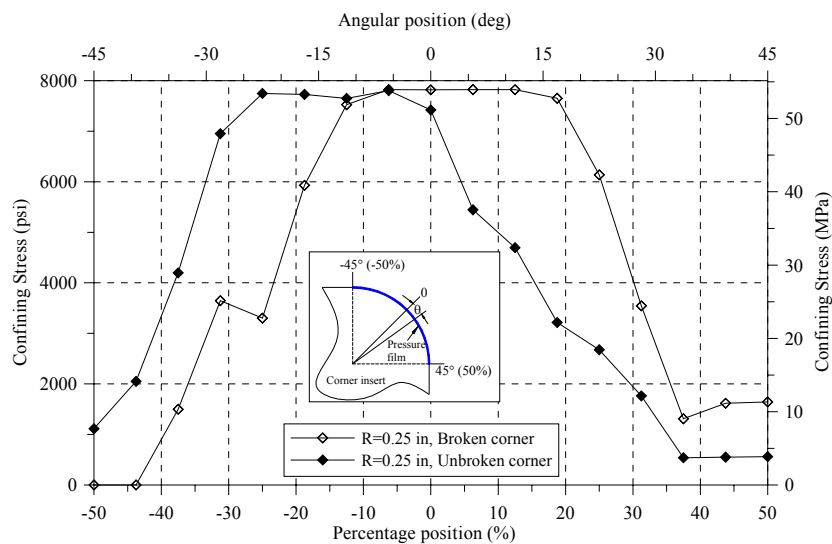


Fig. 45 Confining stress between curvature changing points ( $R=6.35$  mm (0.25 in))

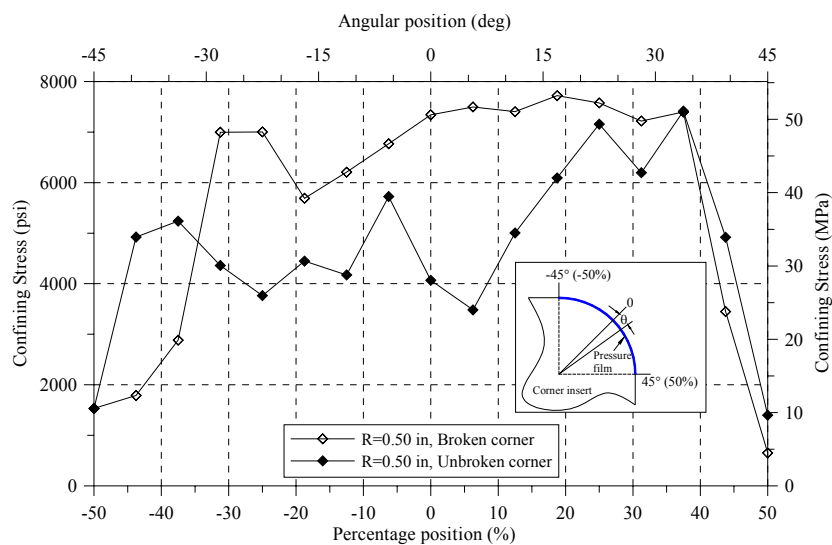


Fig. 46 Confining stress between curvature changing points ( $R=12.7$  mm (0.5 in))

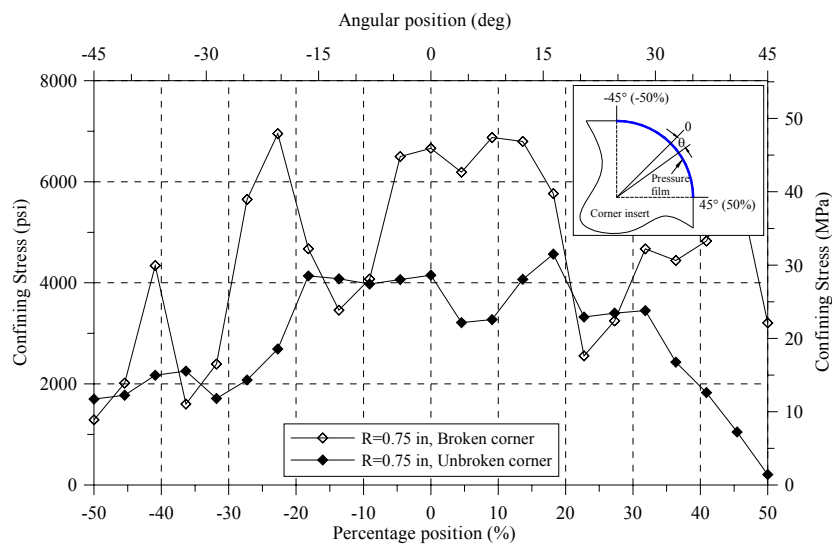


Fig. 47 Confining stress between curvature changing points ( $R=19.0$  mm (0.75 in))

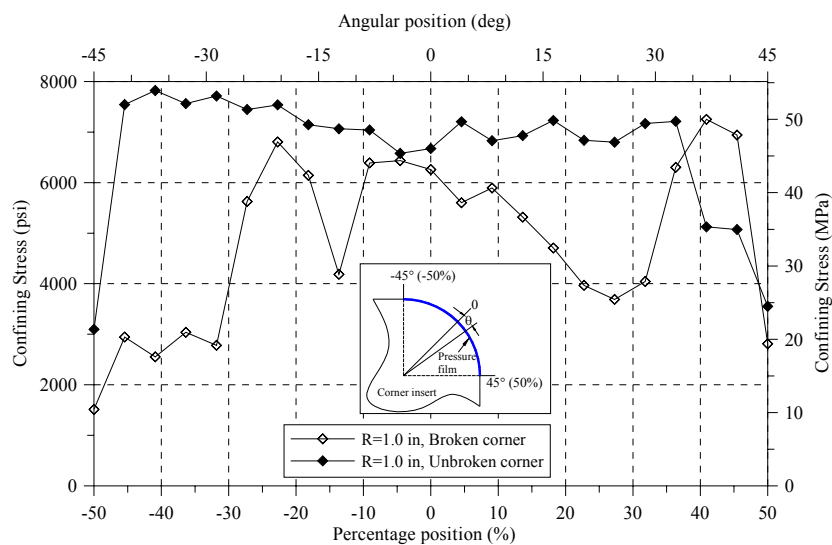


Fig. 48 Confining stress between curvature changing points ( $R=25.4$  mm (1.0 in))

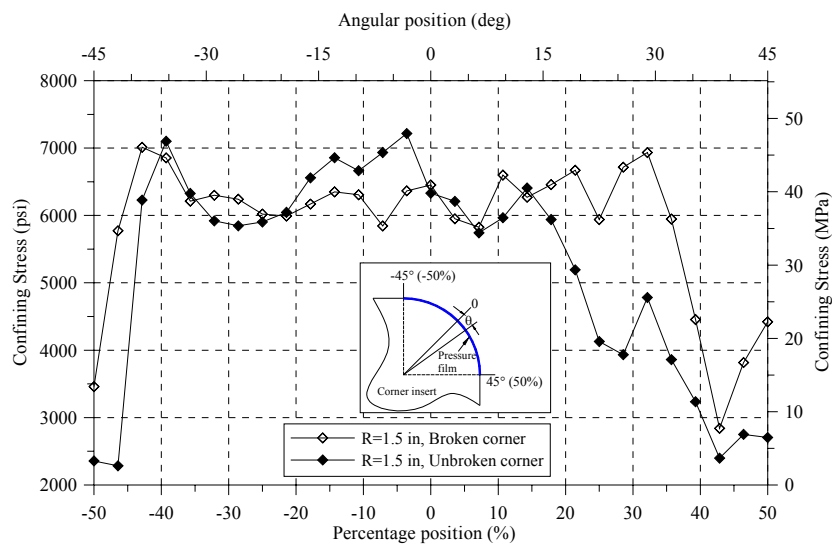


Fig. 49 Confining stress between curvature changing points  
( $R=38.1$  mm (1.5 in))

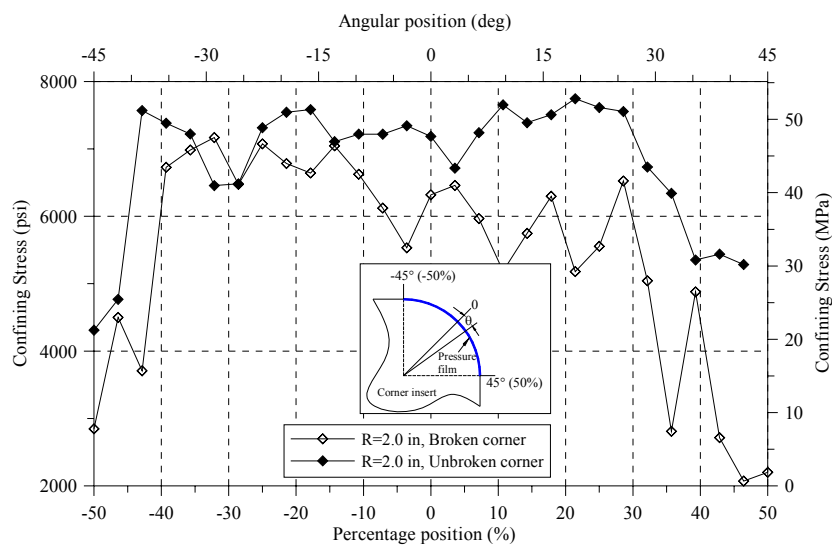


Fig. 50 Confining stress between curvature changing points  
( $R=50.8$  mm (2.0 in))

## **APPENDIX 4**

### **Load Strain Curve of Lap Spliced CFRP Laminates**

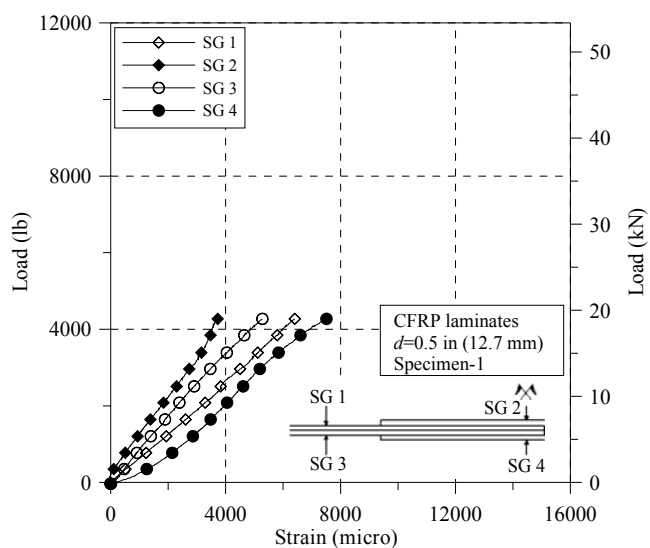


Fig. 1 Load strain curve of lap spliced CFRP laminates (Lap splice length  $d=12.7$  mm, specimen 1)

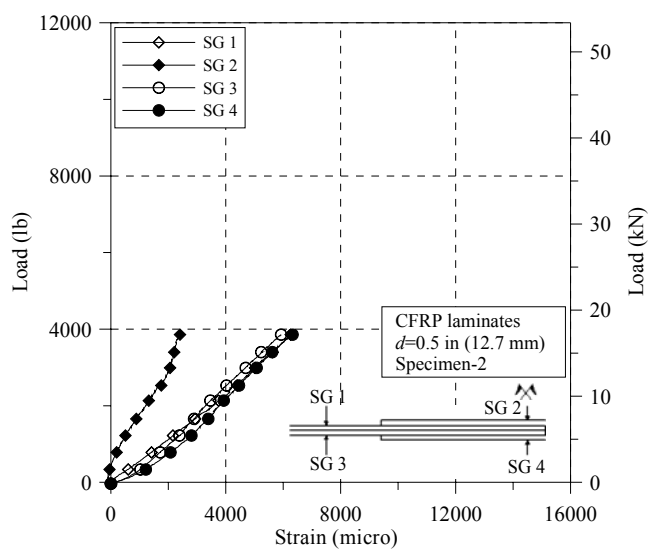


Fig. 2 Load strain curve of lap spliced CFRP laminates (Lap splice length  $d=12.7$  mm, specimen 2)

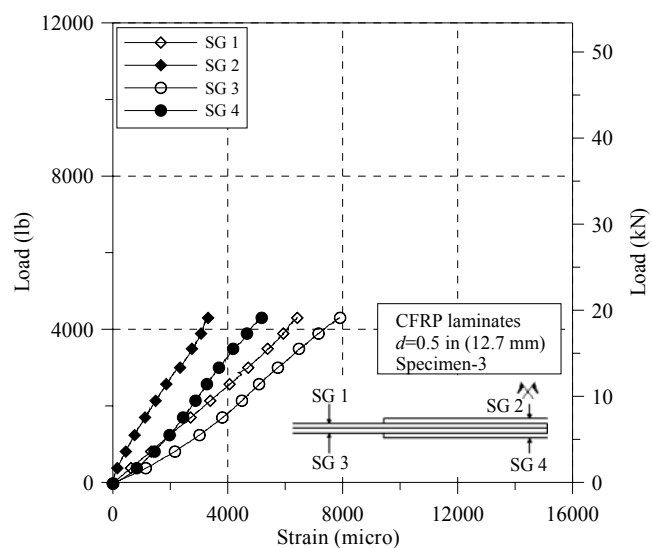


Fig. 3 Load strain curve of lap spliced CFRP laminates (Lap splice length  $d=12.7$  mm, specimen 3)

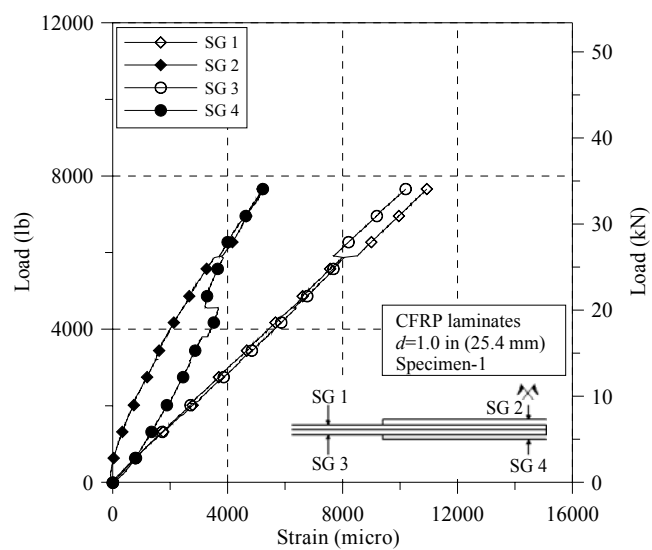


Fig. 4 Load strain curve of lap spliced CFRP laminates (Lap splice length  $d=25.4$  mm, specimen 1)

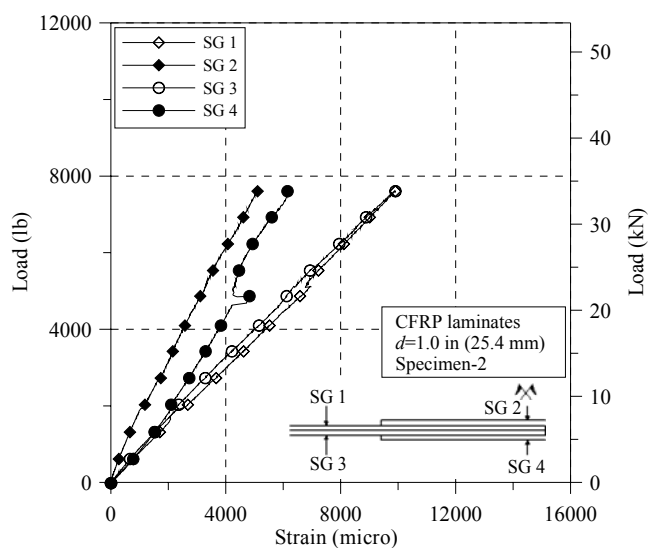


Fig. 5 Load strain curve of lap spliced CFRP laminates (Lap splice length  $d=25.4$  mm, specimen 2)

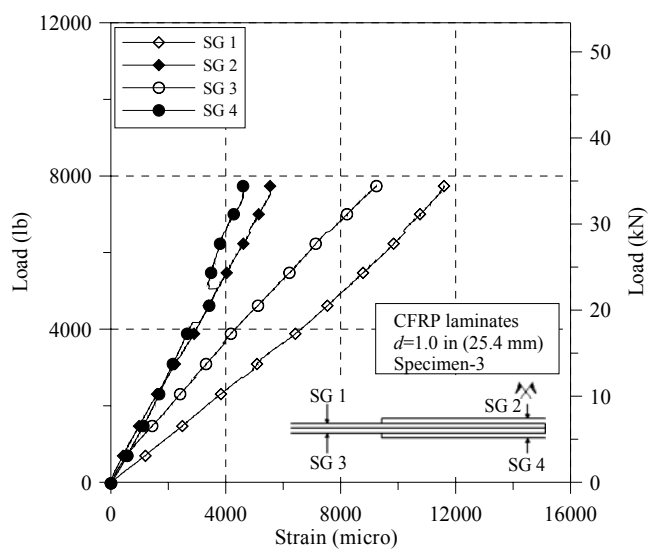


Fig. 6 Load strain curve of lap spliced CFRP laminates (Lap splice length  $d=25.4$  mm, specimen 3)

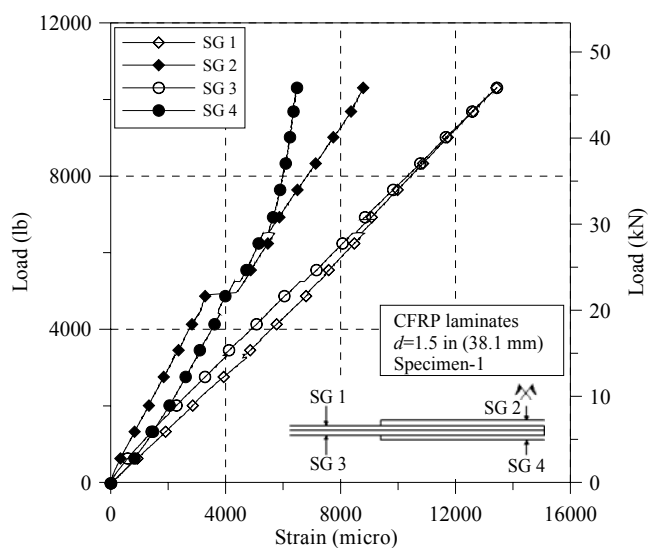


Fig. 7 Load strain curve of lap spliced CFRP laminates (Lap splice length  $d=38.1$  mm, specimen 1)

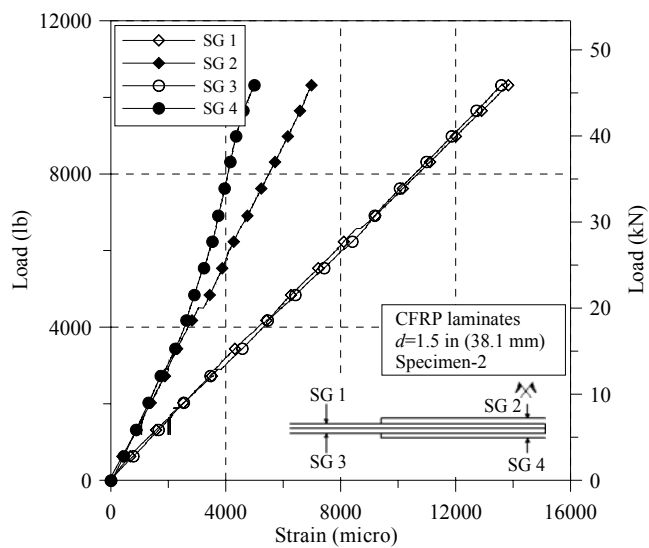


Fig. 8 Load strain curve of lap spliced CFRP laminates (Lap splice length  $d=38.1$  mm, specimen 2)

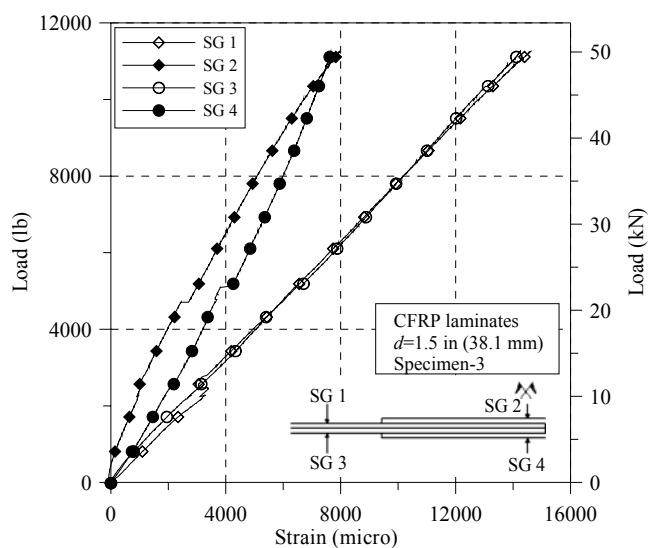


Fig. 9 Load strain curve of lap spliced CFRP laminates (Lap splice length  $d=38.1$  mm, specimen 3)

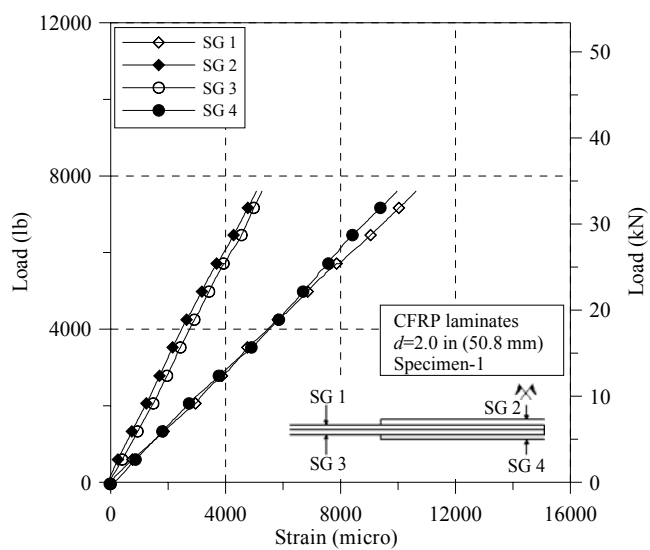


Fig. 10 Load strain curve of lap spliced CFRP laminates (Lap splice length  $d=50.8$  mm, specimen 1)

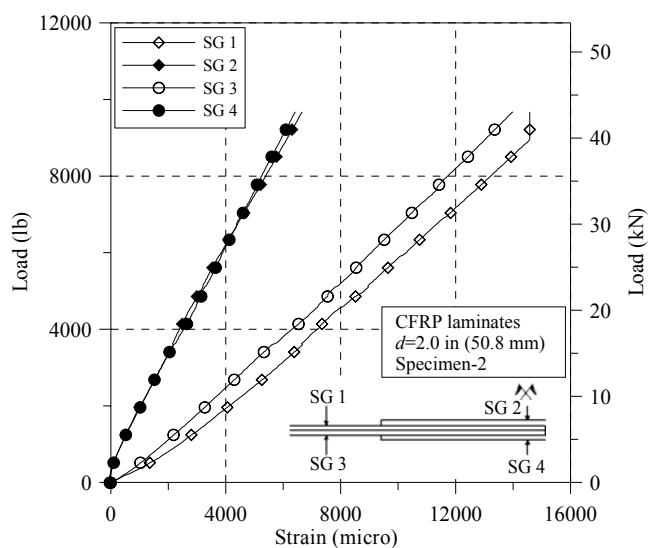


Fig. 11 Load strain curve of lap spliced CFRP laminates (Lap splice length  $d=50.8$  mm, specimen 2)

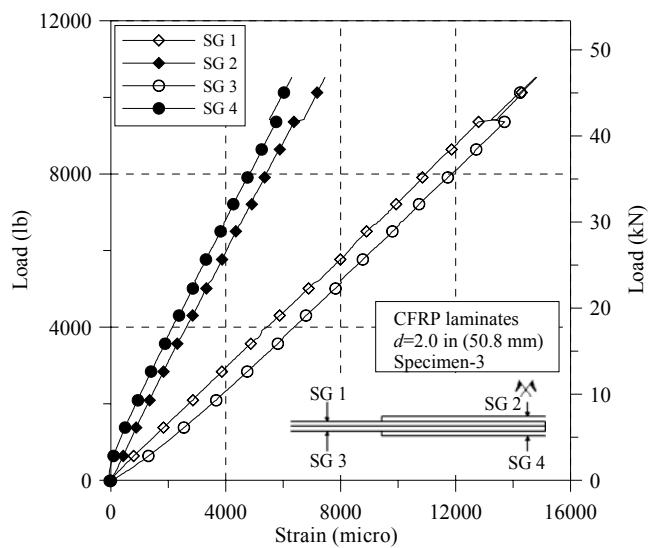


Fig. 12 Load strain curve of lap spliced CFRP laminates (Lap splice length  $d=50.8$  mm, specimen 3)

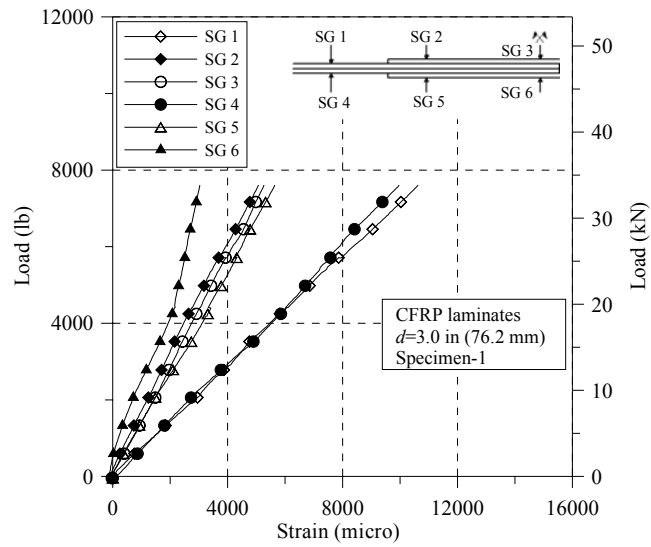


Fig. 13 Load strain curve of lap spliced CFRP laminates (Lap splice length  $d=76.2$  mm, specimen 1)

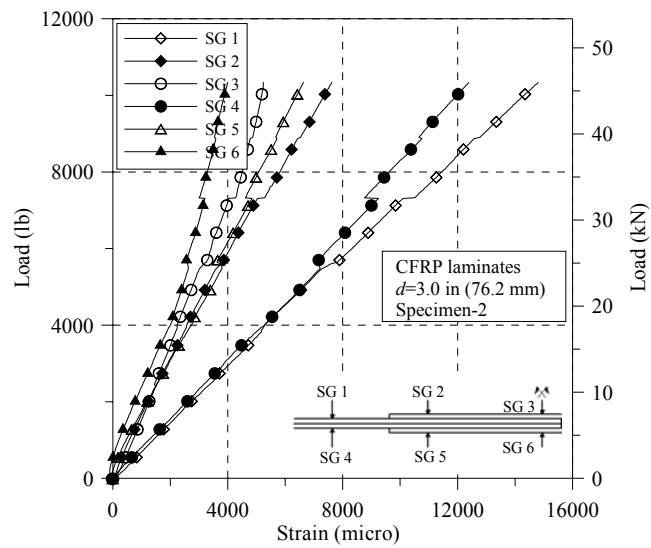


Fig. 14 Load strain curve of lap spliced CFRP laminates (Lap splice length  $d=76.2$  mm, specimen 2)

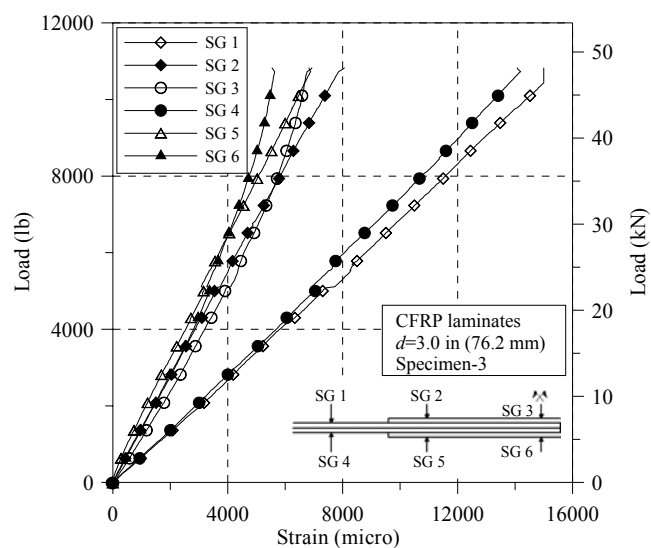


Fig. 15 Load strain curve of lap spliced CFRP laminates (Lap splice length  $d=76.2$  mm, specimen 3)

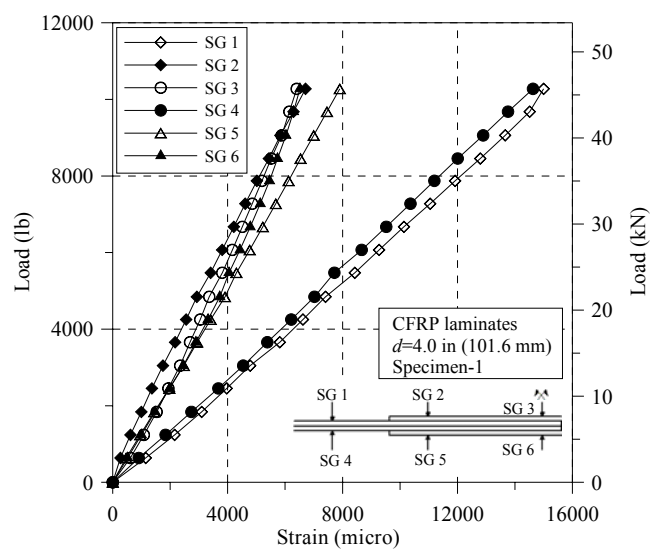


Fig. 16 Load strain curve of lap spliced CFRP laminates (Lap splice length  $d=101.6$  mm, specimen 1)

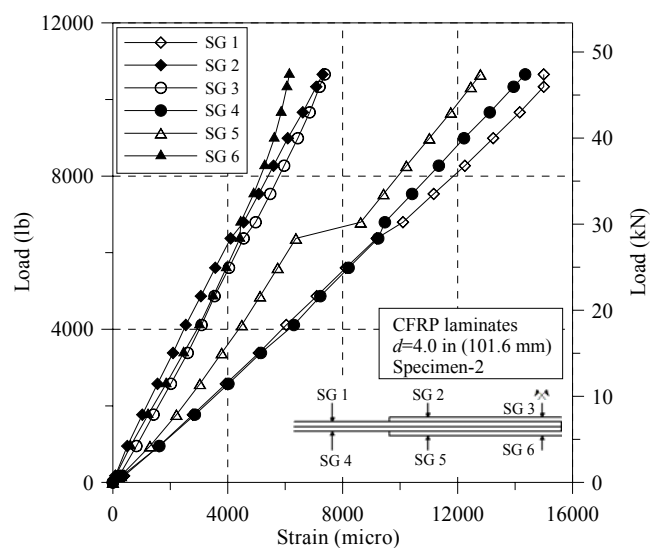


Fig. 17 Load strain curve of lap spliced CFRP laminates (Lap splice length  $d=101.6$  mm, specimen 2)

## **APPENDIX 5**

**Recommendations to the AASHTO LRFD Design  
Specifications, US Units, Second Edition, 1998**

## INTRODUCTION

The following recommendations are made for the AASHTO LRFD Design Specifications, US Units, Second Edition, 1998. Recommendations for the incorporation of FRP reinforcement in strengthening concrete structures are placed in either the Specifications or Commentary portion in the manual depending on which one is most appropriate. The recommendations are based on the investigations on the three critical aspects of installation of externally bonded FRP laminates included in this thesis. References are provided to assist in evaluating the intent of recommendations.

### SPECIFICATIONS

### COMMENTARY

#### 5.1 SCOPE

The provisions of this section also combine the requirements for externally bonded FRP reinforcement used in strengthening concrete structures.

#### 5.2 DEFINITIONS

add:

FRP - fiber reinforced polymer

CFRP - carbon fiber reinforced polymer

AFRP – aramid fiber reinforced polymer

GFRP – glass fiber reinforced polymer

$A_{fl}$  – Area of FRP laminate, in<sup>3</sup>

$d$  – Lap splice length of FRP laminate, in

$E_f$  – Modulus of Elasticity of FRP, ksi

$F_{fu}^*$  - Guaranteed tensile strength of FRP laminate, ksi

$F_u$  – Static ultimate strength of lap-spliced FRP laminate, ksi

$f_{fu}$  – Design strength of FRP laminate, ksi

#### 5.4.3.2 Modulus of Elasticity

The modulus of elasticity of FRP

#### C5.4.3.2

The modulus of elasticity of FRP

laminate should be specified by manufacturer or obtained by conducting testing according to ASTM D-3039/3039M

### 5.5.3 Fatigue Limit State

#### 5.5.3.1 General

For externally bonded FRP laminates when a lap splice is used during installation, fatigue of the laminate need not be checked provided that the bonded length exceeds 4.0 in.

##### 5.5.3.2.1

The stress range in lap-spliced CFRP laminate should not exceed  $0.4F_u$ , where  $F_u$  is the static ultimate strength of lap-spliced CFRP laminate.

If more than one lap splice is present, staggering is required.

laminate is dependent on the fiber type and volumetric content of FRP laminate. It also depends on the quality of installation. For example, fiber misalignment will cause significant stiffness reduction if the angle exceeds 5 degree (Paper 1 and 2)

#### C5.5.3.1

Tests indicate that for 4 in lap-spliced CFRP laminates with the maximum stress less than 40% of its ultimate strength, no fatigue failure is observed after 2.5 million cycles of repeated loading (Paper 6). Continuous CFRP laminates have excellent fatigue performance. Fatigue limit state needs not to be checked for CFRP.

##### C5.5.3.2.1

$F_u$  should be provided by the manufacturer or from coupon testing. In the case of multiple plies, failure could be initiated at one lap splice joint followed by immediate failure of the other lap splice joint causing a reduction in ultimate strength (Paper 6).

$F_u$  is computed using the net fiber area in the laminates. If  $F_u$  is not known, it can be taken as 80% of the design strength for FRP.

Lap splice should be avoided in bends or

### 5.7.3 Flexural Members

#### 5.7.3.2 Flexural Resistance

##### 5.7.3.2.5

The resistance from FRP should be added to  $M_n$  in Equation 5.7.3.2.1-1

other situations where local stress concentration may be incurred.

##### C5.7.3.2.5

Resistance component from FRP should be added by considering FRP reinforcement as a linear material, which is elastic up to failure. Perfect bonding between externally bonded FRP reinforcement and concrete may be assumed.

Strength reduction should be applied if the FRP reinforcement does not take the same direction of the main reinforcement (Paper 1 and 2).

### 5.10.11 Provisions for Seismic Design

#### 5.10.11.4.1.f Splices of Main Reinforcement.

Add:

##### 5.10.11.4.1g

Splice of Externally Bonded FRP Reinforcement

To maintain the continuity of FRP reinforcement wrapping columns or piers, bonded lap splice may be used. Following requirements shall be satisfied:

- Lap splice joint should not be put on cross sectional corners.
- Lap splice length should be at least 4 in. for CFRP

##### C5.10.11.4.1g

In paper 4 and 5, the investigation shows that corner radius has a significant effect on the mechanical properties of CFRP laminate. At best, 67% of the static ultimate strength can be developed even for circular cross sections. Stress concentration exists around the corners depending on the radius.

In paper 6, it is indicated that 4 in. lap splice can develop both the ultimate

Add:

#### **5.10.11.4.1.h**

##### Column Cross Section Configuration

Sharp corners should be avoided in strengthening columns with FRP laminate. For rectangular or square cross section, the corners should be rounded off with a radius of not less than 1.0 in.

Add:

#### **5.11.7**

##### Splices of External FRP Reinforcement

When FRP laminate is used to strengthen concrete structures, the length of lap for lap splices should not be less than 4.0 in. for carbon and 6.0 in for aramid FRP.

strength and fatigue performance of CFRP laminate.

#### **C5.10.11.4.1.h**

Circular cross section should be preferred in regard to easy installation of FRP jacket and stress concentration can be avoided (Paper 6). On the other hand, it is hard to make the laminate perfectly contact the concrete surface at the corners for cross sections with sharp corners.

#### **C5.11.7**

Only the lap splice length for carbon FRP is specified here (Paper 6). From the tests, 1.5 in. is sufficient to develop the static ultimate strength of carbon FRP laminate. 3.0 in. is sufficient for aramid FRP to develop the ultimate strength. However, 6.0 in. is recommended for aramid FRP. The lap splice length for glass FRP is not specified here due to lack of investigation on this composite material.

## VITA

Xinbao Yang was born on May 25, 1969, in Anhui Province, People's Republic of China. He received his BS degree and MS degree in structural engineering in 1991 and 1994, respectively from Shanghai Institute of Railway Technology, Shanghai, China. After he received his MS degree, he went to Tongji University, Shanghai, China as a research engineer. After working in Tongji University for three years, he went to Shanghai Municipal Engineering Administration Bureau as a structural engineer. He enrolled in the program in Structural Engineering at the University of Missouri-Rolla as a PhD candidate in August 1998. He is an associate member of ASCE and a student member of ACI and EERI. He is also an active member of Chi Epsilon, the National Civil Engineering Honor Society.